



3 4456 0452165 8

ORNL/TM-8100

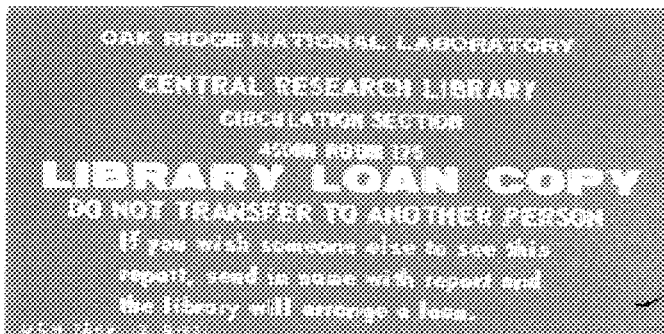
# ORNL

OAK  
RIDGE  
NATIONAL  
LABORATORY

UNION  
CARBIDE

## Design and Analysis of a 5-MW Vertical-Fluted-Tube Condenser for Geothermal Applications

G. H. Llewellyn



DEVELOPED BY  
UNION CARBIDE CORPORATION  
FOR THE UNITED STATES  
DEPARTMENT OF ENERGY

United States of America. Available from  
National Technical Information Service  
U.S. Department of Commerce  
5205 Port Royal Road, Springfield, Virginia 22161  
703/546-4501

This report was submitted to an account of work sponsored by an agency of the  
Department of Defense. Neither the United States Government nor any agency  
or employee of the Government makes any warranty, express or implied, or  
assumes any responsibility whatsoever for the accuracy, completeness, or  
usefulness of the information, apparatus, method, or process disclosed in  
this report. The views expressed in this report are those of the author(s) and do not  
necessarily represent the views of the Defense Science and Technology Information Agency.  
The mention of trade names or trademarks does not constitute an endorsement by  
the Defense Science and Technology Information Agency of the products or services  
of the companies mentioned. The use of registered service marks of the Defense Science and  
Technology Information Agency and the Defense Science and Technology Information Agency  
is not intended to indicate that such marks are registered or used by the Defense Science and  
Technology Information Agency.

ORNL/TM-8100  
Dist. Category UC-66d

Contract No. W-7405-eng-26

Engineering Division for ORNL Energy Division

DESIGN AND ANALYSIS OF A 5-MW VERTICAL-FLUTED-TUBE  
CONDENSER FOR GEOTHERMAL APPLICATIONS

G. H. Llewellyn

Date Published - March 1982

OAK RIDGE NATIONAL LABORATORY  
Oak Ridge, Tennessee 37830  
operated by  
UNION CARBIDE CORPORATION  
NUCLEAR DIVISION  
for the  
DEPARTMENT OF ENERGY



3 4456 0452165 8



## CONTENTS

	<u>Page</u>
LIST OF FIGURES . . . . .	v
LIST OF TABLES . . . . .	vii
ABSTRACT . . . . .	1
1. INTRODUCTION . . . . .	1
2. SUMMARY . . . . .	5
3. HISTORY OF FLUTED TUBES . . . . .	7
4. INDUSTRIAL APPLICATIONS . . . . .	11
5. FLUTED TUBE MANUFACTURE . . . . .	13
6. EXPERIMENTAL WORK AT ORNL . . . . .	19
7. HEAT TRANSFER CALCULATIONS . . . . .	31
7.1 Properties of Liquid and Vapor Streams . . . . .	31
7.2 Tubeside Heat Transfer Coefficient . . . . .	32
7.3 Shellside Heat Transfer Coefficient . . . . .	36
7.4 Fouling . . . . .	40
7.5 Overall Heat Transfer . . . . .	42
7.6 Log Mean Temperature Difference . . . . .	44
8. PRESSURE DROP CALCULATIONS . . . . .	47
8.1 Tubeside Pressure Drop . . . . .	47
8.2 Shellside Pressure Drop . . . . .	49
9. DESIGN VARIABLES AND OPTIMIZATION . . . . .	55
10. CONDENSER DESIGN . . . . .	61
10.1 Design Criteria and Code Requirements . . . . .	62
10.2 Design Description . . . . .	63
10.3 Vibrational Analysis . . . . .	71
10.4 Data Acquisition and Instrumentation . . . . .	75
10.5 Site Testing . . . . .	78
11. RELATED PRESENT AND FUTURE WORK . . . . .	81
12. CONCLUSIONS AND RECOMMENDATIONS . . . . .	85
ACKNOWLEDGMENTS . . . . .	87
REFERENCES . . . . .	89

	<u>Page</u>
BIBLIOGRAPHY . . . . .	95
Appendix A. CONVERSIONS (METRIC/ENGLISH, ENGLISH/METRIC) . . . .	103
Appendix B. PROPERTIES OF ISOBUTANE . . . . .	105
Appendix C. PROPERTIES OF WATER . . . . .	109
Appendix D. SHELLSIDE PRESSURE DISTRIBUTION . . . . .	111

LIST OF FIGURES

<u>Figure</u>	<u>Page</u>
1 Modifications to test loop at the Geothermal Components Test Facility at East Mesa, California . . . . .	3
2 Fluted tube showing the Gregorig effect . . . . .	8
3 Production method used by Toshiba Metal Products Division, Tokoyo, Japan showing typical flute patterns . . . . .	14
4 Tube-rolling machine developed by Grob, Inc., Grafton, Wisconsin . . . . .	16
5 Design specifications for the manufacture of the E-tube . . . . .	17
6 Photomicrograph of a cross section of a carbon steel E-tube produced by Grob, Inc. . . . . .	17
7 Enhancement factors for condensing R-115 on E- and F-tubes compared with smooth tubes with no drainage skirts as functions of heat flux . . . . .	21
8 Enhancement factors for condensing R-113 on E- and F-tubes compared with smooth tubes with no drainage skirts as functions of heat flux . . . . .	22
9 Enhancement factors for condensing R-11 on E- and F-tubes compared with smooth tubes with no drainage skirts as functions of heat flux . . . . .	22
10 Enhancement factors for condensing various refrigerants on E-tubes as functions of heat flux . . . . .	23
11 Effect of length on condensation coefficients of R-11 on A- and F-tubes at heat fluxes from 9,450 to 28,000 W/m <sup>2</sup> (3,000 to 9,000 Btu/h·ft <sup>2</sup> ) . . . . .	25
12 Effect of length of F-tube on the condensing coefficients for various vapors at different heat fluxes . . . . .	25
13 ORNL 40-tube vertical-fluted-tube condenser tested at the East Mesa Geothermal Test Site . . . . .	26
14 ORNL 104-tube vertical-fluted-tube condenser tested at Raft River Geothermal Test Site . . . . .	27

<u>Figure</u>	<u>Page</u>
15 Comparison of tubeside heat transfer correlations in East Mesa condenser for turbulent flow as functions of flow rate at 300 K (80°F) . . . . .	35
16 Inundation correction factor for single smooth tube horizontal condensers as a function of the number of vertical rows . . . . .	37
17 Effect of air concentration on the condensing coefficient of steam . . . . .	39
18 Experimental shellside condensing coefficients obtained for E-tubes . . . . .	41
19 Overall heat transfer coefficient as a function of the condensing coefficient for the East Mesa condenser at a coolant flow rate of 0.22 m <sup>3</sup> /s (3500 gpm) . . . . .	43
20 Tubeside and shellside temperature distribution as a function of length for the East Mesa condenser . . . . .	46
21 Component shellside pressure drops in the East Mesa condenser . . . . .	52
22 Cross section of ORNL 5-MW vertical-fluted-tube condenser . . . . .	64
23 Detail showing condenser gas sample and vent tubes . . . . .	67
24 Tube bundle of ORNL 5-MW vertical-fluted-tube condenser . . . . .	68
25 Exterior view of ORNL 5-MW vertical-fluted-tube condenser showing header details . . . . .	69
26 Full-length exterior view of ORNL 5-MW vertical-fluted-tube condenser . . . . .	70
27 Tube vibration criteria diagram . . . . .	73
28 Acoustic resonance diagram . . . . .	76
29 Relative cost of saline resistant tube materials (March 15, 1981) . . . . .	82

LIST OF TABLES

<u>Table</u>	<u>Page</u>
1   Characteristics of A-, E-, and F-tubes . . . . .	20
2   Comparison of refrigerant properties at 311 K (100°F) . . . . .	20
3   Comparison of ORNL condensers tested at geothermal test facilities . . . . .	28
4   Heat load on East Mesa condenser using direct contact heat exchanger . . . . .	57
5   Tube requirements for East Mesa condenser . . . . .	58
6   Allocation of downcomers on baffles . . . . .	65
7   Natural frequencies in tube passes for 5-MW ORNL East Mesa condenser . . . . .	72



DESIGN AND ANALYSIS OF A 5-MW VERTICAL-FLUTED-TUBE  
CONDENSER FOR GEOTHERMAL APPLICATIONS

G. H. Llewellyn

ABSTRACT

This report covers the design and analysis done at the Oak Ridge National Laboratory of an industrial-sized vertical-fluted-tube condenser. The condenser is used to condense superheated isobutane vapor discharged from a power turbine in a geothermal test facility operated for the U.S. Department of Energy. The 5-MW condenser has 1150 coolant tubes in a four-pass configuration with a total heat transfer area of  $725 \text{ m}^2$  ( $7800 \text{ ft}^2$ ). The unit is being tested at the Geothermal Components Test Facility in the Imperial Valley of East Mesa, California. The condenser design is based on previous experimental research work done at the Oak Ridge National Laboratory on condensing refrigerants on a wide variety of single vertical tubes. Condensing film coefficients obtained on the high-performance vertical fluted tubes in condensing refrigerants are as much as seven times greater than those obtained with vertical smooth tubes that have the same diameter and length. The overall heat transfer performance expected from the fluted tube condenser is four to five times the heat transfer obtained from the identical units employing smooth tubes. Fluted tube condensers also have other direct applications in the Ocean Thermal Energy Conversion (OTEC) program in condensing ammonia, in the petroleum industry in condensing light hydrocarbons, and in the air conditioning and refrigeration industry in condensing fluorocarbon vapors.

1. INTRODUCTION

The U.S. Department of Energy (DOE), Division of Geothermal Energy, asked the Oak Ridge National Laboratory (ORNL) to design and evaluate a 5-MW ( $17 \times 10^6 \text{ Btu/h}$ ) vertical-fluted-tube condenser based on previous experimental work on condensing refrigerants on single fluted tubes.

To demonstrate the feasibility of obtaining energy from geothermal brine deposits, test facilities were developed in the western states. A test loop has been built at the Geothermal Component Test Facility (GCTF) at East Mesa, California, by Barber-Nichols Engineering Company of Arvada, Colorado. The work has been under the direction of Lawrence Berkeley Laboratories (LBL).

The facility loop that normally employs evaporative condensers for tubeside condensation of isobutane is being modified to provide a means of testing the ORNL condenser. The evaporative condensers will be used to provide cooling for the ORNL condenser.

The modified test loop, shown in Fig. 1, provides either a system for mixing liquid isobutane with hot brine in the direct-contact heat exchanger (DCHX) or a Supercritical Heat Exchanger Field Test (SHEFT) unit to produce superheated vapor that drives the turbine, thus producing power. The turbine discharges the superheated isobutane into the ORNL condenser, which desuperheats and condenses the isobutane vapor. The condensate is collected in a hot well where water (less than 2% by weight) carried over from the DCHX is separated from the immiscible isobutane. The condensate is then returned to the DCHX by a turbopump driven by the brine discharged from the DCHX. When using the SHEFT system, the brine does not come in contact with the working fluid. The turbogenerator delivers 0.5 MW of utilizable electric power.

The objectives of this report are to present the pertinent details of the design, analyses, operation, and anticipated performance of the condenser. Referenced background material is included for both the history and technical basis of the high performance of the fluted tubes.

Fluted tube condensers are normally designed to operate at low approach temperatures and low heat fluxes where the performance is the highest. The fluted tubes have a great potential for use in low-temperature-waste-heat-utilization systems that normally operate under these conditions. In a geothermal power plant, about two-thirds of the total equipment cost is attributed to heat exchange equipment where efficiency of the heat exchangers often determines the economic feasibility of the project. The most economic condenser is the unit that, regardless of its efficiency, will condense the most vapor per dollar of cost over the plant write-off period.

Articles by K. J. Bell<sup>1</sup> and Vehara Heuvo<sup>2</sup> shed some light on the state of the art of condenser technology, the current knowledge of heat transfer, and related phenomena involved in condensation and applicability of specific condenser types for various condensing conditions. Both of these papers cite the role of fluted tubes in condenser technology.

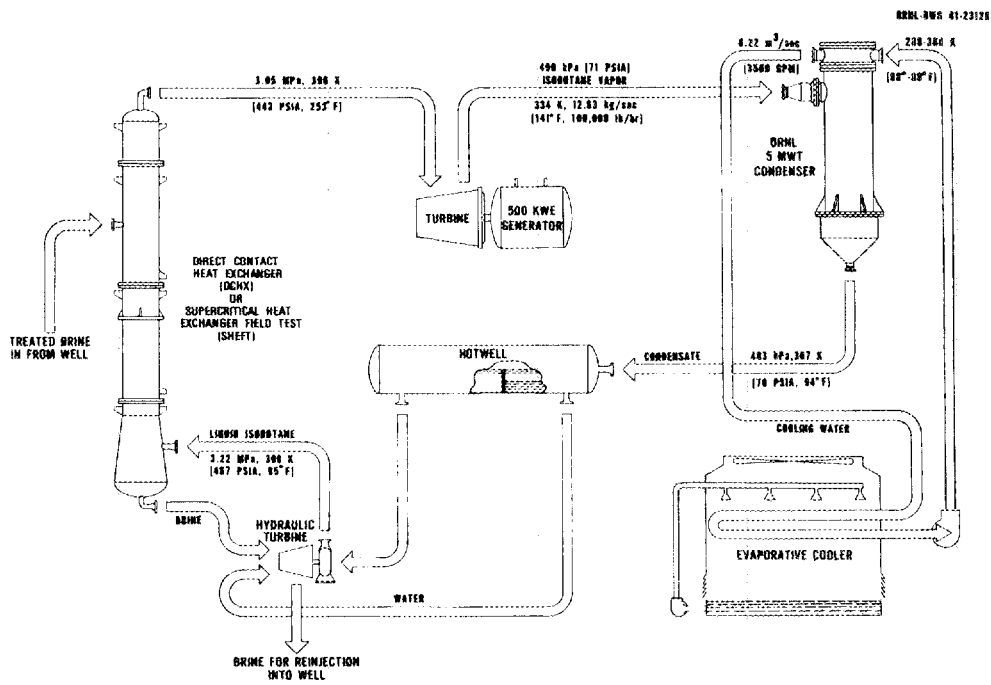


Fig. 1. Modifications to test loop at the Geothermal Components Test Facility at East Mesa, California.

Recent articles by Jerry Taborek of the Heat Transfer Research Institute (HTRI) concerning the state of the art in heat exchanger design<sup>3</sup> and in design techniques<sup>4</sup> were found to be excellent sources of information. These ideas were used to formulate a design for the ORNL condenser. The main points gleaned from review of these references is that:

1. Film condensation of multicomponent mixtures containing immiscibles and noncondensables involving vapor shear is a very complex problem. Even with the aid of the computer, it has been impossible to find nonproprietary methods expressing the relationships of all these variables.

2. The effect of noncondensables is not fully understood, particularly with vapor shear.
3. Too often, the failure of an exchanger is attributed to not using the "right" fouling factor rather than acceptance of the fact that an exchanger was poorly designed.

One objective in the design of this exchanger is to obtain the highest allowable tubeside and shellside velocities using average fouling conditions while transferring the specified heat load. The controlling factor on the thermal design of the condenser is the flow rate and pressure drop for the tubeside and shellside fluids. The mechanical design is controlled by the operating temperature and pressure and the pertinent code requirements.

## 2. SUMMARY

Over the past thirty years, many types of fluted surfaces have been developed for condensing steam, ammonia, hydrocarbons, and fluorocarbons; these surfaces can be custom designed for specific vapors. ORNL has done extensive testing in condensing refrigerants on a wide variety of fluted tubes.

Based on this testing, ORNL has become actively engaged in the design, procurement, and testing of vertical-fluted-tube condensers (VFTC) over a wide capacity range. Units containing 2, 40, 104, and 1150 tubes have been built to date, and a 2500 tube unit is currently being investigated. Carbon steel, aluminum, titanium, admiralty, cupronickels, and special saline-resistant stainless steel alloys have been used to fabricate the fluted tubes.

As a part of the DOE Waste Heat Rejection Program (AM Program), ORNL has developed, designed, and built a 1150-tube VFTC that will be tested and evaluated at the GCTF at East Mesa, California. This report is concerned with the details of the development and design of this 1150-tube unit. The U.S. Navy has recently indicated interest in VFTC application for steam turbine condensers, and the power industry in Japan is also investigating possible application. Incentives derived from ORNL experience using fluted tubes for shellside condensation can be summarized as follows where enhancements refer to comparison in condensing heat transfer coefficients obtained on vertical fluted tubes to those obtained on vertical smooth tubes.

- Commercial installations have reported enhancements in condensing heat transfer coefficients as high as 10 when condensing light hydrocarbons at high vapor velocities.
- The overall heat transfer from a vertical-fluted-tube condenser is expected to be 4 to 6 times that for a horizontal unit with the same total length of smooth tubes at lower vapor velocities. Additional performance can be gained by providing closer baffle spacing at the expense of higher cost and shellside pressure drop. The majority of this enhancement is attributed to the fluted tubes.

- Cost per unit length of fluted tubes is 1.25 to 4 times higher than for smooth tubes and depends on the tube material used. With mass production, it is conceivable that fluted tubes could be produced at a cost premium of less than 25%.
- The cost of a vertical condenser with carbon steel fluted tubes can be as much as 40% higher than a horizontal-smooth-tube unit but would transfer about 6 times the heat.
- Vertical-fluted-tube condensers can be built at 40 to 50% of the cost of horizontal-smooth-tube units having the same heat load.
- Custom-made flutes can be fabricated into standard-sized tubing using most commercially available malleable metal or metal alloys.

### 3. HISTORY OF FLUTED TUBES

The high performance of the fluted tubes employed on these exchangers is primarily due to the Gregorig effect, in which the surface tension forces move the condensate from the crest of the flute into the troughs where it drains by gravity (shown in Fig. 2).

In 1957, R. Gregorig<sup>5</sup> obtained increases in condensing coefficients of 2 to 8 times in condensing steam on vertical-fluted surfaces compared with vertical-smooth surfaces. Gregorig, however, did not present a formulation for design in this disclosure and left things rather vague as to optimization of the design surface.

R. L. Webb<sup>6</sup> of Pennsylvania State University recently developed a method of optimizing the Gregoric condensing surface but based his calculations on ideal conditions. Webb concluded from his studies that each condensable has an optimum flute pattern based on the physical properties of the condensate.

In 1965, T. C. Carnavos<sup>7</sup> reported obtaining condensing enhancements from 4.5 to 7. Alexander and Hoffman<sup>8</sup> in 1971 obtained enhancements in the overall heat transfer as high as 7 in condensing steam.

In 1968, D. G. Thomas<sup>9,10</sup> obtained condensing enhancement factors as high as 9 using loosely clamped wires and longitudinal fins attached to the tubes. As a result of his experiments, Thomas was convinced that higher enhancements could be obtained with properly designed, closely spaced fins than with sinusodial flutes.

Most of the previously mentioned experimental work on single-fluted tubes has been done in condensing steam on the exterior surface of the tube. Recent surveys of data on single-phase heat transfer experiments in condensing ammonia on vertical fluted tubes have been made by A. E. Bergles and M. K. Jensen<sup>11</sup> and were directed toward Ocean Thermal Energy Conversion (OTEC) application. S. K. Combs of ORNL has done experimental work in condensing ammonia on the exterior surface of both vertical<sup>12</sup> and inclined<sup>13</sup> fluted tubes.

Panchal and Bell<sup>14</sup> have analyzed isothermal flow and gravity-controlled flow on vertical fluted surfaces for Nusselt-type condensation

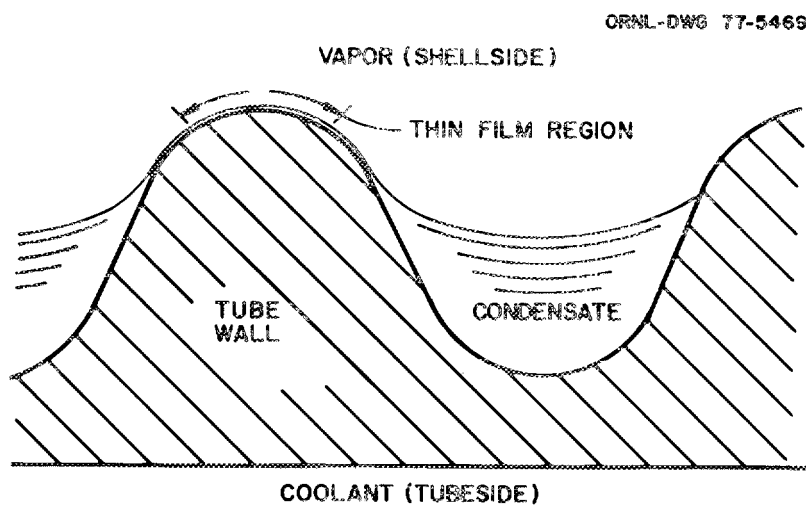


Fig. 2. Fluted tube showing the Gregorig effect.

and presented a method of predicting a flooding Reynolds number. This article also relates the pitch and amplitude of the flutes to the Nusselt number and correlates these analytical predictions with experimental data.

Optimizations of condensing performance on vertical fluted surfaces have been determined by Y. Mori and K. Hijikati from the Tokyo Institute of Technology and by Hirasawa and W. Nakayamo of Hitachi Ltd.<sup>15</sup> These researchers used R-113 to check analytical predictions of condensation rates with fin shape, tube length, and pitch. This paper shows a definite preference for the flat-bottom, grooved fin that provides significantly larger drainage area for the condensate. The paper reinforces the author's thoughts and those of D. G. Thomas at ORNL. This type of fin, which resembles a gear shape and has come to be known as the E-tube at ORNL, has produced superior results on condensing isobutane (R-600a).

It is thought possible that this design might be optimized even further with additional experimental work.

The factors that determine the lineal condensation rate on a vertical fluted tube at given vapor and coolant conditions are summarized:

- condensate properties,
- flute configuration,
- baffle spacing,
- vapor contaminants (oil, water, noncondensables),
- tubeside fouling,
- shellside fouling, and
- tube material.

In horizontal condensers, as the number of the tube rows is increased, the condensate is successively dumped on the lower row of tubes causing a thicker condensate film to build up, consequently increasing the thermal resistance. This phenomenon is known as inundation. Carryover called "rain" associated with a vertical tube bundle is present, but it does not exhibit the pronounced reduction in heat transfer observed in horizontal units. The flutes curtail striping of the condensate from the tubes and reduce the amount of rain generated in vertical units. The ratio of shellside condensing heat transfer coefficients for a single smooth horizontal tube to an equal length ( $L$ ) smooth vertical tube is  $0.77 (L/D)^{1/4}$ , where  $D$  is the tube diameter. The ratio of condensing coefficients ranges from 1.5 to 2.5 for commercial-sized condensers.

Inundation can reduce the total condensation rate on horizontal units by factors up to one-third depending on whose correlation is being used, the noncondensable, the velocities involved, and the gas being condensed.

The question of the economic feasibility of maintaining short condensation lengths by rolling each tube into each baffle and tube supports with extension rollers still remains to be determined. The cost is about \$2 per roll, and the feasibility involves the risk of overexpanding the tube and the cost of having to plug the tube if it is ruptured in the process of expanding it.

If all these factors are taken into account and the designs compared, a vertical-fluted-tube condenser requiring 18300 m (60K ft) of 1.0-in.-diam tubing could conceivably replace a horizontal smooth tube unit requiring 91,400 m (300K ft) of 1.0-in.-diam tubing considering equal fouling on both units.

#### 4. INDUSTRIAL APPLICATIONS

Union Carbide Corporation has commercially fabricated hundreds of vertical-fluted-tube condensers through development work by C. F. Gottzmann and P. S. O'Neill of the Linde Division, Tonawanda, N. Y., and P. E. Minton of the Plastics Division, South Charleston, W. Va.<sup>16</sup>

The high performance condensers utilize fluted surfaces on the shellside for condensing hydrocarbon vapors and employ a patented Linde porous metallic surface to promote nucleate boiling on the inside of the tubes. These units have been used commercially to condense ethane and butane on the shellside while boiling propylene on the tubeside surface, which results in enhancement factors in the overall heat transfer as high as five.

Linde Division has designed most of their "UC-High Flux" exchangers with an approach temperature of 2.8K (5°F),<sup>17</sup> although approach temperatures as low as 1.1K (2°F) have been used. The UC exchangers also operate with pressure drops as high as 2 MPa (300 psi) with correspondingly high vapor velocities. Actual overall coefficients as high as 3400 W/m<sup>2</sup>·K (600 Btu/h·ft<sup>2</sup>·°F) have been obtained<sup>18</sup> in condensing hydrocarbons with estimated condensing film coefficient as high as 5675 W/m<sup>2</sup>·K (1000 Btu/h·ft<sup>2</sup>·°F).



## 5. FLUTED TUBE MANUFACTURE

Currently there are only a few fabricators in the world interested in or actively engaged in the production of fluted tubes. There are several factors to consider in selecting a design for fluted tubes. Designs are enhanced by employing short tube lengths that call for sealing the tube at each baffle. If the tubes are to be rolled into the baffles, skips must be provided in the fluting, a procedure that is practically impossible to accomplish during a drawing operation. If glue or a braze is used to make this seal, there is the problem of excess material running down the flute and plugging it. Grommets were considered, but the number involved on large exchangers (1000 tubes or more) make one look for more expeditious means. Plastic baffles with O-ring seals were seriously considered but dropped when development costs were considered. Another conceivable method of attachment is to partially melt or deform plastic baffles to obtain the seal by heating the tubes to the melting point of the plastic.

Extruding the tubes through a dye requires controlling the tolerance to less than 0.025 mm (1 mil) and controlling the length of the draw. The extrusion also requires the ability to draw certain materials. Copper, copper-base alloys, and aluminum can readily be used for this purpose. A disadvantage of drawing tubes is that the tube has to be "defluted" on the ends to roll it into the tubesheet.

There are companies in North America that can furnish continuously drawn fluted tubing to specification in lengths up to 6 m (20 ft). These include the Teledyne Tubular Products Corporation, the Noranda Tubing Company, and Southwest Alloys. Noranda can furnish tubing with flutes on either or both the inside or outside in either straight or spiral configurations.

Yorkshire Industries, Ltd., of Leeds, England, can furnish skips but only two pitch-spacing options are available for fluting configurations. Maximum enhancements in overall heat transfer of no better than two are expected from these tubes in condensing steam at a cost of about 20% higher than for smooth tubes. The corrugated tubes are available

in copper, bronzes, brasses, aluminum brass, and copper-nickel. Lengths up to 18 m (60 ft) can be obtained.

Toshiba Metal Products of Tokyo, Japan, produces fluted tubes in titanium by rolling flat plate with the desired fluting configuration, bending the plate around a mandril, and seam welding the tube parallel to the axis (Fig. 3). The cost of titanium fluted tubing was about \$26/m (\$8/ft); change of material to carbon steel did not significantly reduce the cost. Toshiba built and supplied condensers for the Sunshine Geothermal Project at Sapporo, Japan.

Grob, Inc., of Grafton, Wisconsin, was the only company that could flute the tubes for the East Mesa condenser at a reasonable cost \$4.92/m (\$1.50/ft) within specification. The work done by Grob using a rolling operation was precise and of excellent quality. The Grob method is suitable for rolling even or odd numbers of uniform teeth spaced on a cylindrical blank.

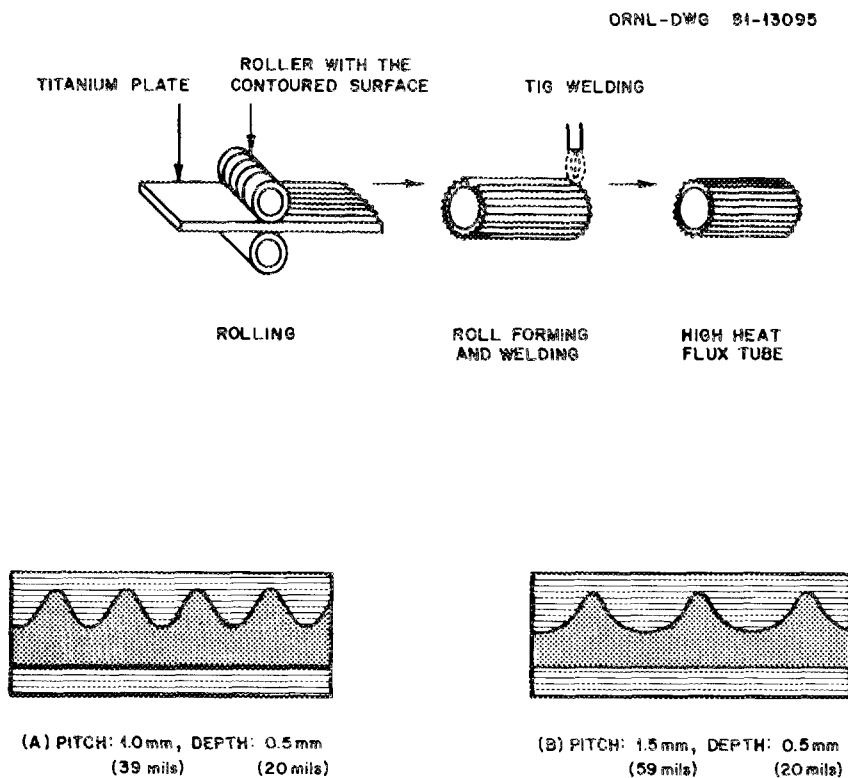


Fig. 3. Production method used by Toshiba Metal Products Division, Tokoyo, Japan showing typical flute paterns.

According to Grob, any ductile material can be rolled. The tubes must be uniform in ductility and cross section to produce an accurate form. Work hardening depends on material composition, the hardness before rolling, the tooth depth, and the feed rate. Some material work hardens so fast that it is impossible to form a deep tooth.

The Grob rolling machine is shown in Fig. 4. The figure shows a rod being fluted, but a tube can be fabricated in the same manner depending on the wall thickness. One or more pair of planetary rollers penetrate a tubular blank for a short part of their cycle. The rollers then leave the blank for the rest of the cycle, during which time the blank indexes. A new roller contact is then made. The blank is continuously longitudinally advanced. The rollers have the exact negative shapes in the contact area as the finished blank has. Each flute pattern requires a different set of rollers. Tubes having thin walls can be reinforced with mandrels that have to be extracted after the fluting operation at additional cost. The work input into the process depends on the amount of metal that is moved. The minimum tube-wall thickness that Grob recommends is governed by the strength of the tubing and the fin depth. Grob used 25-mm- (1.0-in.)-outside diameter by 1.65-mm- (65-mil)-wall low-carbon steel tubing for producing fluted tubes for the East Mesa Condenser. These tubes (Fig. 5) have an outside diameter of 25.6 mm (1.01 in.) and an inside diameter of 22 mm (0.862 in.).

At present, Grob offers no quantity discounts and bases the cost per lineal foot on the metal moved during the fluting operation, which can be related to the number and size of the flutes.

A photomicrograph of a cross section of a carbon steel fluted tube rolled by Grob is shown in Fig. 6. This figure will give the reader some idea of the precision involved. There is speculation that there are German companies that produce fluted tubes on special order, but as yet they have not been located.

ORNL-Photo 3340-81

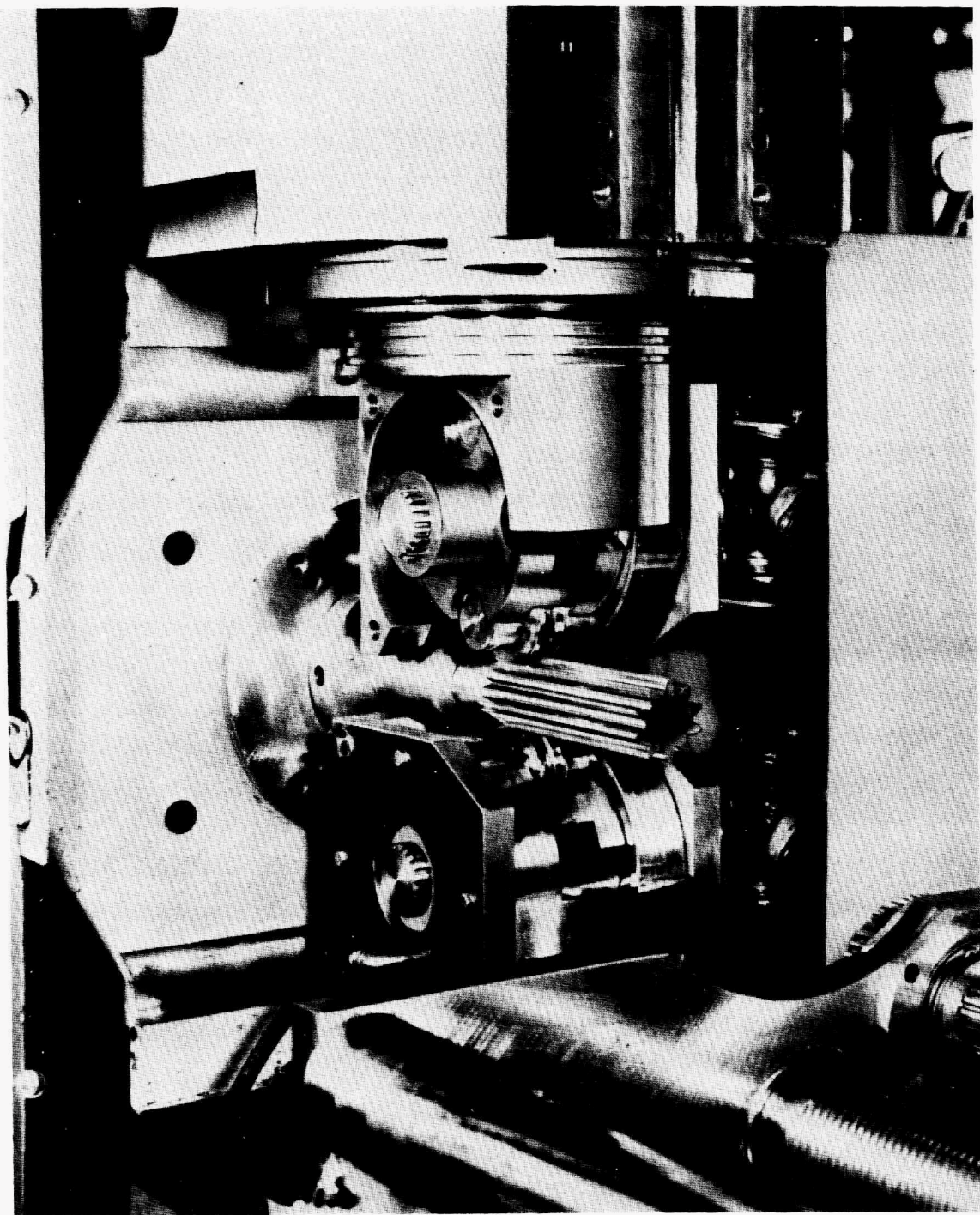


Fig. 4. Tube-rolling machine developed by Grob, Inc., Grafton, Wisconsin.

ORNL-DWG 81-13093

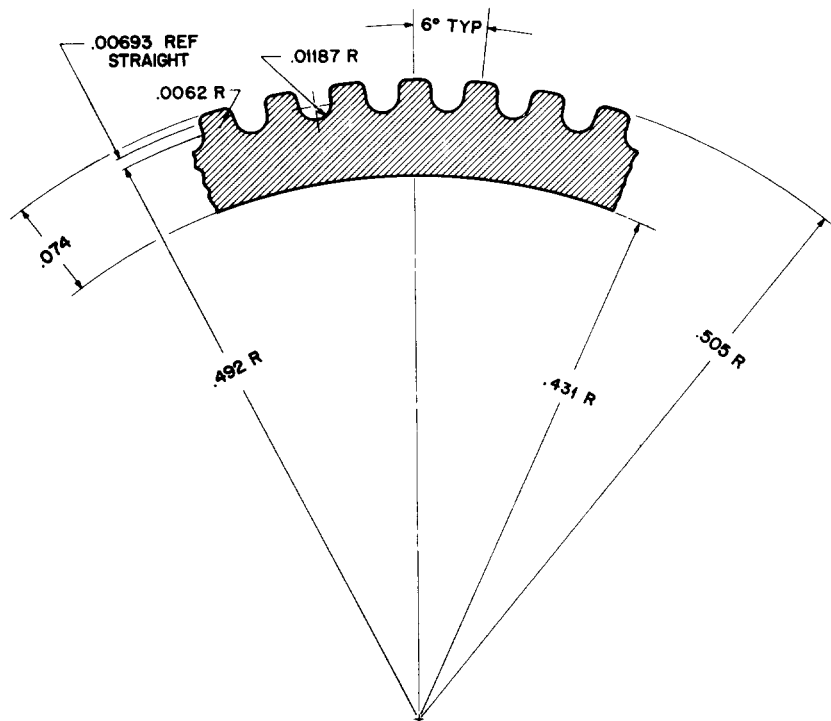


Fig. 5. Design specifications for the manufacture of the E-tube.

ORNL-DWG 81-15255

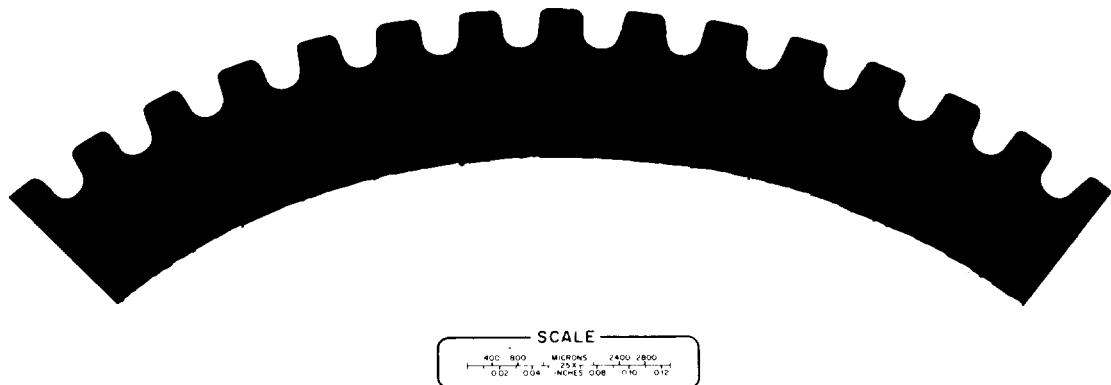


Fig. 6. Photomicrograph of a cross section of a carbon steel E-tube produced by Grob, Inc.



## 6. EXPERIMENTAL WORK AT ORNL

Recent experiments at ORNL by S. K. Combs, G. S. Mailen and R. W. Murphy<sup>19</sup> in condensing refrigerants on a variety of vertical 25-mm (1.0-in.) diam fluted tubes have provided enough data to make optimizations and predictions of heat transfer. They used Wilson plots to establish the condensing film coefficient on the tube wall as a function of the heat flux.

Combs et al made tests on a variety of external surfaces on 25-mm diam tubes having heat transfer areas up to 3.2 times (J-tube) the area of the smooth tube of equal length. R-11, R-21, R-22, R-113, R-114, R-115, and R-600a (isobutane) refrigerants were condensed on the tubes by them to obtain the experimental data. From this data it was concluded that the most promising tube was the aluminum E-tube, which provided more condensate per unit length than any of the others for condensing isobutane.

A comparison of the characteristics of the standard A-tube, the gear-shaped E-tube, and the flute-shaped F-tube are shown in Table 1. It will be noted that the ratio of internal to external heat transfer area is the greatest for the E-tube. Table 2 shows the pertinent properties of each of the refrigerants.

The test by Combs et al did not include condensing each of the refrigerants on all of the tubes. Additional data were provided on the F-tube in condensing R-11 on tubes with drainage skirts spaced at 0.15, 0.30, 0.61, 1.22 m (6, 12, 24, and 48 in.). To try to correlate this data, enhancement factors were calculated comparing condensing film coefficients for the fluted tubes with the condensing film coefficients for a smooth vertical tube. These comparisons were made for various heat fluxes.

Figure 7 shows the enhancement factors as a function of heat flux in condensing R-115 with various skirt spacings for the F-tube compared with a 1.22-m E-tube with no skirts. At low heat fluxes [around 6300 W/m<sup>2</sup> (2000 Btu/h·ft<sup>2</sup>)], it will be noted that the E-tube with skirts spaced 1.22 m apart has about the same enhancement as the F-tube with skirts spaced 0.15 m apart. The maximum enhancement obtained with

Table 1. Characteristics of A-, E-, and F-tubes

Tube type	Configuration	Flute diameter		Inside diameter		External area		Ratio $A_o/A_i$	Number of flutes
		cm	in.	cm	in.	$m^2/m$	$ft^2/ft$		
A	Smooth	2.540	1.000	2.261	0.870	0.0243	0.2618	1.1494	0
B	Gear	2.565	1.010	2.189	0.862	0.0391	0.4208	1.8647	60
F	Sine wave	2.540	1.000	2.286	0.900	0.0258	0.2775	1.1777	48

Table 2. Comparison of refrigerant properties at 311 K (100°F)

Property	Units	R-11	R-21	R-22	R-113	R-114	R-115	R-600a	R-717	H <sub>2</sub> O
Saturation pressure	psia MPa	23.46 0.1618	40.04 0.2761	210.6 1.452	10.48 0.073	45.85 0.3161	182.73 1.260	72.04 0.4967	212.0 1.461	0.95 0.007
Thermal conductivity	Btu/h·ft·°F W/m·K	0.049 0.084	0.056 0.097	0.047 0.082	0.042 0.073	0.035 0.061	0.027 0.046	0.059 0.102	0.261 0.452	0.363 0.628
Dynamic viscosity	lb/ft·h Pa·s × 10 <sup>4</sup>	0.894 3.700	0.690 2.840	0.440 1.840	1.380 5.700	0.710 2.900	0.400 1.650	0.350 1.450	0.300 1.230	1.580 6.530
Density	lb/ft <sup>3</sup> kg/m <sup>3</sup>	90.20 1445.0	83.40 1335.0	71.20 1141.0	95.80 1534.0	88.40 1416.0	76.00 1217.0	33.40 535.0	36.40 583.1	62.00 993.2
Heat of vaporization	Btu/lb J/kg × 10 <sup>-5</sup>	75.20 1.749	95.10 2.211	72.80 1.693	64.50 1.498	52.90 1.230	35.60 0.832	133.1 3.094	477.8 11.10	1037.0 24.10
Heat capacity	Btu/lb·°F J/(kg·K)	0.210 895.0	0.260 1090.0	0.310 1310.0	0.230 971.0	0.250 1040.0	0.300 1259.0	0.630 2623.0	1.160 4845.0	1.000 4175.0
Surface tension	lb/ft N/m	0.00114 0.0167	0.00112 0.0163	0.00044 0.0065	0.00117 0.0171	0.00072 0.0171	0.00026 0.0105	0.00057 0.0084	0.00120 0.0175	0.00480 0.0699
Cost	US \$/lb US \$/kg	0.470 1.034	0.540 1.188	0.870 1.914	0.720 1.584	0.810 1.782	0.750 3.850	1.000 2.200	0.250 0.550	0.010 0.022

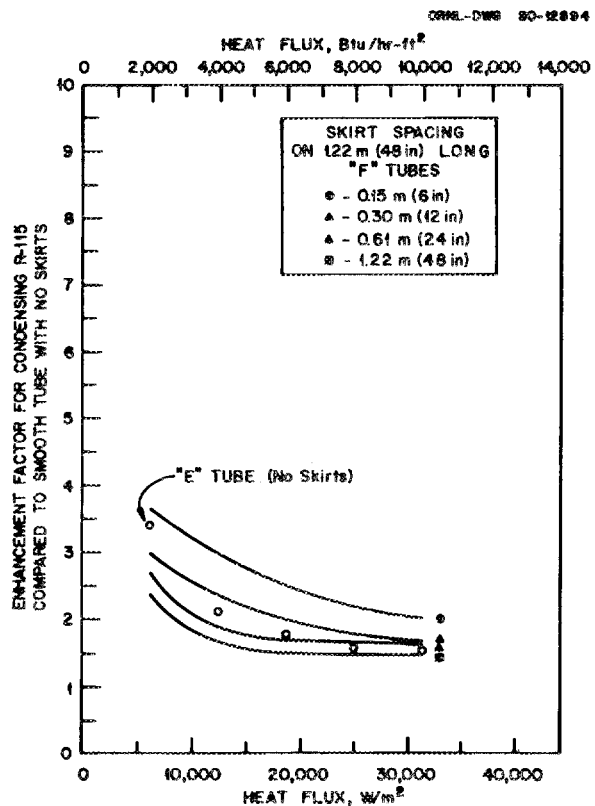


Fig. 7. Enhancement factors for condensing R-115 on E- and F-tubes compared with smooth tubes with no drainage skirts as functions of heat flux.

R-115 is about 3.75. The skirt spacing with R-115 seems more effective at low heat fluxes with an increase in enhancement of about 1.6; at high fluxes the increase is reduced to 1.3.

Figure 8 shows the same relationships when condensing R-113 refrigerant where the maximum enhancement is 6.75 with the 0.15-m skirt spacing on the F-tubes. An E-tube with skirt spaced at 1.22-m intervals could achieve about the same enhancement as the F-tubes with 0.15-m spacing. The enhancement in the condensing film coefficient is increased by a factor of 1.5 at low fluxes to 2.7 at the high fluxes by reducing the skirt spacing from 1.22 m to 0.15 m.

Figure 9 shows the relationships when condensing R-11 vapor, which yields enhancement factors as high as 8.0 by using 0.15-m skirt spacing. The effect of skirt spacing is not quite as sensitive here, with the

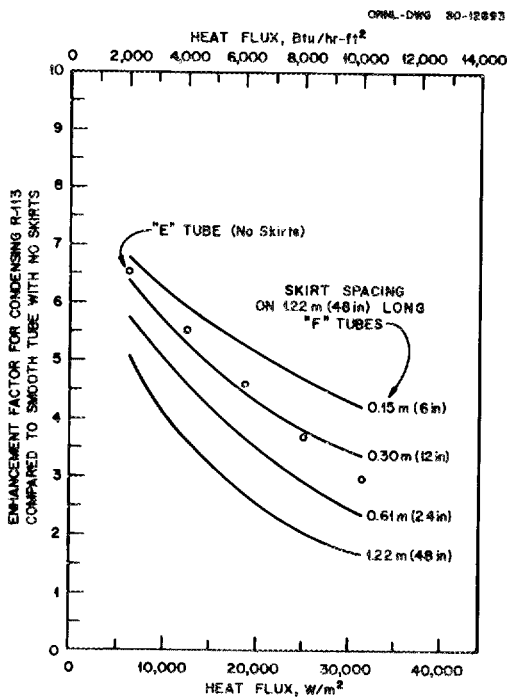


Fig. 8. Enhancement factors for condensing R-113 on E- and F-tubes compared with smooth tubes with no drainage skirts as functions of heat flux.

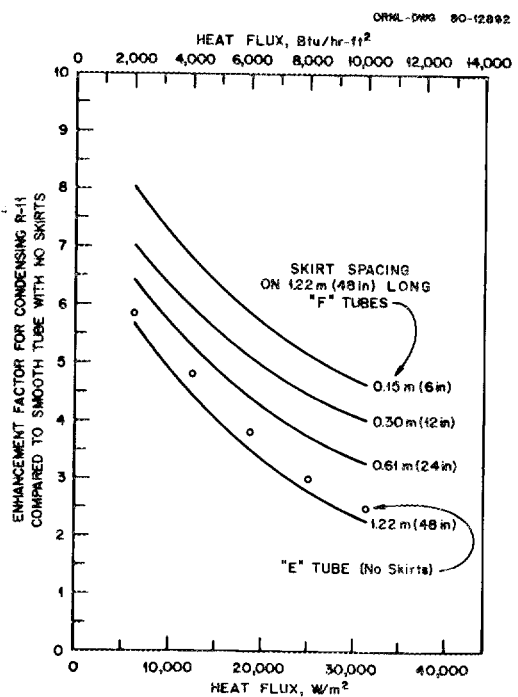


Fig. 9. Enhancement factors for condensing R-11 on E- and F-tubes with smooth tubes with no drainage skirts as functions of heat flux.

increase ranging from 1.43 to 2.11 when decreasing the skirt spacing from 1.22 m to 0.15 m. The E-tube with 1.22-m skirt spacing produces about the same enhancement as the F-tube with the same spacing.

Figure 10 shows the relative enhancement in condensing various refrigerants on E-tubes with 1.22-m (48-in.) skirt spacings. The fluorocarbon exhibiting the most similar enhancement to isobutane vapor (R-600A) is R-11. It is quite difficult to obtain permission from the ORNL fire marshall to test hydrocarbons in the laboratory testing facility, which is the main reason why so few runs were made with isobutane. Referring to R-11, it would seem that 20% enhancements might be expected at low heat fluxes using skirt spacings of 0.61 m and 30% increases with spacings of 0.3 m. No allowances for this increase have been considered in this design (see Sect. 7.3).

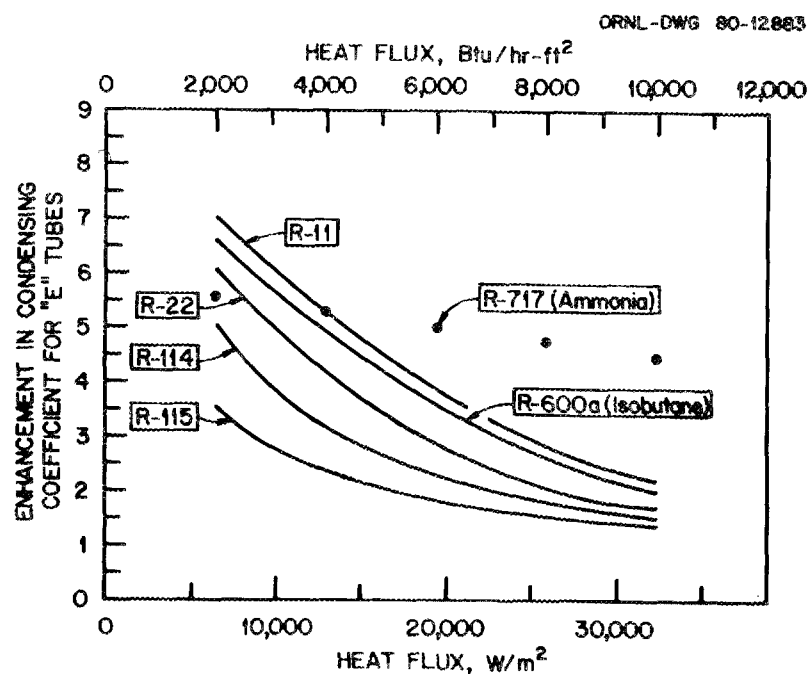


Fig. 10. Enhancement factors for condensing various refrigerants on E-tubes as functions of heat flux.

Figure 11 shows the condensing heat transfer coefficient as a function of effective tube length for several tube types for high and low heat fluxes as given in Ref. 20. Several trends can be seen from this figure. It appears that increases in effective tube length reduce the condensing heat transfer coefficient more drastically, particularly at low fluxes, for the smooth tube than it does for an equal length increase in the fluted tubes. The condensing coefficients in most cases seem to be reduced more at high heat fluxes than at low heat fluxes for fluted tubes.

Figure 12 shows the effect of tube length on the condensing coefficients on an F-tube for several selected refrigerants. It can be seen that the length has practically no effect at low heat fluxes of  $9500 \text{ W/m}^2$  ( $3000 \text{ Btu/h}\cdot\text{ft}^2$ ) when condensing ammonia (R-717) and only a slight effect at high heat fluxes of  $28,000 \text{ W/m}^2$  ( $9000 \text{ Btu/h}\cdot\text{ft}^2$ ). From review of all of the relationships pertaining to the effect of condensation length on enhancement at low fluxes, it might generally be said that increasing tube length from 0.15 m (6 in.) to 1.22 m (48 in.) roughly decreases the condensing heat transfer coefficient by as much as 15%. The net result of decreasing the tube length from 1.22 m to 0.3 m (12 in.) results in increasing the total heat transfer by 5 to 10%. Conversely, increasing the length from 1.22 m (4 ft) to 4.88 m (16 ft) could conceivably decrease the overall heat transfer by a similar amount.

Before the design of the 1150-tube unit, a  $4.2-\text{m}^2$  (45-ft $^2$ ) 40-tube condenser was designed and tested by ORNL at the East Mesa facility.<sup>21</sup> The 40-tube condenser shown in Fig. 13 contains aluminum F-type fluted tubes. The 25-mm (1.0 in.) F-tube has 48 flutes on the outside that resemble a sine wave having amplitudes of about 0.25 mm (10 mils). The field test results of the 40-tube condenser indicated an overall heat transfer of less than one-fourth of the anticipated values for the larger East Mesa condenser currently being investigated.

Tests were also made on a 104-vertical-fluted-tube condenser shown in Fig. 14 that was tested at the Geothermal Test Facility located at Raft River, Idaho. A separate report is being prepared on the testing of this condenser, which performed considerably better than the 40-tube unit tested at East Mesa. It will be noted that the 104-tube unit has

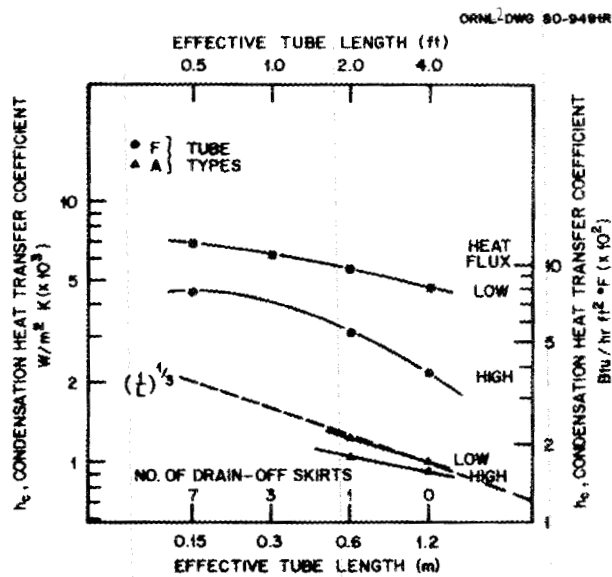


Fig. 11. Effect of length on condensation coefficients of R-11 on F- and A-tubes at heat fluxes from 9450 to 28,000 W/m<sup>2</sup> (3000 to 9000 Btu/h·ft<sup>2</sup>).

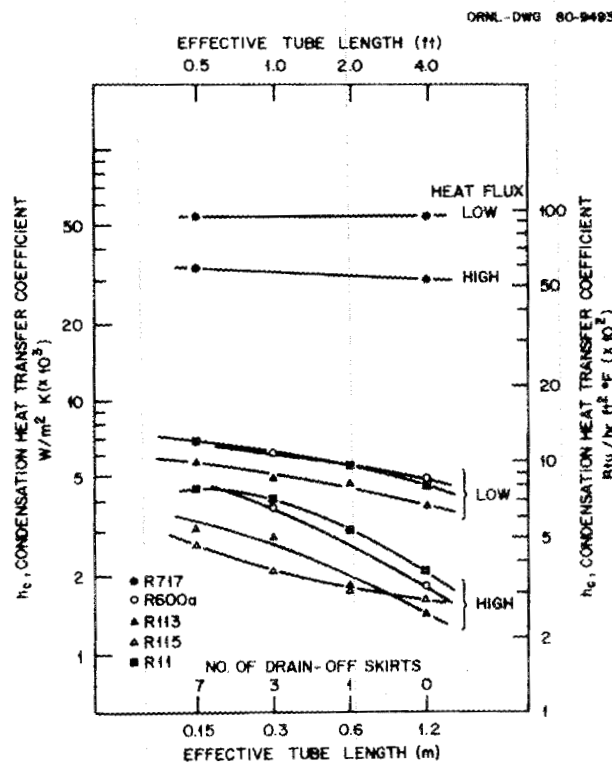


Fig. 12. Effect of length of F-tube on the condensing coefficient for various vapors at different heat fluxes.

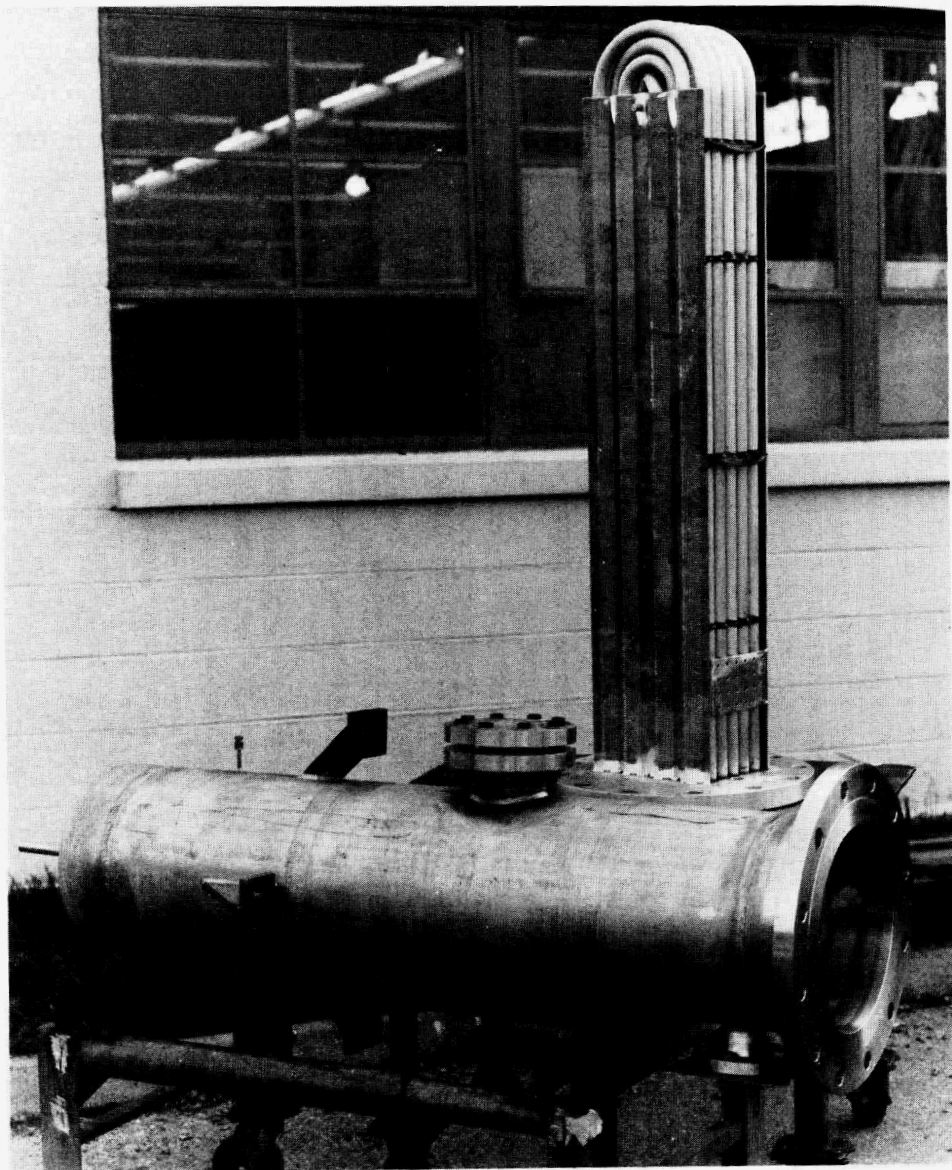


Fig. 13. ORNL 40-tube vertical-fluted-tube condenser tested at the East Mesa Geothermal Test Site.

the vapor supply located at the base of the condenser. Table 3 shows the pertinent design and operating parameters and compares the performance of two ORNL condensers tested to date with the 1150-tube condenser being tested at East Mesa.

ORNL-DWG 80-10760R

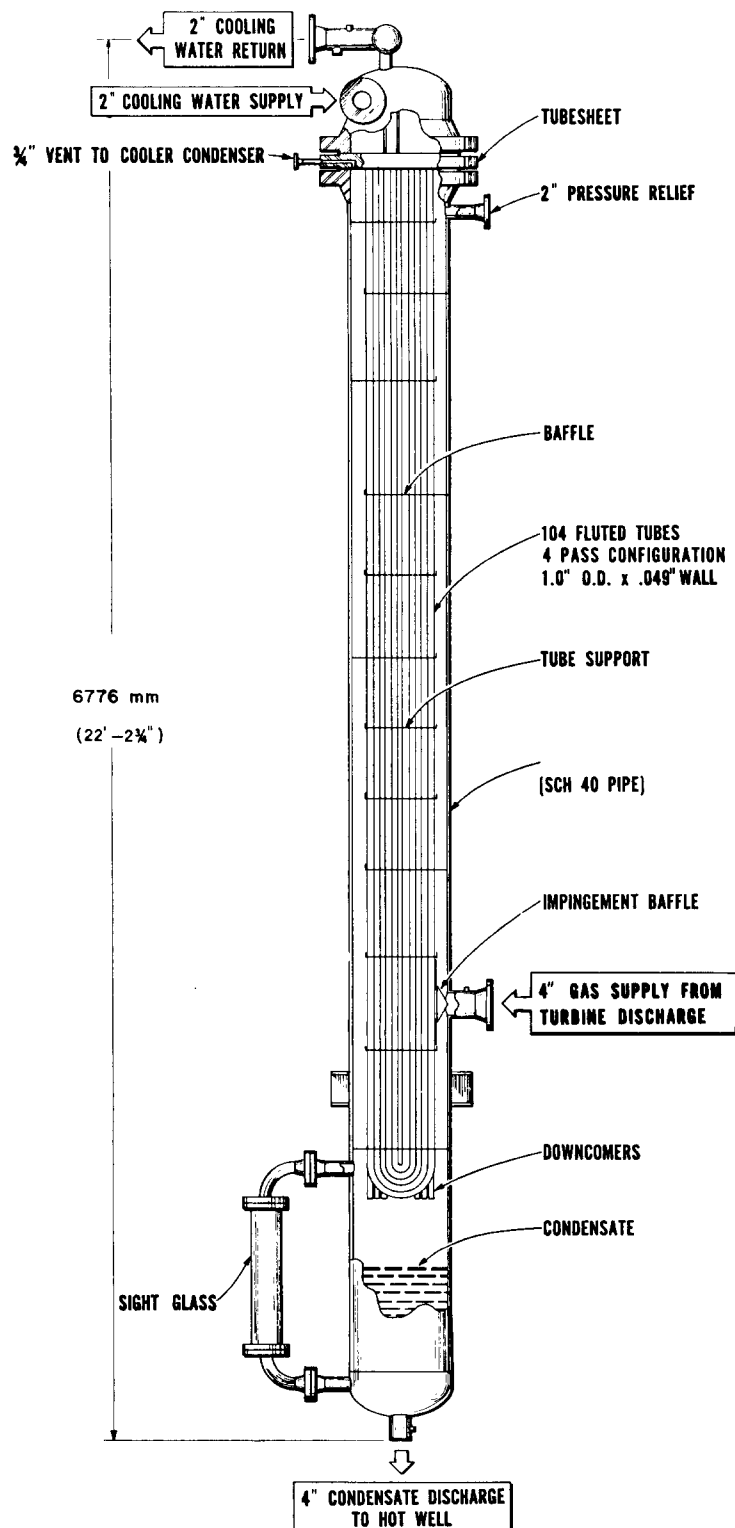


Fig. 14. ORNL 104-tube vertical-fluted tube condenser tested at the Raft River Geothermal Test Site.

Table 3. Comparison of ORNL condensers tested at geothermal test facilities

	Units	40-tube condenser	104-tube condenser	1150-tube condenser
Test facility		East Mesa, Calif.	Raft River, Idaho	East Mesa, Calif.
Heat transferred	MW(t) Btu/h	0.0586 200,000	0.5 1,706,500	5.0 17,065,000
Heat transfer area <sup>a</sup>	m <sup>2</sup> ft <sup>2</sup>	4.46 48	52.6 566	688 7400
Heat flux	W/m <sup>2</sup> Btu/h·ft <sup>2</sup>	13,134 4167	9471 3005	7269 2306
LMTD	K °F	22-28 40-50	4.26 7.66	4.6 8.2
Overall U	W/m <sup>2</sup> ·K Btu/h·ft <sup>2</sup> ·°F	450-600 80-105	2205 392	1700-2800 300-500 (predicted)
Water flow rate	m <sup>3</sup> /s gpm	0.006 90	0.019 300	0.221 3500
Water velocity	m/s ft/s	1.38 4.54	1.98 6.5	2.04 6.70
Vapor flow rate	kg/s lb/h	0.190 1500	1.65 13,000	12.63 100,000
Vapor velocity	m/s ft/s	0.806 2.65 (maximum)	1.83 6.0	3.05 10.0
Tube material		Aluminum	Admiralty	Carbon steel
Tube type		F	E	E
Baffle material		Rubber	Carbon steel	Carbon steel
Baffle attachment		Glued	Rolled	Rolled
Downcommers		None	6	38
Shrouds		Yes	Yes	Yes
Water vapor		Yes (amount?)	Yes	1.37 wt %
Noncondensibles		CO <sub>2</sub> (amount?)	N <sub>2</sub> (amount?)	CO <sub>2</sub> 0.16 wt %

<sup>a</sup>Discounts plugged tube (2 at Raft River and 12 at East Mesa).

The values quoted on the smaller units are those involving the highest overall heat transfer coefficients in a direct-contact binary cycle. For complete details on the testing of these units, the reader is referred to forthcoming reports on the individual tests.

There are several differences in these condensers that are worth mentioning. The noncondensable gas at East Mesa is carbon dioxide, while at Raft River it is nitrogen. The 1150-tube unit contains the more efficient E-tubes having 60 flutes, about 1.5 times the coolant velocity of the 40-tube unit. The 1150-tube unit maintains a fairly constant vapor velocity on the shellside, which is about twice the maximum velocity as obtained in the 40-tube unit. The baffles in the 40-tube unit were fabricated from 0.38-mm (15-mil) resilient rubber, whereas the baffles of the larger unit are fabricated from 9.5-mm (3/8-in.)-thick carbon steel plates into which the tubes are rolled. The latter arrangement provides a more stable flow path for the vapor and promotes more predictable uniform velocities.



## 7. HEAT TRANSFER CALCULATIONS

The heat transfer calculations for the condenser involve the physical properties of the liquid and vapor phases of the shellside fluid, the physical properties of the liquid phase of the tubeside fluid, and the thermodynamic properties of the shellside fluid. The total heat transfer is obtained by calculation of the tubeside heat transfer coefficient, and estimation of the tubeside and shellside fouling factors. The design area of the condenser is obtained from a combination of experimental and calculated data (along with some educated guesses). The heat transfer and pressure drop relationships have been correlated and computerized using a Gibbs-type phase rule for selecting the equations and variables for sizing the condenser.

### 7.1 Properties of Liquid and Vapor Streams

The determination of the heat content of the vapor streams can present problems in evaluating the condenser performance. The actual vapor composition might contain several light hydrocarbons, water, and some noncondensable gases.

The Benedict-Webb-Rubin (BWR), Hans-Starling (HS), Redlich-Kwong (RK) and Peng-Robinson (PR) equations of state are all popular contenders for accurate means of determining the thermodynamic properties of hydrocarbon vapors. N. A. Samurin and J. R. Shields<sup>22</sup> of the Elliott Company have compared the BWR, PR, and HS equations with General Electric's Mark V proprietary computer code. The HS correlation was found to predict lower saturation temperatures at pressures below 500 psia, and as much as 5% difference was noted in the saturation temperature at 50 psia.

The HS equations were used by the system designers of East Mesa for evaluating the thermodynamic properties of gases for the 500-kW(e) system now operational at the geothermal test site. Thermodynamic properties of light hydrocarbons and gases using the Starling-Benedict-Webb-Rubin correlation were compiled and computerized by K. E. Starling.<sup>23</sup> Because of its polarity, water was not included.

The desired analytical scheme is to evaluate the vapor-liquid equilibrium constants from the fugacities and ultimately to predict a bubble point and dew point as a function of pressure (and location) in the exchanger. The situation is further complicated for a mixed hydrocarbon vapor containing both immiscibles and noncondensables.

D. H. Riemer et al.<sup>24</sup> of the University of Utah have also compiled a program using the Starling-Benedict-Webb-Rubin correlation to evaluate the pure component thermodynamic properties of 12 light hydrocarbons. Eventually, we would like to use Starlings computerized data that have been expanded to allow for water composition as a subroutine for obtaining thermodynamic properties of the mixtures.

Physical and thermodynamic property data for isobutane over the pertinent temperature and pressure range are shown in Appendix B. These data were obtained from the American Institute of Petroleum Engineers (API) Data Book<sup>25</sup>. Figures B.1 through Fig. B.3 show the latent heat, vapor pressure, and specific heat as functions of temperature. Figure B.4 shows the enthalpy as a function of both temperature and pressure. Figure B.5 shows the solubility of both propane and isobutane in water as functions of temperature, and Fig. B.6 shows the solubility of both propane and isobutane as functions of temperature. Appendix C shows the physical properties of water used in the tubeside heat transfer correlations tabulated over the appropriate temperature range. These data can be used for making quick checks on the correlations employed in the design.

## 7.2 Tubeside Heat Transfer Coefficient

The condenser design is based on the availability of 0.22 m<sup>3</sup>/s (3500 gpm) of cooling water supplied at temperatures ranging from 282 to 300K (50 to 80°F). A tubeside velocity 0.09 m/s (0.3 ft/s) in the E-tubes is sufficient to produce turbulent flow with a resulting tubeside heat transfer coefficient of about 570 W/m<sup>2</sup>·K (100 Btu/h·ft<sup>2</sup>·°F), but it takes a velocity of 2.7 m<sup>3</sup>/s (8.9 ft/s) to obtain a heat transfer coefficient of 9080 W/m<sup>2</sup>·K (1600 Btu/h·ft<sup>2</sup>·°F) based on the Dittus-Boelter correlation.

According to Kays and Perkins,<sup>26</sup> the most applicable equations for calculating turbulent flow inside smooth tubes are the Dittus-Boelter, Colburn, and the Sieder-Tate correlations.

The Dittus-Boelter correlation shown in Eq. (1) defines the Nusselt number, Nu, for heating fluids in circular tubes and is recommended when there is less than a 5.6K (10°F) drop across the water film:

$$\text{Nu} = 0.023 \text{ Re}^{0.8} \text{ Pr}^{0.4} = h \cdot D / k \quad (1)$$

Equation (1) is based on extensive experimental data covering ranges in Reynold numbers from 10,000 to 120,000, Prandtl numbers from 0.7 to 120, and for L/D ratios greater than 60. The Reynolds number in the final condenser design is about 45,000, the Prandtl is about 6.8, and the L/D ratio is over 225. The physical properties used in Eq. (1) are to be evaluated at the mean bulk-fluid temperature. The Colburn correlation defines the Nusselt number for both heating and cooling of fluids in circular tubes as shown in Eq. (2)

$$\text{Nu} = 0.023 \text{ Re}^{0.8} \text{ Pr}^{1/3} = St \cdot Pr \cdot Re = h \cdot D / k \quad (2)$$

and extends the correlation to include the j-factor defined in several ways in Eq. (3):

$$j = St \cdot Pr^{2/3} = 0.023 \text{ Re}^{-0.2} = f/8 \quad (3)$$

In the Colburn correlation, it is recommended that the physical properties be evaluated at the mean temperature between the average bulk-fluid temperature and the average tube-wall surface temperature. This correlation also provides a method of evaluating the friction factor used in the determination of the pressure drop.

The Sieder-Tate correlation as shown in Eq. (4) allows for radial variations in the viscosity. The viscosity ratio term tends to increase the tubeside heat transfer coefficient when the fluid is being heated and decrease it when the fluid is being cooled.

$$\text{Nu} = 0.027 \text{ Re}^{0.8} \text{ Pr}^{0.4} (\mu / \mu_s)^{0.14} = h \cdot D / k \quad (4)$$

An approximate heat transfer coefficient<sup>27</sup> for the turbulent flow of water inside tubes in the temperature range of 5 to 104K (40 to 220°F) is shown in Eq. (5) and depends only on the size of the conduit, the velocity, and temperature.

$$h = C (1 + 0.011t_b) V_1^{0.8}/D_1^{0.2} \quad (5)$$

where in Eqs. (1 through 5)

- Nu = dimensionless Nusselt number =  $h \cdot D/k$ ,
- Pr = dimensionless Prandtl number =  $C_p \mu/k$ ,
- Re = dimensionless Reynolds number =  $DG/\mu$ ,
- St = dimensionless Staunton number =  $h/C_p \cdot G = Nu/Re \cdot Pr$ ,
- $h$  = tubeside heat transfer coefficient,  $W/m^2 \cdot K(Btu/h \cdot ft^2 \cdot ^\circ F)$ ,
- $D$  = inside tube diameter, m(ft),
- $D_1$  = inside tube diameter, inches,
- $k$  = thermal conductivity of fluid evaluated at  $t_b$ ,  $W/m \cdot K(Btu/h \cdot ft \cdot ^\circ F)$ ,
- $C_p$  = specific heat evaluated at  $t_b$ ,  $J/kg \cdot K(Btu/lb_m \cdot ^\circ F)$ ,
- $\mu$  = dynamic viscosity evaluated at  $t_b$ , Pas(lb/ft·h),
- $\mu_s$  = dynamic viscosity evaluated at  $t_s$ , Pas(lb/ft·h),
- $f$  = dimensionless Darcy-Weisbach friction factor,
- $t_w$  = inside the tube wall temperature, K( $^\circ F$ ),
- $t_b$  = bulk fluid temperature, K( $^\circ F$ ),
- $t_s$  = average film temperature =  $0.5 (t_w + t_b)$ , K( $^\circ F$ ),
- $G$  = coolant mass velocity =  $V\rho \text{ kg/m}^2 \text{s}$ ,  $3600 V\rho \text{ lb/ft}^2 \text{h}$ ,
- $V$  = fluid velocity m/s (ft/h),
- $V_1$  = fluid velocity, ft/s,
- $\rho$  = fluid density evaluated at  $t_b$ ,  $kg/m^3$  ( $lb/ft^3$ ),
- $j$  = dimensionless Colburn  $j$ -factor,
- $C$  = 851.25 for metric units, 150 for English units,

Changes in the coolant supply temperature of  $\pm 5.6K$  ( $10^\circ F$ ) will cause a corresponding change from 6 to 9% in calculating the heat transfer coefficients in any of the above equations. In midsummer when the coolant supply is running hot, the tubeside coefficient will be

higher, but so will the condensing pressure and consequently the temperature of the isobutane because it is close to the temperature of the condensing surface. The small increase in overall heat transfer coefficient will result in a slight decrease in the rise in the bulk water temperature and the log mean temperature difference. This results in the condensing temperature being slightly below the temperature that would have resulted if the thermal effect on the coefficient had not been considered.

The relationships for the four correlations for the inside heat transfer coefficient are plotted as functions of coolant flow rate at a temperature of 300K (80°F) in Fig. 15. The relationships indicate variations caused by temperature changes for each correlation. Equation (1) was used to calculate the tubeside heat transfer coefficient, and it is assumed to be accurate within 1 to 2%.

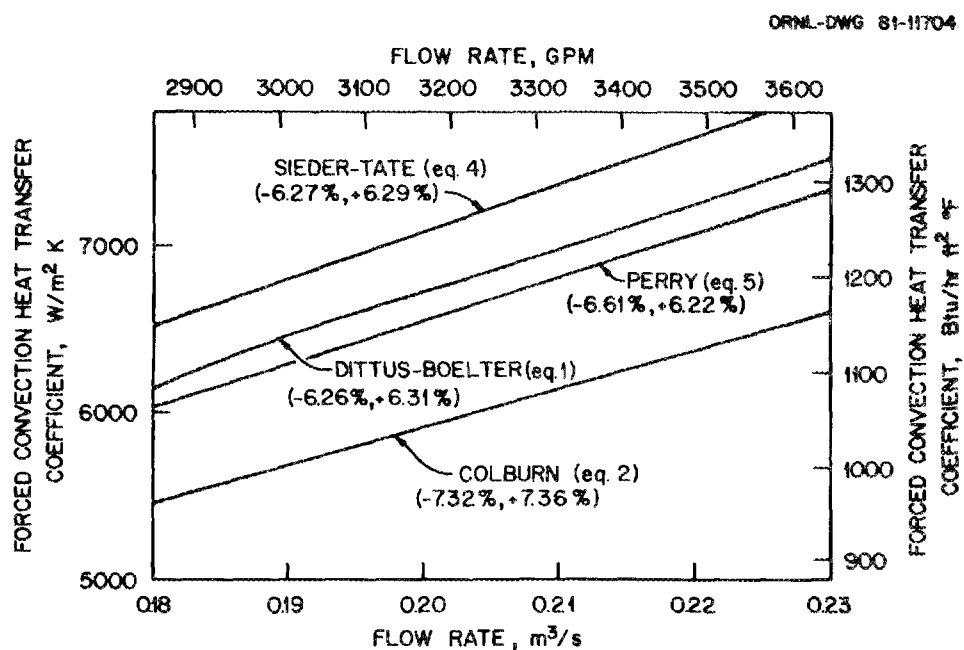


Fig. 15. Comparison of tubeside heat transfer correlations in East Mesa condenser for turbulent flow as functions of flow rate at 300 K (80°F).

At a constant wall heat flux, the thermal entry length was investigated for a Reynold number of 45,000 and a Prandtl of 6.0; it takes about 6 tube diameters (0.13 m or 5 in.) to obtain fully developed thermal flow. To obtain fully developed thermal and hydraulic flows, an entry length of about 30 tube diameters (0.66 m or 26 in.) is required. These facts considered and knowing that the tube has an (L/D) ratio of 237, no allowance was made for the differences in the regime of developing flow.

### 7.3 Shellside Heat Transfer Coefficient

Equation (6) shows the Nusselt correlation for calculating the condensing coefficient on the outside of horizontal rows of smooth tubes:

$$h_h = 0.725 \left[ \frac{k^3 \rho (\rho - \rho_v) \lambda g}{\mu D_o (t_{sat} - t_w)} \right]^{1/4} \phi . \quad (6)$$

Equation (7) shows the basic Nusselt correlation for calculating the condensing coefficient on the outside of a single vertical tube:

$$h_v = 0.943 \left[ \frac{k^3 \rho (\rho - \rho_v) \lambda g}{\mu L (t_{sat} - t_w)} \right]^{1/4} \quad (7)$$

where

- $\rho_v$  = vapor density,
- $k$  = liquid thermal conductivity,
- $\rho$  = liquid density,
- $h_v$  = condensing coefficient on vertical tube,
- $h_h$  = condensing coefficient for n rows of horizontal tubes,
- $\lambda$  = latent heat of condensation (vaporization),
- $g$  = acceleration due to gravity,
- $\mu$  = dynamic viscosity,

$D_o$  = outside tube diameter,  
 $t_{sat}$  = saturation temperature of vapor,  
 $t_w$  = wall temperature,  
 $\phi$  = loss factor due to inundation (Fig. 16), =  $f$  (number of rows of tubes), N

If Eq. (7) is divided by Eq. (6), the ratio R,  $(h_v/h_h)$ , is shown in Eq. (8):

$$R = h_v/h_h = 1.30 (D/L)^{1/4} \phi . \quad (8)$$

Assuming an L/D of 24 for a single tube, it would appear that a smooth vertical tube could condense only 60% of the vapor that could be condensed on the same tube in a horizontal position. This is probably close to reality for a single tube. If we consider the inundation loss incurred with a horizontal exchanger having as many as 100 tubes in a vertical row, the vertical unit could condense twice as much vapor. Only ten rows of tubes are needed before equal condensation is expected from both units based on  $\phi$  using the Nusselt correlation. Increasing the number of vertical tubes does not significantly decrease the heat transfer per tube. Shellside condensation takes on further complexities when noncondensables and other components are added to the vapor stream.

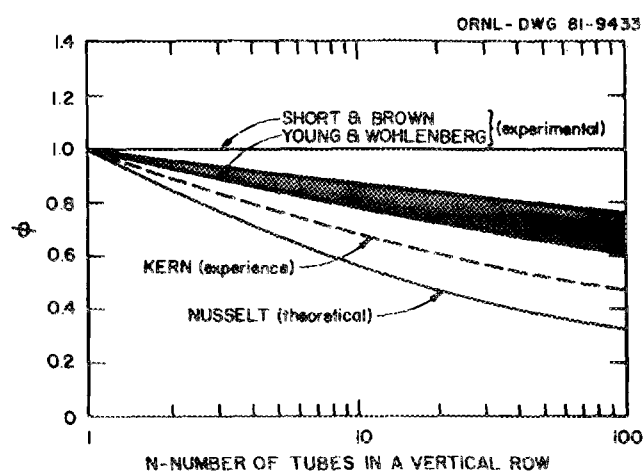


Fig. 16. Inundation correction factor for single smooth tube horizontal condensers as a function of the number of vertical rows.

There are concentration gradients and temperature gradients as functions of distance through the condenser in the shellside condensation of a multicomponent mixture. The higher boiling components will condense out first and in higher concentrations in the condensate and lower concentration in the vapor/gas mixture. The lower boiling components will come out further down the condenser.

Quantitatively, because of the diffusion and nonequilibrium involved, the analysis is extremely complex and seldom are there enough data, either experimental or theoretical, to warrant an exact analysis. The thermodynamics must supply the vapor-liquid equilibrium so that a dew-point and bubble point can be determined preferably at each row of tubes in the condenser. Computer codes are required for this purpose and usually are of a proprietary nature. Both the Heat Transfer Research Institute (HTRI) at Alhambra, California, and Heat Transfer and Fluid System (HTFS),<sup>28</sup> Harwell, England, have computer codes for handling this type of problem. We have tried, without success, several other proprietary codes using ternary mixtures with CO<sub>2</sub> present as a noncondensable.

The case when noncondensables are present in a pure component gas has presented problems since the first boiler went into operation. Othmer<sup>29</sup> predicted in 1929 that in condensing steam, the condensing coefficient could be reduced by as much as 50% with as little as 1% noncondensable (air) present in the steam. From his experiments where stagnant steam was being condensed on 0.23-m (9-in.) diameter tubes, this was quite true. When the vapor is moving at high velocities and vapor-shear becomes involved, not only would the presence of 1% noncondensable go unnoticed, but there also would be a remarkable increase in the overall heat transfer due to the vapor shear.

In a recent article F. C. Standiford<sup>30</sup> demonstrated the effects of noncondensables at velocities ranging from 0.2 to 2 m/s (1 to 7 ft/s) are not nearly as severe: more like 10% air at the vent point causing a 5% reduction in the "air free" coefficient (Fig. 17). However, this effect appears to be a function of the condenser design. Other sources of information indicate that the effect of a noncondensable is also

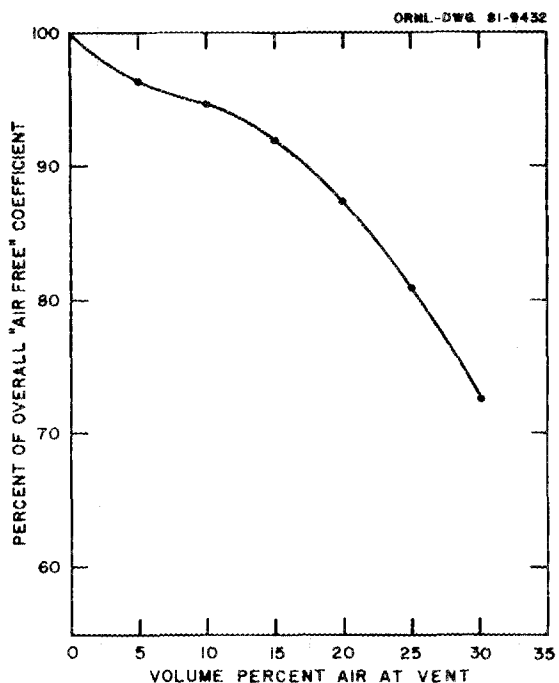


Fig. 17. Effect of air concentration on the condensing coefficient of steam.

proportional to the ratio of the densities or the molecular weights of the noncondensable to the condensable vapor. The standard treatment for a noncondensable in the presence of a single condensable is the Colburn-Houghton<sup>31</sup> method.

Collections of subroutines have been gathered by G. R. E. Franks<sup>32</sup> that give the designer the capability of performing a row-by-row analysis for shellside condensation. Franks presented a method of calculation of the shellside condensing coefficient for multicomponent vapor with noncondensables without considering the presence of water and vapor shear.

A more recent in-depth treatment of this subject has been covered by John Prausnitz et al.,<sup>33</sup> that allows the thermodynamic contribution of water to be evaluated realistically while also considering vapor shear that produces much higher condensing heat transfer coefficients.

The overall heat transfer is calculated in the same manner regardless of how the shellside condensing coefficient is evaluated, so rather

than calculating or even estimating the effect of these variables, it would seem to be wiser to use the experimental results obtained for the 1.22-m (4-ft) E-tube with no skirts. This approach is believed to be conservative. No credit is taken in the East Mesa condenser design for vapor shear or the fact that the skirt spacing on the condenser is 0.61 m (2 ft) or less. Allowance was not made in the East Mesa condenser design for the presence of noncondensable in the vapor stream, but previous assumptions should more than compensate for this omission.

It is planned eventually to correlate the data from these experiments into basic equations for calculating the shellside heat transfer coefficient. This shellside correlation might ultimately involve consideration of the composition, quality, and velocity of the vapor, the temperature of the condensing surface, and the tube configuration. To develop shellside correlations, some degree of precision must be maintained in the experiments in the evaluation of the LMTD and the inside heat transfer coefficient; the heat flux is easier to evaluate.

For the evaluation of the shellside condensing coefficient for the East Mesa condenser, single tube experimental data are used that were gathered by Combs et al., in condensing isobutane on a 1.22-m (4-ft) long aluminium E-tube.<sup>19</sup> Similar data were acquired by N. Domingo of ORNL in condensing R-11 on both 1.22-m (4-ft) long carbon steel and aluminum<sup>34</sup> E-tube. The data (Fig. 18), obtained from Wilson plots and including the wall resistance, were fitted to polynomial expressions for use in the computer programs.

#### 7.4 Fouling

C. H. Gilmore<sup>35</sup> of Union Carbide has claimed that fouling can be reduced to practically nothing when tubes are chrome plated internally and externally and the velocities are kept high.

The tubeside fouling estimation for the East Mesa condenser was based on several factors. The tube material was low-carbon steel with a carbon content of less than 0.10%, almost like Swedish steel. The coolant is treated, recirculated water that is to be totally contained within the

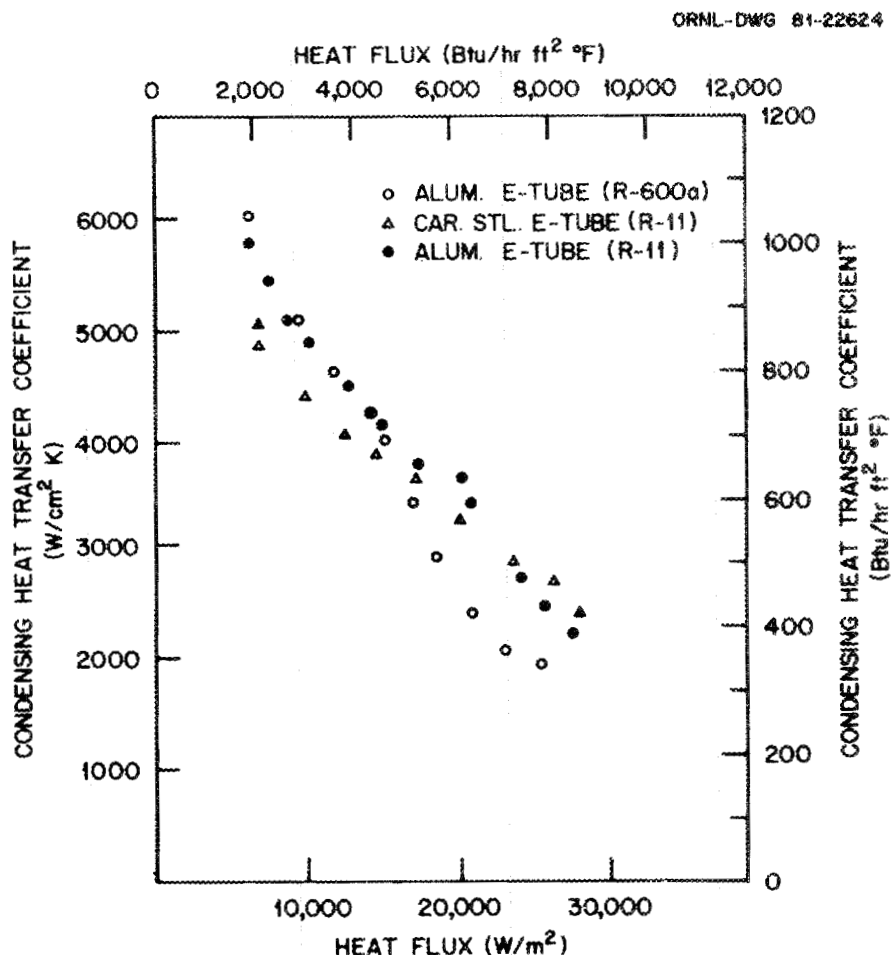


Fig. 18. Experimental shellside condensing coefficients obtained for E-tubes.

pipes and never comes in contact with any geothermal brines. The water velocity is relatively high at about 2.1 m/s (7 ft/s). Maximum anticipated fouling from treated cooling tower water is  $0.00018 \text{ m}^2 \cdot \text{K/w}$  ( $0.001 \text{ h} \cdot \text{ft}^2 \cdot {}^\circ\text{F/Btu}$ ) and for design purposes  $2/3$  of this value will be used, or  $0.00012 \text{ m}^2 \cdot \text{K/W}$  ( $0.00066 \text{ h} \cdot \text{ft}^2 \cdot {}^\circ\text{F/Btu}$ ). This value has to be multiplied by the ratio of the outside to inside heat transfer area of 1.85.

The maximum shellside fouling for clean hydrocarbons is taken as  $0.00009 \text{ m}^2 \cdot \text{K/w}$  ( $0.0005 \text{ h} \cdot \text{ft}^2 \cdot {}^\circ\text{F/Btu}$ ); 50% of this value or  $0.000045 \text{ m}^2 \cdot \text{K/w}$  ( $0.00025 \text{ h} \cdot \text{ft}^2 \cdot {}^\circ\text{F/Btu}$ ) will be used for the design value.

A total fouling factor of  $0.000259 \text{ m}^2 \cdot \text{K/W}$  ( $0.00147 \text{ h} \cdot \text{ft}^2 \cdot {}^\circ\text{F/Btu}$ ) is then used in calculating the area requirements for the East Mesa condenser. The above mentioned fouling factors are referenced in TEMA<sup>36</sup> and Kern<sup>37</sup> and are used by most heat exchanger manufacturers.

### 7.5 Overall Heat Transfer Coefficient

The overall heat transfer coefficient may be calculated by the summation of all the component resistances with corrections for the ratios of the heat transfer area. As in electrical flow, parallel conductances are additive and series resistances are additive as shown by combining the five component resistances in series in Eq. (9)

$$U_o = 1.0 / [(1/h_o) + (A_o/h_i A_i) + f_o + (A_o f_i / A_i) + (A_o L / A_m k)] \quad (9)$$

where

$U_o$  = the overall heat transfer coefficient  $\text{W/m}^2 \cdot \text{K}$  ( $\text{Btu/h} \cdot \text{ft}^2 \cdot {}^\circ\text{F}$ ),  
 $A_o$  = outside area of tube,  $\text{m}^2$  ( $\text{ft}^2$ ),  
 $A_i$  = inside area of tube,  $\text{m}^2$  ( $\text{ft}^2$ ),  
 $A_m$  = log-mean average tube area,  $\text{m}^2$  ( $\text{ft}^2$ ),  
 $h_i$  = tubeside heat transfer coefficient  $\text{W/m}^2 \cdot \text{K}$  ( $\text{Btu/h} \cdot \text{ft}^2 \cdot {}^\circ\text{F}$ ),  
 $f_i$  = tubeside fouling factor  $\text{m}^2 \cdot \text{K/W}$  ( $\text{h} \cdot \text{ft}^2 \cdot {}^\circ\text{F/Btu}$ ),  
 $h_o$  = shellside heat transfer coefficient  $\text{W/m}^2 \cdot \text{K}$  ( $\text{Btu/h} \cdot \text{ft}^2 \cdot {}^\circ\text{F}$ ),  
 $f_o$  = shellside fouling factor  $\text{m}^2 \cdot \text{K/W}$  ( $\text{h} \cdot \text{ft}^2 \cdot {}^\circ\text{F/Btu}$ ),  
 $k$  = thermal conductivity of tube material  $\text{W/m} \cdot \text{K}$  ( $\text{Btu/h} \cdot \text{ft} \cdot {}^\circ\text{F}$ ),  
 $L$  = tube wall thickness  $\text{m}$  ( $\text{ft}$ ).

Because the experimental data used to obtain the condensing coefficient was done using the Wilson plot, which includes the wall resistance of the tube, the last term in Eq. (9) will be deleted in the calculation. The ratio of the outside to inside area of the E-tube,  $(A_o/A_i)$ , is 1.850.

In discussing the enhancement of the fluted tube, it should be pointed out that if the tubeside resistance is controlling, improvement

in the overall heat transfer is not as apparent with improvement in the shellside coefficient. For the case at hand, the coolant flow rate of 3500 gpm and a fouling factor of  $0.0012 \text{ m}^2 \cdot \text{K/W}$ , ( $0.00066 \text{ h} \cdot \text{ft}^2 \cdot {}^\circ\text{F/Btu}$ ) results in a total tubeside resistance of  $0.000296 \text{ m}^2 \cdot \text{K/W}$  ( $0.001681 \text{ h} \cdot \text{ft}^2 \cdot {}^\circ\text{F/Btu}$ ). When fouling is neglected, the tubeside resistance is reduced to  $0.000233 \text{ m}^2 \cdot \text{K/W}$  ( $0.001324 \text{ h} \cdot \text{ft}^2 \cdot {}^\circ\text{F/Btu}$ ). The total shellside resistance which includes the wall resistance could vary from a minimum of  $0.000185 \text{ m}^2 \cdot \text{K/W}$  ( $0.000883 \text{ h} \cdot \text{ft}^2 \cdot {}^\circ\text{F/Btu}$ ) to a maximum of  $0.000230 \text{ m}^2 \cdot \text{K/W}$  ( $0.001303 \text{ h} \cdot \text{ft}^2 \cdot {}^\circ\text{F/Btu}$ ). A plot of the overall heat transfer coefficient as a function of the condensing coefficient with and without anticipated fouling is shown in Figure 19. It will be noticed that the shellside resistance is controlling up to a shellside coefficient of  $3900 \text{ W/m}^2 \cdot \text{K}$  ( $687 \text{ Btu/h} \cdot \text{ft}^2 \cdot {}^\circ\text{F}$ ) at a constant coolant flow rate of  $0.2 \text{ m}^3/\text{s}$  (3500 gpm).

Several facts can be deduced from this plot. (1) Fouling is more devastating to enhanced exchangers than unenhanced exchangers. (2) Enhancement is more apparent when the film on the enhanced surface is not the controlling resistance. (3) To make the shellside resistance

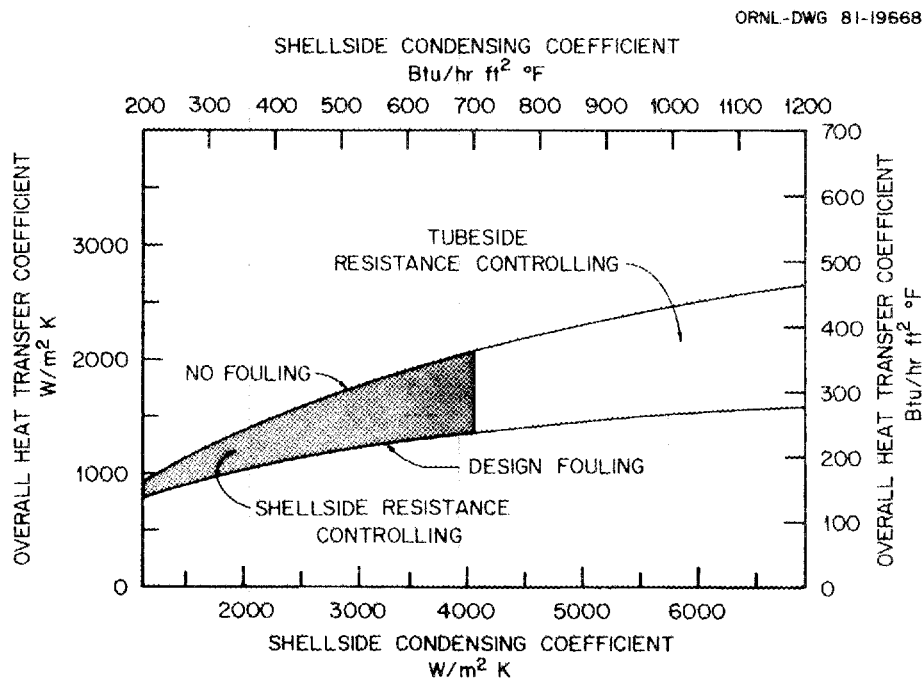


Fig. 19. Overall heat transfer coefficient as a function of the condensing coefficient for the East Mesa condenser at a coolant flow rate of  $0.22 \text{ m}^3/\text{s}$  (3500 gpm).

controlling requires increasing the tubeside velocity, which is quite costly, with the pumping cost being proportional to the cube of coolant flow rate. To achieve a controlling resistance with a maximum anticipated condensing coefficient of  $5820 \text{ W/m}^2 \cdot \text{K}$  ( $1025 \text{ Btu/h} \cdot \text{ft}^2 \cdot {}^\circ\text{F}$ ) a coolant flow rate of  $0.322 \text{ m}^3/\text{s}$  (5100 gpm) would be required.

Fouling can often be reduced by the proper selection of tube material, addition of inhibitors to the coolant, and periodic cleaning of the tubes. The tubeside resistance can be reduced by increasing the pumping capacity of the tubeside coolant. The shellside resistance can be reduced by limiting the noncondensables in the condenser, but insufficient condensation of the shellside vapor in a given condenser is rarely improved by increasing the flow rate of the vapor. In the case of the East Mesa condenser, a coolant flow rate of  $0.322 \text{ m}^3/\text{s}$  would require a 303-hp pump requiring 0.283 Mw of power, which is 57% of the total power produced by the turbo generator.

### 7.6 Log Mean Temperature Difference

The log mean temperature difference (LMTD) for a counter-current or cocurrent liquid-liquid heat exchanger is calculated in a straight forward manner. Consider cold fluid on the tubeside of a heat exchanger entering the exchanger at a temperature  $t_i$  and leaving at a temperature  $t_o$ . Hot fluid is on the shellside entering at a temperature  $T_i$  and leaving at  $T_o$ . The average temperature of the hot stream is  $(T_o + T_i)/2$ , and the average temperature of the cold stream is  $(t_o + t_i)/2$ . The average temperature difference between these two streams is the sum of the two streams  $(T_o + T_i)/2 - (t_o + t_i)/2$  regardless of whether the flow is cocurrent or counter-current. The LMTD between these streams is defined for counter-current flow in Eq. (10):

$$\text{LMTD} = (T_i - t_o) - (T_o - t_i) / \ln ((T_i - t_o) / (T_o - t_i)) . \quad (10)$$

If the flow is cocurrent the LMTD is calculated as shown in Eq. (11),

$$\text{LMTD} = (T_i - t_i) - (T_o - t_o) / \ln [(T_i - t_i) / (T_o - t_o)] . \quad (11)$$

Assuming a constant condensing temperature of 307.4K (94°F), a water supply temperature of 299.7K (80°F), and a water flow rate of 0.221 m<sup>3</sup>/s (3500 gpm), the rise in the coolant temperature is 5.44K (9.79°F). With an average temperature difference between the two streams of about 5K (9°F) both the counter-current and cocurrent LMTD is 4.55K (8.19°F), a difference of 10%, which could mean \$3700 in tubing cost. The four-tube-pass configuration for condensation is both counter-current and cocurrent, depending on the pass. Many investigations have been made on calculation of LMTD for multipass liquid-liquid heat exchangers.

Because we are dealing with a relatively small approach temperature 2.3K (4.2°F) and a small average temperature difference of 5K (9°F), it seems unwise to use correction factors correlated for liquid-liquid exchangers where the efficiency is either zero or infinite when a constant temperature is employed because the methods don't allow for heat transfer with a change of phase. Therefore, 4.55K (8.19°F) LMTD will be used for the design. Figure 20 shows the temperature distributions in both streams as a function of the length in the exchanger.

Some explanation should be given for this approach<sup>38</sup> because some designers still break the condenser into component parts. Desuperheating, condensing, and subcooling sections or regimes are often evaluated with corresponding heat transfer coefficients, LMTDs, and areas for each section. This approach provides from two to five times the area actually required. In the East Mesa condenser, most of the desuperheating being done is in the first half of the first pass across the tube bank. About 13% of the total heat is superheat. If the desuperheating is based on a gas film coefficient of about 285 W/m<sup>2</sup>·K (50 Btu/h·ft<sup>2</sup>·°F), 520 m<sup>2</sup> (5600 ft<sup>2</sup>) of heat transfer area is required, which is 72% of the design area of the East Mesa condenser, thus

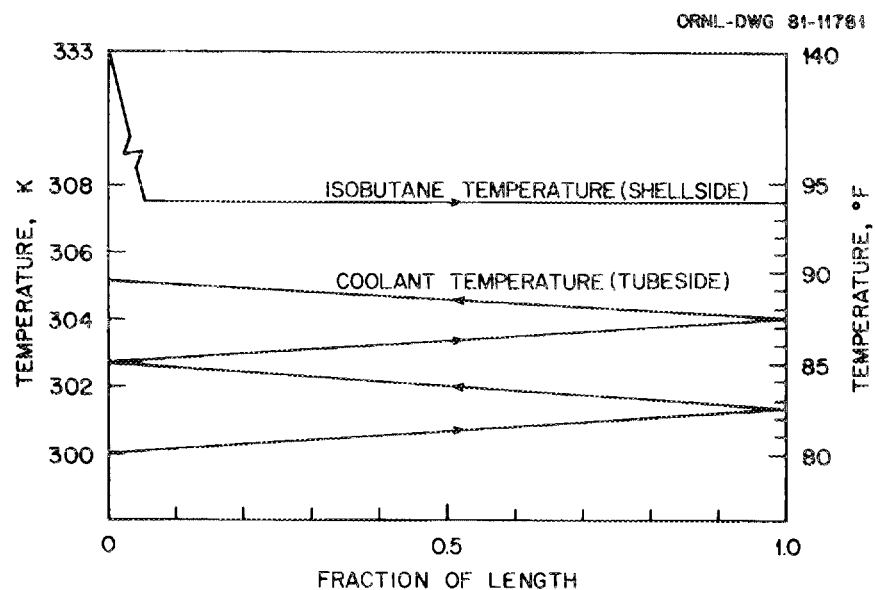


Fig. 20. Tubeside and shellside temperature distribution as a function of length for the East Mesa condenser.

leaving insufficient area for condensing. Using this method of calculation would require a much larger condenser. Instead of the three stages happening separately, they actually occur simultaneously, with desuperheating requiring about the same percentage (13%) of the total surface area or  $93 \text{ m}^2$  ( $1000 \text{ ft}^2$ ).

## 8. PRESSURE DROP CALCULATIONS

When the flow rates are increased in a given condenser, there are usually noticeable increases in heat transfer and obviously corresponding increases in pressure drops. Generally the heat transfer is limited by the pumping head or the allowable pressure drops across the tubeside and shellside of the condenser. If the pressure cannot be supplied, it must be compensated for by adding more heat transfer area with a loss of efficiency because velocities must be reduced to avoid exceeding the allowable pressure drops. When in doubt about an untested or new design concept, most heat exchanger manufacturers will usually guarantee the heat transfer or the pressure drop but not both. It is just as important to obtain reliable pressure drop correlations as it is to obtain reliable heat transfer correlations.

The tubeside pressure drops in the analysis of this condenser are relatively easy to calculate because we are dealing with a single-phase fluid in uniform channels. The shellside pressure drops are more difficult to evaluate. Two-phase flow is involved in evaluating the shellside pressure drop involving a constantly changing flow area with the condensate being constantly removed.

### 8.1 Tubeside Pressure Drop

It is desirable to have a relationship that can be used to calculate the friction factor for any flow regime as functions of the Reynolds number and the relative roughness of the conduit. S. W. Churchill<sup>39</sup> of the University of Pennsylvania has developed Eq. (12), which accomplishes this.

$$f = 8.0 [(8/Re)^{1/2} + 1.0/(A + B)^{3/2}]^{0.0833} \quad (12)$$

where

$$\begin{aligned} A &= [2.457 \ln (1.0/(7/Re)^{0.8} + 0.27 E)]^{1/6}, \\ B &= (37,530/Re)^{1/6}, \end{aligned}$$

$Re$  = dimensionless Reynolds number,  
 $\epsilon$  = surface roughness, m (ft),  
 $= 1.52 \times 10^{-6}$  m ( $5 \times 10^{-6}$  ft) for smooth tubing,  
 $D$  = inside tube diameter, m (ft),  
 $f$  = dimensionless Darcy-Weisbach friction factor,  
 $E$  = dimensionless relative roughness =  $\epsilon/D$ .

Entrance loss for the tubes will vary from a minimum of zero for specially rounded openings to a maximum of 1/2 velocity head,  $V^2/4g$ . To be conservative, the maximum entrance loss has been assumed for design purposes based on the coolant velocity in the tubes.

The exit loss is expressed as one velocity head multiplied by  $(1.0 - A_t/A_s)$  where  $A_t$  is the tube area and  $A_s$  is the area of the discharge section. The maximum loss is incurred as  $A_s$  becomes infinite, so the maximum loss is one velocity head or  $V^2/2g$ . This drop is independent of the shape of the exit. There are four separate tube entrances and four separate tube exits that must be accounted for in calculating the total tubeside drop.

There is a pressure loss each time the fluid changes direction. This loss can be evaluated by assuming a loss of one velocity head for each  $90^\circ$  turn in the fluid of a constant velocity. There is a turn when the coolant direction is changed in going from the entrance nozzle into the first tube pass with a flow area  $A_1$ . Two turns are encountered ( $180^\circ$  turn) associated with area  $A_2$  in going from the tubes in the first pass to the tubes in the second pass. Two more turns are encountered in the header in the center section in going from the second to the third pass associated with an associated area  $A_3$ . Two more turns are encountered in going from the third to the fourth pass associated with area  $A_2$ . Finally, there is one turn associated with area  $A_1$  when the fluid moves from the tubes in the fourth pass to the coolant discharge nozzle.

The total tubeside pressure drop,  $\Delta P_t$ , in the condenser is obtained by summation of the component pressure drops as given in Eq. (13) for the multipass configuration.

$$\Delta P_t = P(\Delta P_1 + \Delta P_2) + \Delta P_3 + \Delta P_4 + \Delta P_5 + \Delta P_6 + \Delta P_7 + \Delta P_8 \quad (13)$$

where

- $\Delta P_t$  = total tubeside pressure drop, m (ft) of fluid,
- $\Delta P_1$  = maximum pressure loss at tube entrance =  $V^2/4g$ ,
- $\Delta P_2$  = maximum pressure loss at tube exit =  $V^2/2g$ ,
- $\Delta P_3$  = pressure loss due to friction =  $(fL/D) V^2/2g$ ,
- $\Delta P_4$  = maximum entrance loss in header =  $V_p^2/4g$ ,
- $\Delta P_5$  = maximum exit loss in header =  $V_p^2/2g$ ,
- $\Delta P_6$  = turning loss in outer channels of header =  $2V_1^2/2g$ ,
- $\Delta P_7$  = turning loss in floating head =  $4 V_3^2/2g$ ,
- $\Delta P_8$  = turning loss in center header channel =  $2 V_3^2/2g$ ,
- L = length of flow channel, m (ft) =  $PZ/N$ ,
- Z = length of tube in a single tube pass, m (ft),
- N = number of tubes,
- P = number of tube passes,
- D = inside diameter of tube, m (ft),
- V = tubeside fluid velocity, m/s (ft/s),
- g = acceleration due to gravity m/s<sup>2</sup> (ft/s<sup>2</sup>),
- $V_p$  = velocity in coolant pipe =  $W/A_p$ , m/s (ft/s),
- $V_n$  = velocity in headers =  $W/A_n$ ,
- W = coolant mass flow rate, kg/s (lb/s),
- $A_1$  = area of outer header channels, m<sup>2</sup> (ft<sup>2</sup>),
- $A_2$  = area of channel in floating head, m<sup>2</sup> (ft<sup>2</sup>),
- $A_3$  = area of center header channel m<sup>2</sup> (ft<sup>2</sup>),
- $A_p$  = area of coolant nozzle m<sup>2</sup> (ft<sup>2</sup>).

## 8.2 Shellside Pressure Drop

In the design of the ORNL VFTC, it was recommended that the shell-side pressure drop be kept below 7 kPa (1.0 psi). With this criteria, the condenser is considered to be pressure-drop limited. Design changes such as increased tube pitch, decreased tube length, or use of multisegmental baffles can be made to reduce the shellside pressure drop.

First of all, it was desirable to obtain some idea of the allowable baffles assuming 15% baffle cut with tubes in the window and equal baffle spacing. These relationships were found in an empirical equation proposed by D. G. Kern,<sup>40</sup> which uses one-half of the pressure drop calculated for the total flow of the vapor through the entire shell. With a vapor flow rate of 12.63 kg/s (100,000 lb/h) it was found that six equally spaced baffles would cause a pressure drop of 5.9 kPa (0.9 psi) while seven baffles resulted in a pressure drop of 8.9 kPa (1.3 psi), therefore exceeding the design requirements.

Using six baffles, it was decided to rearrange the spacing so that an approach to a uniform vapor velocity could be obtained through each shell pass. A computer program was written to make the task easier by providing a row-by-row analysis of the pressure drop as shown in Appendix D.

The program requires knowledge of the number of tubes on each row, the baffle spacing at each pass, the area of the segmental opening that is void of tubes, and the mass flow rate of the vapor. It is assumed that the condensation is equally distributed over the total length of tubes about 8.06 kg/m (5.40 lb/ft). This assumption does not appear to be conservative because of the superheat involved. It is estimated that the superheat is probably dissipated in the first half of the first shellside pass. This assumption would probably result in slightly higher pressure drop in the first pass, with the total shellside drop remaining about the same.

The summation of the component pressure drops on the shellside of the condenser,  $\Delta P_s$ , is given in Eq. (12)

$$\Delta P_s = \Delta P_1 + \Delta P_2 + \sum_{j=1}^{jt} \sum_{i=1}^{it} \Delta P_3 + \sum_{k=1}^{kt} \Delta P_4 \quad (12)$$

where

$\Delta P_s$  = total shellside pressure drop, m (ft) of fluid,

$\Delta P_1$  = maximum pressure loss in concentric expansion from 12-in. pipe, to 24-in. pipe =  $K V_1^2 / 2g$ ,

$V_1$  = velocity in 12-in. pipe, m/s (ft/s),  
 $\beta^2 = (d_1/d_2)^2 = 0.2784$ ,  
 $K = (1 - \beta^2)^2 = 0.5207$ ,  
 $d_1$  = inside diameter of 12-in. Sch 40 pipe, m (ft),  
 $d_2$  = inside diameter of 24-in. Sch 40 pipe, m (ft),  
 $V_2$  = velocity in 24-in. pipe m/s (fps),  
 $\Delta P_2$  = maximum entrance loss into condenser =  $0.5 V_2^2/2g$ ,  
 $g$  = acceleration due to gravity m/s<sup>2</sup> (ft/s<sup>2</sup>),  
 $\Delta P_3$  = pressure loss due to flow of vapor through jth row of tubes  
 and ith pass having a flow area  $A_{ij} = f_{ij} V_{ij}^2/2g$ ,  
 $A_{ij} = B_i (N_j + 1) (P - D)$ ,  
 $N_j$  = number of tubes on jth row,  
 $P$  = tube pitch, m (ft),  
 $D$  = O.D. of tube, m (ft),  
 $B_i$  = baffle spacing for ith pass m (ft),  
 $f_{ij}$  = dimensionless Darcy-Weisbach friction factor =  
 $0.8 \cdot Re_{ij}^{-0.2}$  evaluated at i<sub>th</sub> pass and j<sub>th</sub> row,  
 $Re_{ij}$  = dimensionless Reynolds number evaluated at i<sub>th</sub> pass and j<sub>th</sub>  
 row =  $D W_{ij} / \mu A_{ij}$ ,  
 $W_{ij}$  = mass flow rate of vapor at i<sub>th</sub> pass and j<sub>th</sub>  
 row =  $(W_{i+1,j} - C_{ij})/2$ ,  
 $C_{ij}$  = mass flow of condensate condensed at i<sub>th</sub> pass and j<sub>th</sub> row,  
 $\Delta P_4$  = pressure drop across baffle windows  
 = 1 velocity head =  $1.0 V_k^2/2g$ ,  
 $V_k$  = velocity at k<sub>th</sub> baffle =  $W_k / \rho A_b$ ,  
 $V_{ij}$  = velocity at i<sub>th</sub> pass and j<sub>th</sub> row =  $W_{ij} / \rho A_{ij}$ ,  
 $W_k$  = mass flow rate of vapor through k<sub>th</sub> baffle,  
 $A_b$  = baffle area =  $0.118 \text{ m}^2$  ( $1.28 \text{ ft}^2$ ),  
 $i$  = pass number,  
 $it$  = total number of tube passes = 6 (see Fig. 21),  
 $j$  = row number,  
 $jt$  = total number of tube rows = 32,  
 $k$  = turn number,  
 $kt$  = total number of flow reversals (turns) = i-1,  
 $\rho$  = vapor density, kg/m<sup>3</sup> (lb/ft<sup>3</sup>),  
 $\mu$  = vapor viscosity, Pa·s (lb/ft·h).

ORNL-DWG 81-13094

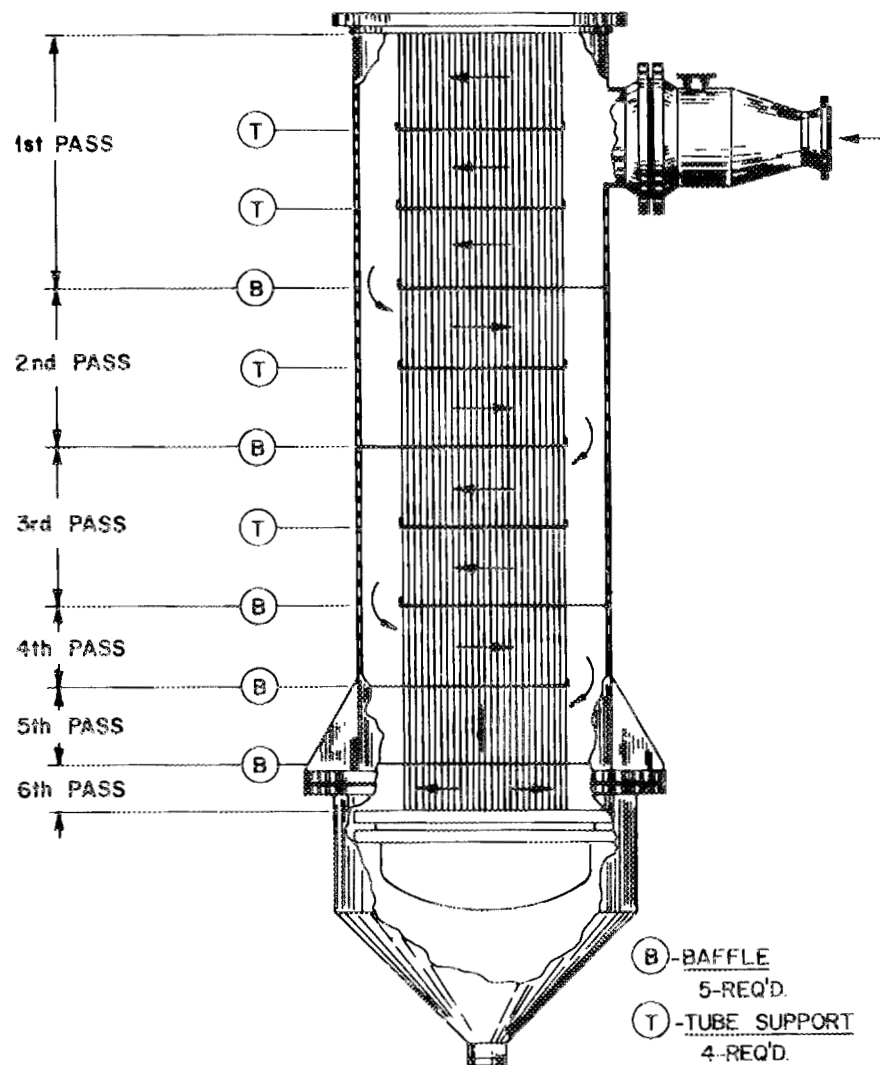


Fig. 21. Component shellside pressure drops in the East Mesa condenser.

In the calculation of shellside pressure drop, the Bell-Delaware<sup>41</sup> or Taborek<sup>42</sup> methods are normally used. These methods allow for streams or leakages through annular voids between the baffle hole and the tubes. The East Mesa condenser was fabricated with all of these holes sealed and with shrouds provided to offer almost perfect "cross flow," which gives justification for neglecting the perturbations considered in these classical methods.

In equation 12, the entrance loss into the condenser,  $\Delta P_2$ , is calculated from relationships given in Ref. 43 and the friction factor,  $f_{ij}$ ; across any tube row is given in Ref. 44.

A tabulation of the pressure drop calculated at each row for each of the six passes of the East Mesa condenser is given in Appendix D.1 through D.6.



## 9. DESIGN VARIABLES AND OPTIMIZATION

In general, the number of degrees of freedom in a unit process equals the difference between the number of pertinent variables and the number of independent design relationships (equations).<sup>45</sup> The term pertinent variables is used because there are variables in the process that have no direct bearing on the system operation or are repetitive quantities. These relationships can be simply stated in Eq. (15).

$$F = V - R \quad (15)$$

where

F = degrees of freedom,

V = pertinent design variables (unknowns),

R = independent design relationships (equations),

and is another way of saying for n unknowns you must have n equations.

The basic equations involved in the condenser design are:

$$Q = W_c C_c (t_2 - t_1) . \quad (16)$$

$$Q = W_g [\lambda + C_g (t_g - t_c)] . \quad (17)$$

$$Q = U A \Delta T_m . \quad (18)$$

$$\Delta T_m = [(t_c - t_1) - (t_c - t_2)] / \ln [(t_c - t_1) / (t_c - t_2)] . \quad (19)$$

$$A = N L Z . \quad (20)$$

$\Delta P_t$  = tubeside pressure drop [see Eq. (13)] .

$\Delta P_s$  = shellside pressure drop [see Eq. (14)] .

The floating variables are used in these equations:

A = the total outside heat transfer area of tubes,  $\text{m}^2$  ( $\text{ft}^2$ ),  
U = overall heat transfer coefficient =  $f(N, P)$ ,  $\text{W}/\text{m}^2 \cdot \text{K}$  ( $\text{Btu}/\text{h} \cdot \text{ft}^2 \cdot {}^\circ\text{F}$ ),  
N = number of tubes,  
P = number of tube passes.

The following variables are set either by choice or prevailing operating conditions:

$w_g$  = mass flow rate of vapor = 12.55  $\text{kg}/\text{s}$  (99,400  $\text{lb}/\text{h}$ ),  
 $w_c$  = mass flow rate of coolant = 220.58  $\text{kg}/\text{s}$  ( $1.747 \times 10^6$   $\text{lb}/\text{h}$ ),  
 $t_1$  = maximum coolant supply temperature = 300 K ( $80^\circ\text{F}$ ),  
 $t_g$  = vapor supply temperature = 333.9 K ( $140.6^\circ\text{F}$ ),  
 $c_g$  = specific heat of the vapor = 0.000117  $\text{J}/\text{kg} \cdot \text{K}$  ( $0.49 \text{ Btu}/\text{lb} \cdot {}^\circ\text{F}$ ),  
 $c_c$  = specific heat of the coolant = 0.000239  $\text{J}/\text{kg} \cdot \text{K}$  ( $1.0 \text{ Btu}/\text{lb} \cdot {}^\circ\text{F}$ ),  
 $p_g$  = vapor supply pressure = 493 kPa (71.5 psia),  
 $\Delta p_s$  = allowable shellside pressure drop = 6.9 kPa (1.0 psi),  
 $\Delta p_t$  = allowable tubeside pressure drop = 69 kPa (10.0 psi),  
 $t_o$  = desired condensing temperature = 307 K ( $94^\circ\text{F}$ ),  
Q = heat load = 4.917 MW ( $16.781 \times 10^6 \text{ Btu}/\text{h}$ ),  
D = inside diameter of tube = 0.0219 m (0.07183 ft),  
X = tube pitch = 0.0318 m (1.25 in.),  
Z = outside surface area per unit length of tube = 0.1283  $\text{m}^2/\text{m}$  ( $0.4208 \text{ ft}^2/\text{ft}$ ),  
L = exposed length of tubing = 4.48 m (16 ft),  
 $f_i$  = tubeside fouling resistance = 0.00012  $\text{m}^2 \cdot \text{K}/\text{W}$   
= ( $0.00066 \text{ h} \cdot \text{ft}^2/\text{Btu}$ ),  
 $f_i$  = shellside fouling resistance = 0.000044  $\text{m}^2 \cdot \text{K}/\text{W}$   
= ( $0.00025 \text{ h} \cdot \text{ft}^2 \cdot {}^\circ\text{F}/\text{Btu}$ ).

The foregoing limitations have actually set some other parameters in the system. The coolant discharge temperature  $t_2$  can be directly calculated from EQ. (14).

$$t_2 = t_1 + Q/C_c \quad W_c = 305 \text{ K } (89.73^\circ\text{F})$$

and then the LMTD can be calculated from Eq. (19)

$$\Delta T_m = 4.55 \text{ K } (8.19^\circ\text{F}) .$$

The distribution of the heat load on the condenser is shown in Table 4. The water vapor that is discharged from the turbine in the DCHX mode arrives at the condenser at a quality of 68%, based on preliminary calculations.

Table 4. Heat load on East Mesa condenser using direct contact heat exchanger

Heat load	Flow rate		Heat		Percentage
	kg/s	lb/h	MW	Btu/h	
Super heat in isobutane	12.359	97,882	0.6827	2,330,000	13.8844
Latent heat in isobutane	12.359	97,882	3.9436	13,459,000	80.2019
Latent heat in water vapor	0.117	930	0.3842	970,000	5.7802
Sensible heat in water	0.055	438	0.0061	20,900	0.1245
Sensible heat in CO <sub>2</sub>	0.019	155	0.0004	1,500	0.0089
Total	12.551	99,400	4.917	16,781,400	100.0000

Trial calculations for various tube passes are made by assuming values for the overall heat transfer coefficient. Based on this assumption, a heat transfer area and a heat flux are calculated that enables the outside heat transfer coefficient to be evaluated. With the allocated fouling resistance and the resistances offered by both films, the overall heat transfer coefficient is calculated and compared

with the assumed value. This procedure is continued until the difference is negligible. The procedure was programmed to obtain the results shown in Table 5. The output includes the tubes required and the pertinent variables obtained using one-, two-, four-, and eight-tube passes with 4.48-m (16-ft)-long tubes.

Table 5. Tube requirements for East Mesa condenser  
(Tube length = 16 ft)

Passes	1	2	4	8
Tubes	3987	1654	1150	968
Condensing coefficient				
W/m <sup>2</sup> ·K	7326	6413	5789	5403
Btu/h·ft <sup>2</sup> ·°F	1291	1130	1020	952
Tubeside coefficient				
W/m <sup>2</sup> ·K	970	3411	7928	15913
Btu/h·ft <sup>2</sup> ·°F	171	601	1397	2804
Overall coefficient				
W/m <sup>2</sup> ·K	431	1044	1504	1782
Btu/h·ft <sup>2</sup> ·°F	76	184	265	314
Clean coefficient				
W/m <sup>2</sup> ·K	488	1430	2463	3320
Btu/h·ft <sup>2</sup> ·°F	86	252	434	585
Tubeside velocity				
m/s	0.14	0.70	2.01	4.78
ft/s	0.48	2.33	6.70	15.92
Tubeside pressure drop				
kPa	7.10	11.86	74.54	721.56
psi	1.03	1.72	10.81	104.65

It can be seen from comparisons made in Table 5 that using eight-tube passes makes the tubeside pressure drop too much while two-tube passes do not provide sufficient velocity to obtain a reasonably good tubeside heat transfer coefficient. The four-pass unit seemed to offer a good compromise for both the pressure drop and the tubeside heat transfer coefficient. Using 968 tubes, the tubeside pressure drop is exceedingly high because we were asked to keep the drop below 69 kPa (10 psi).

Using 1654 tubes reduced the pressure drop to 12 kPa (2 psi). It was found that an exchanger with 1150 tubes could be used and still be close to the required pressure drop at the same time increasing the heat transfer.

Therefore, it was decided to use 1150 tubes in a four-pass configuration having an effective tube length of 4.48 m (16 ft). The total tube length is obtained by adding the thicknesses of the two-tube sheets, the baffles, and the tube supports to the effective length.

The 1150 tubes provide  $719 \text{ m}^2$  ( $7743 \text{ ft}^2$ ) of enhanced heat transfer surface resulting in a mean heat flux of  $6830 \text{ W/m}^2$  ( $2167 \text{ Btu/h}\cdot\text{ft}^2$ ). This choice allows for a permissible fouling of  $0.000117 \text{ m}^2\cdot\text{K/W}$  ( $0.00067 \text{ h}\cdot\text{ft}^2\cdot{}^\circ\text{F/Btu}$ ) on the tubeside, which is close to the assumed value of  $0.000116 \text{ m}^2\text{K/W}$  ( $0.00066 \text{ h}\cdot\text{ft}^2\cdot{}^\circ\text{F/Btu}$ ).

It would seem desirable to have the tubeside coefficient at least equal to the condensing coefficient multiplied by the area ratio of the outside to inside tube areas (1.85), which would necessitate a maximum tubeside coefficient of  $12667 \text{ W/m}^2\cdot\text{K}$  ( $2232 \text{ Btu/h}\cdot\text{ft}^2\cdot{}^\circ\text{F}$ ) requiring a velocity of 3.67 m/s (12.03 fps). At this velocity (and neglecting entrance, exit, and turning losses), a total length of tubing of 10 m (32 ft) could be tolerated to keep the pressure drop within the allocated range. With a four-pass configuration, the tube length would be limited to 2.5 m (8 ft). To keep the heat flux at  $6300 \text{ W/m}^2$  ( $2000 \text{ Btu/h}\cdot\text{ft}^2$ ) where we can utilize the maximum condensing coefficient of  $5900 \text{ W/m}^2\cdot\text{K}$  ( $1040 \text{ Btu/h}\cdot\text{ft}^2\cdot{}^\circ\text{F}$ ), we need  $780 \text{ m}^2$  ( $8390 \text{ ft}^2$ ) of heat transfer area requiring 2490 tubes 8 ft long tending toward a "pancake" exchanger increasing the shellside pressure drop.

A solution can not be obtained by arbitrarily assuming a high heat flux. The arbitrary assumption of a heat flux of  $31,500 \text{ W/m}^2$  ( $10,000 \text{ Btu/h}\cdot\text{ft}^2$ ) would require only 1,216 m (3,988 ft) of tubes and would result in a calculated overall heat transfer coefficient of  $6930 \text{ W/m}^2\cdot\text{K}$  ( $1,221 \text{ Btu/h}\cdot\text{ft}^2\cdot{}^\circ\text{F}$ ) obtained by dividing the heat flux by the LMTD. The calculated overall heat transfer coefficient obtained by summation of the thermal resistances\* is only  $965 \text{ W/m}^2\cdot\text{K}$  ( $170 \text{ Btu/h}\cdot\text{ft}^2\cdot{}^\circ\text{F}$ )

---

\* Based on a 8-tube pass configuration.

requiring 8,730 m (28,643 ft) of tubing, or about seven times the length of tubes obtained in the original assumption. This length however results in one-seventh of the original heat flux assumption.

The pressure drop on the shellside of the exchanger was discussed in Sect. 8.2; tabulated results of the row-by-row analysis is presented in Appendix D.

## 10. CONDENSER DESIGN

The conceptual design of the condenser evolved from several parameters that remained unchanged through the actual manufacture of the unit. These parameters were the external tube surface area, the number of tubes, and the baffle spacing. There are several items that were changed in the final design of the condenser.

The basis for procurement was the condition that the manufacturer (Patterson and Kelley Company) would assume the mechanical responsibility, including adherence to various codes, and UCC-ND would assume the responsibility for the thermal flow performance.

In the conceptual design of the East Mesa condenser, several locations of the vapor inlet nozzle were considered. Originally the nozzle location was at the base of the condenser, as was done with the Raft River condenser. Nitrogen was the noncondensable gas present at the Raft River test site, and it was assumed that the light gas would accumulate at the top of the condenser where the vent line was located in the tubesheet of the condenser. In the case of the East Mesa condenser, carbon dioxide is the noncondensable gas expected to be present in amounts up to 0.2% by weight. Carbon dioxide, having a density less than but almost equal to isobutane, presented a different venting situation from the Raft River condenser. A proper venting system should provide for a continuous vent, a recovery condenser, and a recovery compressor. At the East Mesa facility, it was not possible to provide an adequate compressor for continuous venting because it takes about 1 hp for every 12 kg/h (27 lb/h) of vapor throughput. Therefore, the design was changed to a top vapor inlet so that the vapor stream containing the carbon dioxide has maximum contact with the condensate to facilitate dissolution of the noncondensable isobutane. The dissolved carbon dioxide is eventually disposed of in the isobutane recovery system through the brine returned to the direct-contact heat exchanger.

The ORNL VFTC includes design features that are somewhat unusual and not standard practice in the industry. Condensate downcomers design and fabrication methods are covered. The use of shrouds and impingement

baffles is also covered. A vibrational analysis was performed on the condenser, although with rolling the tubes into each baffle there seemed little need for this to be done leaving unsupported spans of less than 0.6 m (2 ft). The vibrational analysis indicated the design to be free of vibrational problems with maximum vapor velocities of 3 m/s (10 ft/s).

An idea of how the condenser will be installed at the test site and the plans for testing is covered, and finally the instrumentation and data acquisition system is briefly covered to give some idea of the expected accuracy of the forthcoming experiments.

#### 10.1 Design Criteria and Code Requirements

The design criteria for the East Mesa condenser were actually set by the site requirements at the Geothermal Component Test Facility at East Mesa, California, and by the State of California.

The shellside design pressure was specified as 1650 kPa (275 psig) at a temperature of 450 K (350°F). The tubeside design pressure is 690 kPa (100 psig) at 311 K (100°F). This was done to protect the condenser in the event of turbine damage, when the vessel could be exposed to higher instantaneous pressures even though there are pressure relief valves in the lines. The normal operating conditions on the shellside of the condenser are 333 K (140.6°F) and 487 kPa (70.6 psia) with the tubeside cooling water supplied at temperatures from 283-300 K (50-80°F) at a pressure of 618 kPa (75 psig). The tube material was specified as low-carbon steel having a carbon content not exceeding 0.10%. The tube sheet and shell material was specified as SA 515- Grade 70.

The design was in conformance with the following codes: (1) Section 8, Division 1 of the ASME Code for Unfired Pressure Vessels, (2) Tubular Heat Exchangers Manufacturers Association (TEMA) Class B, (3) Uniform Building Code (UBC) for seismic zone 4, and (4) CAL/OSHA Standards Section.

## 10.2 Design Description

A cutaway diagram of the East Mesa VFTC (Fig. 22) shows the arrangement of the unit in the normal operating position, which is installed about 1° off vertical to facilitate drainage of the condensate in the downcomers and otherwise has no effect on the design of the condenser. This inclination is accomplished by mounting the condenser on a sloping pad.

The vapor, at a temperature of 333 K (140.6°F) and a pressure of 487 kPa (70.6 psia), enters the condenser through a 12-in. supply nozzle that is expanded to 24-in. prior to entrance into the condenser. The vapor strikes a perforated impingement baffle fabricated from 6-mm (0.25-in.) steel plate, which protects the tubes from direct exposure to the 4.5 m/s (15 ft/s) inlet velocity of the vapor stream.

The vapor condenses on the cold surface of the fluted tubes and flows down the vertical tube until it reaches the top baffle plate, where the condensate flows by gravity to the downcomer tubes located at the site of the baffle plate. The condensate enters the downcomers and is discharged on the splash plate at the base of the condenser. The downcomers are used to remove the condensate from the process as quickly as possible to minimize subcooling. Subcooling is a disadvantage in recovering heat in a geothermal power system because the heat must be made up at the direct-contact heat exchanger during the vaporization process, thus reducing the overall efficiency. In addition, the downcomers tend to increase the quality of the two-phase flow by removing the condensate from the tube as soon as possible.

The design of the baffle spacing (Sect. 8.2) provides for six traverse vapor passages with baffle spacings ranging from 1.54 m (60 in) to 0.33 m (13 in).

The anticipated condensate accumulated at each condenser baffle plate was obtained from Appendix D and sufficient 2.54-cm (1.0-in.) tubes were provided to allow for adequate drainage. The driving head,  $\rho L$ , of the condensate was equated to the frictional resistance in the tube to calculate the number of tubes required at each baffle. The allocation of the downcomers at each baffle is shown in Table 6.

ORNL-DWG 81-12529

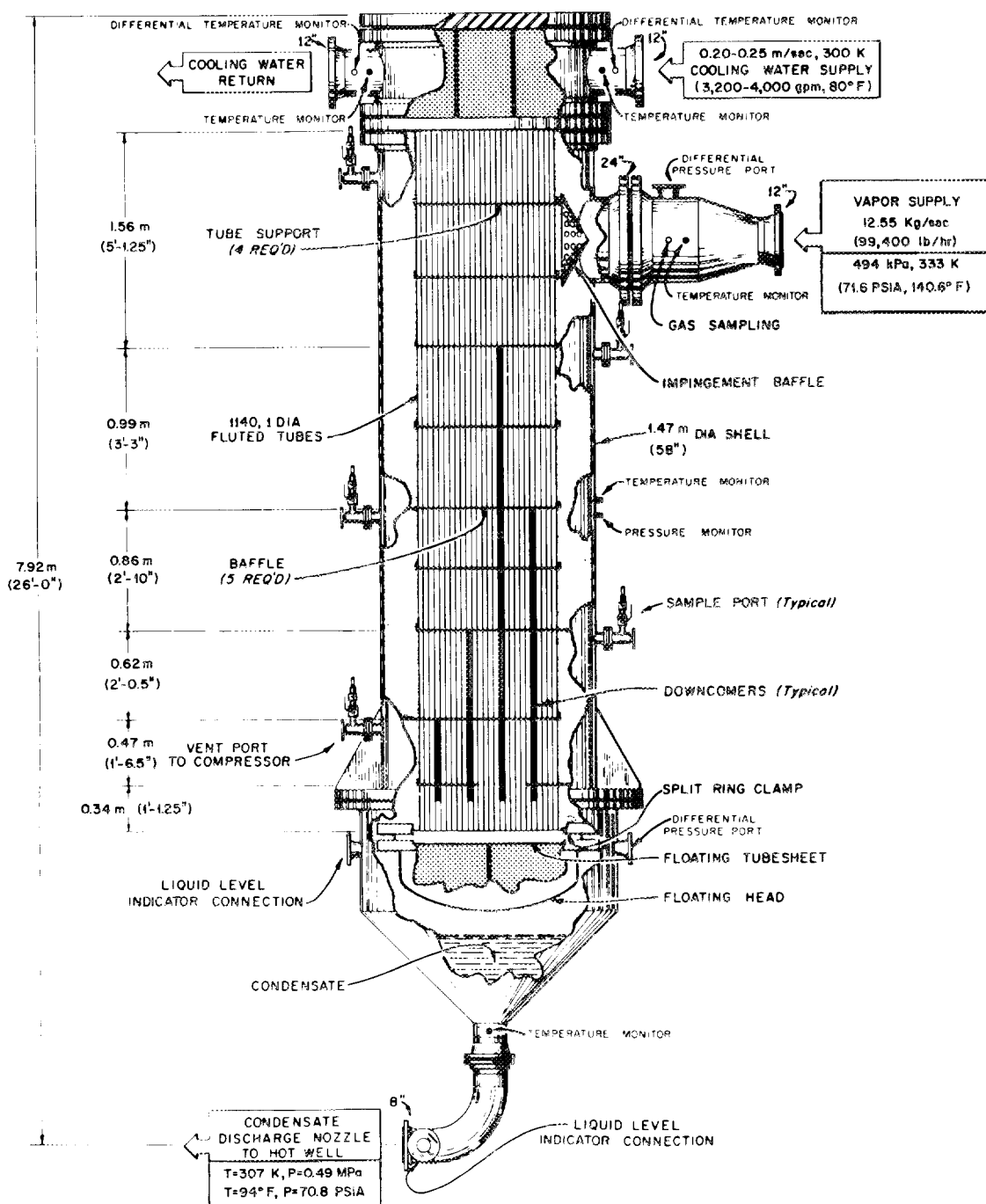


Fig. 22. Cross section of ORNL 5-MW vertical-fluted-tube condenser.

Table 6. Allocation of downcommers (DC) on baffles

Baffle	Downcommers	Condensate		Head required		DC length		Velocity		Pressure drop	
		kg/s	lb/h	m	ft	m	ft	m/s	fps	Pa	Psi
1	13	1.894	30,986	0.20	0.64	3.35	11	1.48	4.86	2482	0.36
2	9	1.380	22,579	0.23	0.76	2.13	7	1.56	5.12	2069	0.30
3	7	1.043	17,071	0.32	1.04	1.22	4	1.52	4.98	1517	0.22
4	5	0.770	12,605	0.35	1.15	0.61	2	1.57	5.15	1379	0.20
5	4	0.962	9,191	0.50	1.64	0.30	1	1.43	4.69	965	0.14

The baffles have a ridge along the edge to provide a holding area for the condensate and to keep the condensate from spilling over the baffles and to discharge the condensate through the downcommers as designed. The condenser was also provided with 3-mm- (0.125-in.-) thick vertical shrouds confining the vapor passage to a true cross flow pattern where the cross flow area is uniformly distributed at each tube row in the condenser to minimize vapor bypassing the tube bundle. The condensate is collected in a funnel-shaped tank at the base of the condenser and discharged to the hot well through a 8-in. Sch 40 pipe at a velocity of 1.65 m/s (5.4 ft/s).

To locate areas in the condenser where the noncondensables collect and to determine the distribution of the noncondensables throughout the condenser, probes were provided at six different locations. Five of the probes penetrate to the vertical midplane of the condenser as shown in Fig. 23. The probes are equipped with valve stations that permit samples of the gas to be extracted from the center of the condenser; temperature and pressure monitors are provided at the extraction point. A continuous or intermittent bleed of noncondensables can be made at any or all of these locations. All of these parts were fabricated from type 316 stainless steel to avoid contamination problems in the vapor analysis. The probes are slipped through the area that is incurred by tube separation allowed for the flow dividers in the header and the tube sheet resulting in a pitch of 44 mm (1.75 in.) at 3 horizontal locations. The probes are vertically positioned 5 cm (2 in.) below the baffles where the noncondensable CO<sub>2</sub> (MW = 44) is expected to accumulate because it is lighter than the isobutane (MW = 58).

The tubes were attached to the tubesheets by welding the tubes to the tubesheets in addition to rolling the tubes into scored holes. This method of attachment is the most efficient means offered by the manufacturer in obtaining leak-tight joints.

The water header is equipped with flow baffles to divide the header into an inlet section, a mixing U-turn section in the center, and a discharge section. In like manner the floating head is divided into two U-turn sections. In each of the sections in the floating head and

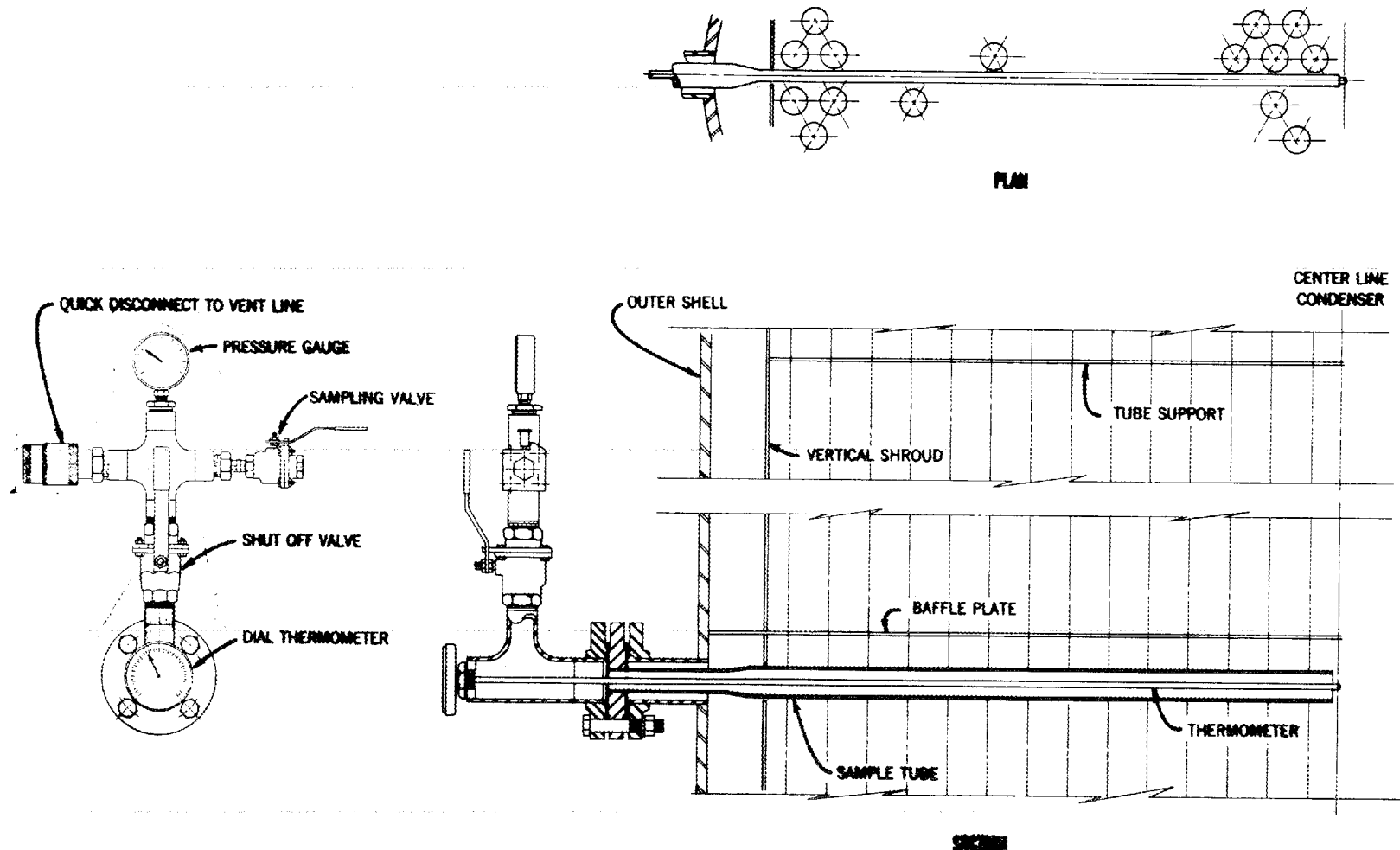


Fig. 23. Detail showing condenser gas sample and vent tubes.

the center section there is a complete flow reversal; in the entrance and exit sections there is a 90° change in direction. The pressure drops in all of these sections have been considered.

The floating head design was chosen for two reasons. First it offered a means of rolling the tubes into the baffles from either end with a 2.5-m (8-ft) extension roller. It was also found to be less costly than fabricating a U-tube bundle. The cost of the U-tube design involved added setup costs in the fluting operation, the cost of section welding the tubes, and bending costs.

Figure 24 shows the tube bundle of the exchanger during the final stages of construction. The impingement baffle can be used to orient the bundle with the shell. The downcomer locations can be identified as the 38 plugged holes to the extreme left of the tubesheet. The shroud between the tubesheet and the first baffle has not yet been attached.

ORNL-Photo 0203-81



Fig. 24. Tube bundle of ORNL 5-MW vertical-fluted-tube condenser.

Figure 25 shows the assembled unit and details of the water header. The six gas sample nozzles can be seen located on the near side of the condenser. The cylinder on top contains dry nitrogen which was used as a cover gas during shipment and storage before erection at the East Mesa test site. The valves shown in the photograph on the top of the water header are air vents on the three water compartments in the header.

ORNL-Photo 0205-81

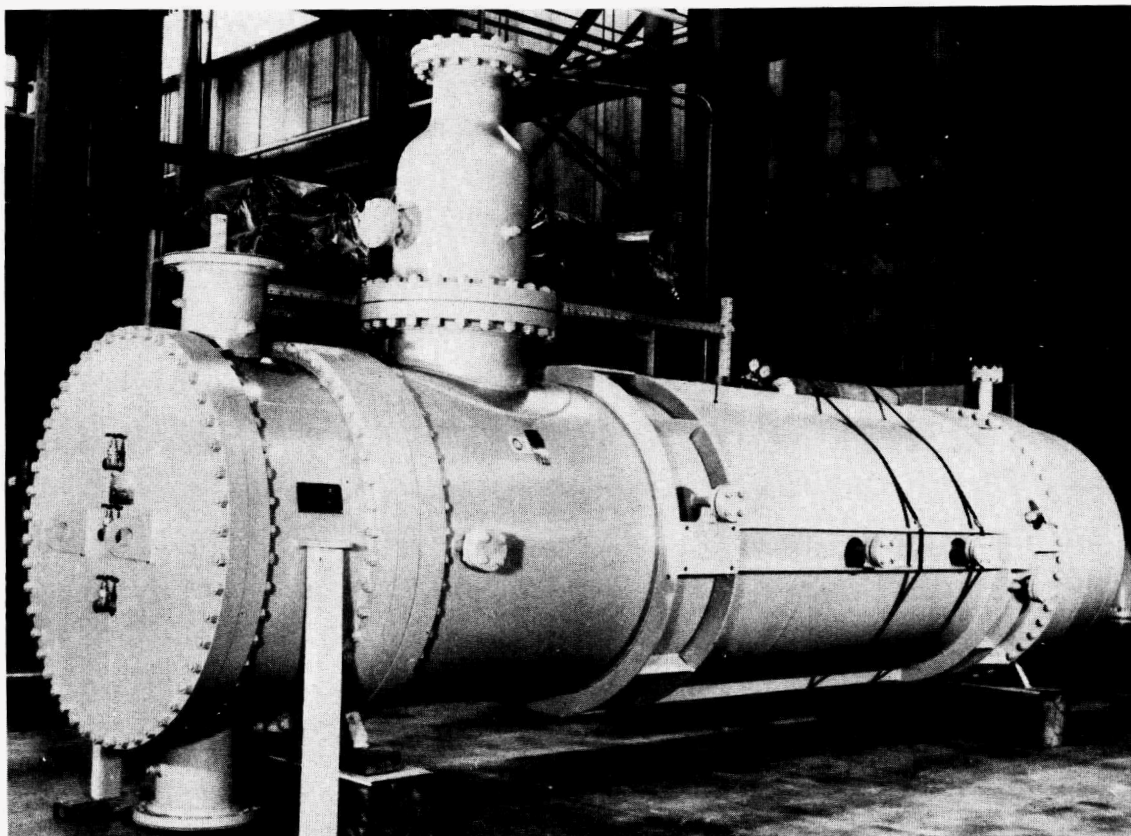
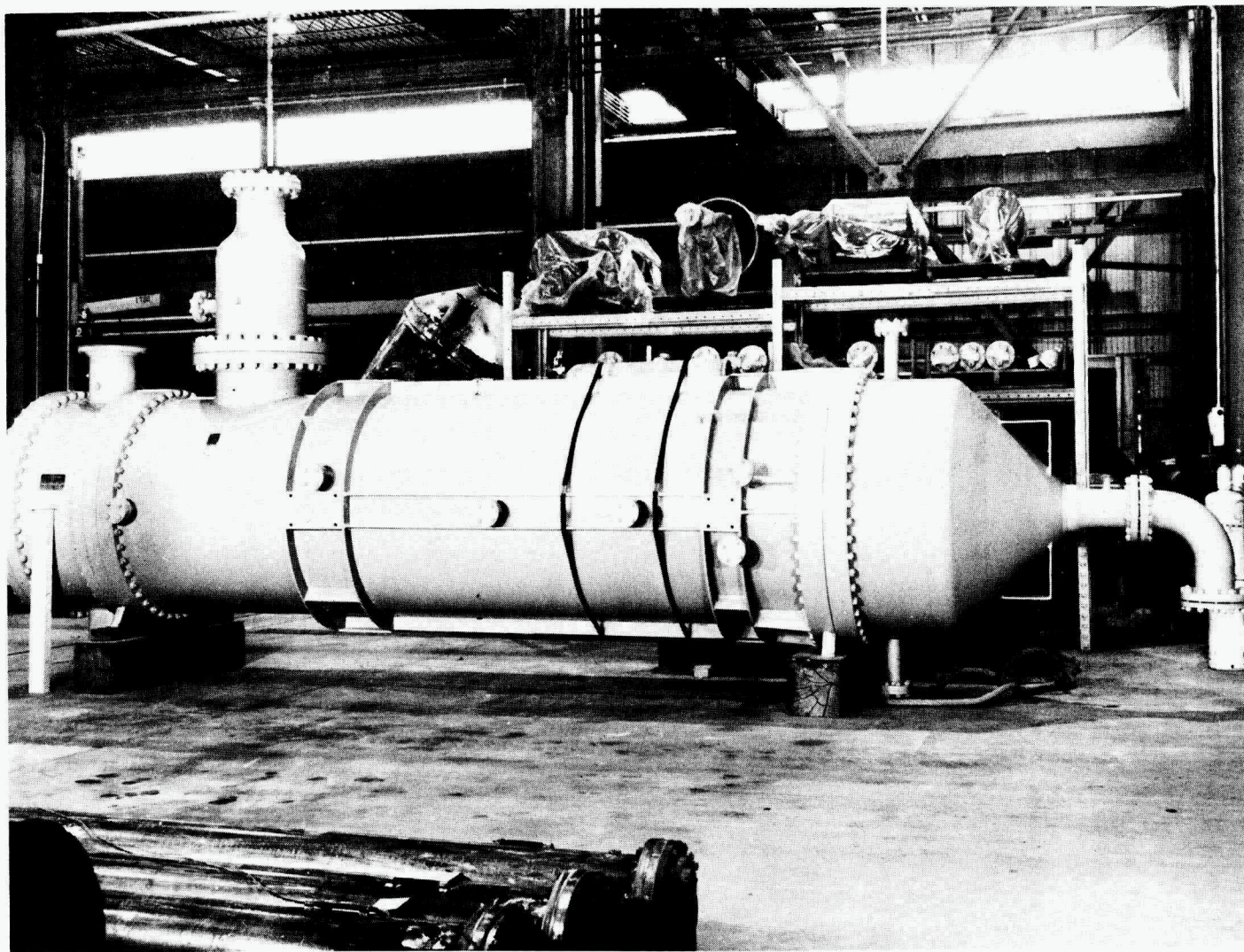


Fig. 25. Exterior view of ORNL 5-MW vertical-fluted-tube condenser showing header details.

Figure 26 shows the full length of the condenser and gives a good view of the condensate discharge nozzle. The reinforcing plates on the site of the condenser are for attaching the support legs and the frame on which the condenser is to be mounted. Special care was taken with the design of the frame because the condenser will be operated in a seismic high risk area.

ORNL-Photo 0204-81



70

Fig. 26. Full-length exterior view of ORNL 5-MW vertical-fluted-tube condenser.

### 10.3 Vibrational Analysis

The six-pass design for the East Mesa condenser was analyzed for potential flow-induced vibrational problems. Three excitation mechanisms were considered: (1) vortex shedding, (2) turbulent buffeting, and (3) fluid elastic instability. Conservative design guidelines were used to check for potential transverse tube vibrations and resonant vibrations.

The basic engineering approach is to use conservative design guidelines to prevent undesirable vibrations from occurring. The design guidelines, in one way or another, are related to the avoidance of the synchronization of the system's natural frequency with the excitation frequencies. Because the degree of conservatism in various guidelines varies, preoperation flow testing is essential in ensuring the performance and reliability of a heat exchanger.

Both tube vibration and acoustic resonance vibration evaluations were considered for the East Mesa condenser, and it was found to be free of vibrational problems.

#### 10.3.1 Tube Vibrational Evaluation

A common approach is to model each tube span as an individual beam under zero axial loading and with either clamped or hinged (simply supported) end supports. This approach is conservative and usually underpredicts the fundamental frequency of the tube. The fundamental frequency of the tube  $f_n$  expressed in Hertz is shown in Eq. (21)<sup>46</sup>

$$f_n = k (E I g_c / M_e)^{0.5} / 2 \pi L^2 \quad (21)$$

where

$k$  = an empirical constant,

= 9.87 for hinged supports used in this analysis,

$E$  = Young's modulus of elasticity =  $6.76 \times 10^8 \text{ kg/m}^2$  ( $26 \times 10^6 \text{ lb/in.}^2$ ),

$I$  = Moment of inertia for tube =  $3.5 \times 10^{-8} \text{ m}^4$  ( $0.084 \text{ in.}^4$ ),

$g_c$  = acceleration due to gravity =  $9.81 \text{ m/s}^2$  ( $32.17 \text{ ft/s}^2$ ),

$M_e$  = effective mass/unit length =  $1.25 \text{ kg/m}$  ( $0.07 \text{ lb/in.}$ ),

$L$  = span length, m (in.).

Substituting the appropriate span lengths in the above equation, the natural frequencies for each pass of the East Mesa condenser were calculated and tabulated in Table 7.

Table 7. Natural frequencies in tube passes  
for 5-MW ORNL East Mesa condenser

Pass	Tube supports	Span m (ft.)	Natural frequency (Hz)
1	2	0.36 (1.71)	165
2	1	0.57 (1.88)	66
3	1	0.43 (1.42)	116
4	0	0.62 (2.04)	56
5	0	0.47 (1.54)	97
6	0	0.35 (1.13)	185

For a given gap flow velocity, the corresponding critical tube span length can be calculated<sup>47</sup> using Eqs. (22), (23), and (24). The resulting values will not be equal. For the East Mesa condenser, the vortex shedding criteria gives the least critical length, while turbulent buffeting gives the greatest. The upper and lower values define an uncertainty region when the critical length is plotted against the gap flow velocity. The design and operation condition should be below the uncertainty region.

$$(L)_{cr} = \left[ \frac{K}{2\pi} \frac{D}{SV} \right]^{1/2} \left[ \frac{EI g_c}{M_e} \right]^{1/4}. \quad (22)$$

$$(L)_{cr} = \left[ \frac{K \ell t}{2\pi D \theta V^2} \right]^{1/2} \left[ \frac{EI g_c}{M_e} \right]. \quad (23)$$

$$(L)_{cr} = [9.87 KD/V]^{1/2} \left[ \frac{M_e \sigma_o}{\rho D^2} \right]^{1/4} \left[ \frac{EI g_c}{M_e} \right]^{1/4} \quad (24)$$

where

V = maximum velocity,

D = tube diameter,

$\ell$  = longitudinal tube spacing,

t = traverse tube spacing,

$K = 0.33$ ,  
 $\ell = 0.80$ ,  
 $\theta = 3.05(1 - D/t)^2 + 0.28$ ,  
 $\rho = \text{gas density}$ ,  
 $\sigma_0 = 0.0033$ ,  
 $f_s = \text{vortex shedding frequency}$ ,  
 $S = \text{Strouhal number} = f_s D/V$ .

These equations have been used to construct the tube vibration criteria diagram (Fig. 27), which can be used to predict vibrational problems in the East Mesa condenser for each tube pass based on the unsupported tube length and cross flow velocity.

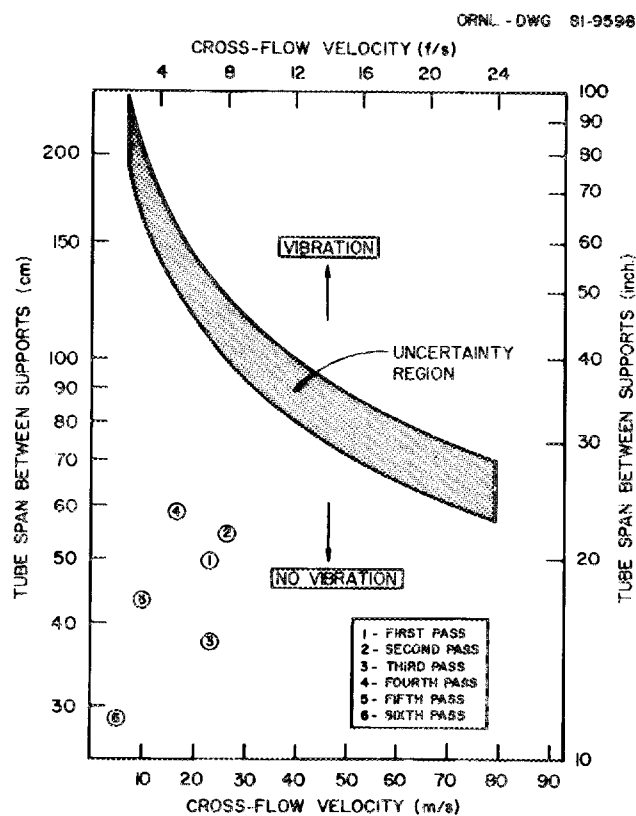


Fig. 27. Tube vibration criteria diagram.

### 10.3.2 Acoustic Resonance Vibration Evaluation

When the shellside fluid is a gas, the fluctuations caused either by vortex shedding or turbulent buffeting can excite the shellside gas column to a resonating condition. An acoustic resonance will produce a loud noise and increase the shellside pressure loss, thus affecting the performance of the heat exchanger.

The frequency of an acoustic standing wave in a cylindrical shell ( $f_a$ ) is given in Eq. (25):

$$f_a = \frac{nc}{a} . \quad (25)$$

where

$n$  = a constant depending on the mode excited,

$c$  = speed of sound in the shellside gas,

$a$  = inside shell diameter.

The mode of primary interest is the first, for which  $n = 0.5861$ . Values of  $n$  for the higher modes can be found in Ref. 48. The speed of sound is given in Eq. (26):

$$d = [z\gamma gRT]^{1/2} \quad (26)$$

where

$z$  = compressibility factor, for isobutane at design conditions = 0.84,

$\gamma$  = specific heat ratio,

$g$  = gravitational constant,

$R$  = gas constant for isobutane,

$T$  = absolute shellside gas temperature.

At the design operating temperature of 307K (94°F), the speed of sound in isobutane is 203.8 m/s (668.7 ft/s).

When the excitation frequency is within  $\pm 20\%$  of the acoustic standing wave frequency, the phenomena of acoustic resonance is likely to occur.

The equations describing the resonant range are:

$$f_s = \beta f_a \quad (27)$$

$$f_t = \beta f_a \quad (28)$$

with

$$0.8 < \beta < 1.2 .$$

Equation (27) applies to vortex shedding and (28) to turbulent buffeting.

For a given gap flow velocity, the range of inside shell diameters that could lead to an acoustic resonance are given by:

$$a = \frac{(0.5861)\beta D_c}{SV} \quad (29)$$

for vortex shedding and for turbulent buffeting:

$$a = \frac{(0.5861)\beta c l t}{V D} \quad (30)$$

where

$$0.8 < \beta < 1.2$$

For a given gap flow velocity V, the smallest and largest inside shell diameter as calculated from Eqs. (29) and (30) define the resonance region. For a safe design, the design operating condition should be outside the resonance region. Figure 28 is a plot of the inside shell diameter against the gap flow velocity; it is observed that the East Mesa condenser is well below the resonance region for all six passes.

#### 10.4 Data Acquisition and Instrumentation

The condenser is fully equipped with instrumentation to provide sufficient data to accurately determine the heat transfer in both the vapor and coolant streams. The accuracy of the instrumentation was made commensurate. It is not good logic or economically feasible to have the capability of determining a temperature difference to within  $\pm 0.1\%$  when the flow rate is determined to within  $\pm 10\%$ . It would be more logical to have both the temperature difference and the flow rate to be within 1% yielding a system accuracy of  $\pm 98\%$  in determining the total heat rate. An excellent article has been written by J. F. Whitbeck<sup>49</sup> in selecting instrumentation for geothermal heat recovery systems and was quite helpful in designing the instrumentation for the East Mesa condenser.

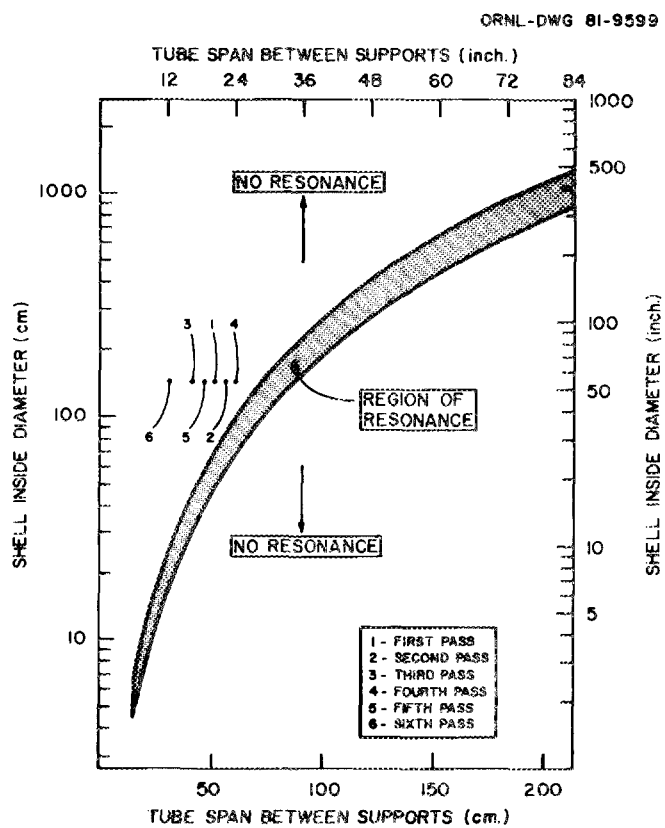


Fig. 28. Acoustic resonance diagram.

The most accurate means of determining the total heat transfer in the condenser is in the coolant stream. It is a single-phase fluid, the pertinent physical properties are essentially constant and reliable, and it is convenient to monitor. The location of the temperature monitor in the water supply stream really doesn't matter because the fluid is assumed to be well mixed as it enters the supply line. The location of the temperature monitor on the coolant discharge was intentionally located downstream of the condenser so that adequate mixing can occur. Resistance thermometers were provided to monitor the minimum, maximum, and temperature difference in the coolant stream. The flow rate is monitored by a calibrated orifice meter. The estimated accuracy at the data logger used for the differential temperature is better than 99.8%. The estimated accuracy at the data logger for the flow meter data is 99%. The recorded data takes into account the total accuracy including the

errors encountered in the instrument, the transmission, and the recording. The accuracy of all temperature determinations is better than 99.8%. All resistance thermometers (RTDs) are installed in thermowells so that they may be replaced without having to shut down the process.

The vapor stream is monitored by a venturi that was installed in the line to the existing system and is probably 98% accurate at the recorder. This isn't too helpful but can be used for making heat balances within  $\pm 2\%$ . The vapor stream pressure and temperature is monitored at three locations in the condenser: the vapor supply line, at the midpoint in shell, and at the condensate discharge. The differential pressure measurement is also monitored and transmitted to the data logger. The expected accuracy of the differential pressure transmitters is better than 99.8%. The accuracy of the pressure at the recorder is better than 99.5%.

A liquid hold up volume is provided in the funnel at the base of the condenser. A differential pressure cell monitors the liquid level in the funnel where the data are transmitted to the data logger.

Dial thermometers with errors of less than 0.6K ( $1^{\circ}\text{F}$ ) have been provided at the six sample ports on the condensers whose location can be seen in Fig. 20. These ports are also equipped with pressure gages with errors of no greater than 1% of the range or 14 kPa (2 psi). More accurate electronic instrumentation can be added at these ports as warranted. It is intended that this instrumentation be used by the person taking the vapor samples to determine any sudden changes in the sampling conditions.

The vapor samples are taken in 1-liter metal containers equipped with 6-mm (0.25-in.) sample nozzles. The samples collected will be analyzed on site using a Varian chromatographic analyzer that can provide quantitative analyses on all of the pertinent hydrocarbons, oxygen, and carbon dioxide. The Karl Fischer method will be used to obtain water content in the vapor and liquid isobutane samples.

### 10.5 Site Testing

The ORNL VFTC was fabricated at Patterson-Kelley's factory at East Stroudsburg, Pennsylvania, and shipped by truck to the geothermal test site at East Mesa, California. The support frame for the condenser was fabricated in Patterson-Kelley's factory at Mineral Wells, Texas.

The ORNL VFTC was connected to the existing system at the 6-2 Wellhead at the test site (as was shown in Fig. 1). Testing is planned for the winter of 1981.

The test site is located in the desert region in the extreme southeastern part of California near Holtville. Holtville is in the Imperial Valley east of El Centro.

The present schedule for testing is to run the condenser with the Supercritical Heat Exchanger Field Test (SHEFT) unit for about two weeks and then switch to the Direct Contact Heat Exchanger (DCHX) for two weeks for supply of the working fluid. The advantages of using the SHEFT unit is that it provides a constant source of relatively pure isobutane gas with a known composition. When the DCHX is used, about 1.5% by weight of water vapor condenser plus CO<sub>2</sub> that accumulates in the vapor stream are carried over into the condenser.

The proposed scheme for evaluating the overall heat transfer coefficient of the condenser in both modes of operation is:

1. Obtain the temperature drop across the condenser, (T<sub>2</sub> - T<sub>1</sub>) from the differential transmitter and inlet and outlet water temperatures T<sub>1</sub> and T<sub>2</sub>.
2. Obtain the coolant water flow rate, W<sub>w</sub>.
3. Calculate directly the overall heat transfer as shown in Eq. (31)

$$U_o = \frac{W_w C_p (T_2 - T_1) \ln[(T_2 - T_c)/(T_1 - T_c)]}{[(T_2 - T_c) - (T_1 - T_c)] A_o} \quad (31)$$

where

C<sub>p</sub> = constant specific heat of water,

A<sub>o</sub> = total outside heat transfer area of condenser = 687 m<sup>2</sup> (7400 ft<sup>2</sup>),

T<sub>c</sub> = condensing temperature.

A second calculation can be made to check the total heat transfer by accounting for the heat on the shellside. This involves knowledge of parameters that are not immediately available such as the quality and content of steam in the vapor supply.

The scheme presented for evaluating the condenser is in reality an effort to find how good our design predictions were and to substantiate the single-tube experimental data. The design conditions need to be produced which means a vapor supply temperature of 333 K (140.6°F) at a pressure of 487 kPa (70.6 psia) and a coolant supply of 0.221 m<sup>3</sup>/s (3500 gpm) at a temperature of 300 K (80°F).

The prime objective in testing the 5-MW condenser is to compare the field test results with results obtained in the laboratory. If these field test results are significantly different, reasonable explanations should be provided to account for the differences.

One of the proposed investigations concerns noncondensables, mainly CO<sub>2</sub>, that accumulate in the working fluid. Complete and accurate solubility data, equilibrium constants, and even composition of the working fluid is often lacking. Solubility data for propane and isobutane in water and water in propane and isobutane can be found in Appendix B.5 and B.6. The plots were obtained using Henry's Law, giving some idea of how solubility is affected by temperature at the operating pressure of the condenser.

During normal operating conditions in the DCHX mode, gas samples will be collected at each of the six sample points at various times to find out where and in what concentrations the noncondensables are collecting. Once this is determined, a permanent vent or vents may be provided, eventually equipped with a cooler condenser to strip the hydrocarbons during the venting process. CO<sub>2</sub> will be introduced intentionally into the system to bring the concentration to a point where it starts to have a significant effect on the heat transfer and find out if the vents provided on the condenser can remove the noncondensable.

The testing procedures will involve independently changing the flow rates of the working fluid and the coolant. Changing the mass flow rate of vapor will cause a proportional increase or decrease in the heat

load as well as the temperature difference in the coolant. Changing the mass flow rate of the coolant should cause a proportional change in both the condensing temperature and the coolant discharge temperature and pressure, although the heat load would remain constant.

It would be desirable to observe the condensing conditions with various amounts of superheat in the vapor using a constant coolant flow rate at a constant coolant supply temperature. Whether or not all the planned operations can be carried out will depend on the system performance, the brine delivery conditions and the wetbulb temperature during the experimental operation period.

After completing each scheduled test with the SHEFT and DCHX units in operation, it is planned to inspect and photograph the inside of the tubes using a borescope. The 1.0-in. vent valves provide sufficient room to introduce the flexible scope into tubes beneath the valves. This procedure will give comparisons of the relative tubeside corrosion incurred in the two processes. The borescope will be used to observe the shellside of the tubes through the vent ports to verify any fouling or oil buildups. Photographs of both the interior and exterior tubes will document such problems that may be encountered.

Similar procedures have been used in controlled tests performed on fluted tube condensers<sup>50</sup> in condensing ammonia for the OTEC program. Work was also done in testing a vertical-fluted-tube evaporator in conjunction with the OTEC project.<sup>51</sup>

## 11. RELATED PRESENT AND FUTURE WORK

The turbine discharge condenser for the recently built 5-MW(e) Raft River power station in Idaho has carbon steel tubes that were designed based on the assumption that a source of fresh coolant make-up water would be available. The smooth tube horizontal U-tube condenser has 7900 19-mm (3/4-in.) diam tubes providing about  $5950 \text{ m}^2$  ( $64,000 \text{ ft}^2$ ) of heat transfer surface. The heat flux on these tubes is about  $6760 \text{ W/m}^2$  ( $2150 \text{ Btu/h}\cdot\text{ft}^2$ ). The expected overall coefficient is about  $695 \text{ W/m}^2\cdot\text{K}$  ( $122 \text{ Btu/h}\cdot\text{ft}\cdot{}^\circ\text{F}$ ). As it turns out, geothermal brine must be used as make-up for the cooling water, and replacement condensers are being considered for this unit where salt water resisting alloys must be utilized.

An in-depth study was made by UCC-ND for the replacement condenser. First of all, manufacturers of plate and frame, spiral, and evaporative units were contacted. All but the evaporative manufacturers declined interest for reasons of size, cost, or materials. Baltimore Air Coil could offer only stainless steel tubes and estimated the total cost to be about \$1.6M (1981); they allowed for the cost of their stainless steel tubed units to be about four times the cost of the units with carbon steel tubes.

Using newly developed alloys such as SEACURE (produced by the Trent Tube Division of Colt Industries) or AL29-4C (a competitive alloy developed by Allegheny-Ludlum), it was found that a horizontal exchanger designed for this application would cost about \$1.8M.

A bayonet-type exchanger requiring only 2,000 vertical fluted tubes providing  $2346 \text{ m}^2$  ( $25,000 \text{ ft}^2$ ) of heat transfer surface could do the job with the cost estimated at less than \$700 K. A more standard unit similar to the mesa condenser is estimated at \$900 K. A total of eight separate designs were investigated and costs estimated using the newly developed saline resistant alloys.

The study included two horizontal units for direct comparison — one fixed and the other U-tube. U-tube units were found to be more

expensive because the tubes had to be section welded as well as bent. It is more economical to use fixed or floating heads in the large size units than to employ the U-tube design.

A study has been made on compatible tubing alloys in contact with salt and brackish water. All of the alloys shown in Fig. 29 are highly resistant to salt water and aerated salt water, which is a more severe case. Grade AS-179 carbon steel is the only material presented (in Fig. 29) that is severely attacked by salt water and is included for cost comparisons.

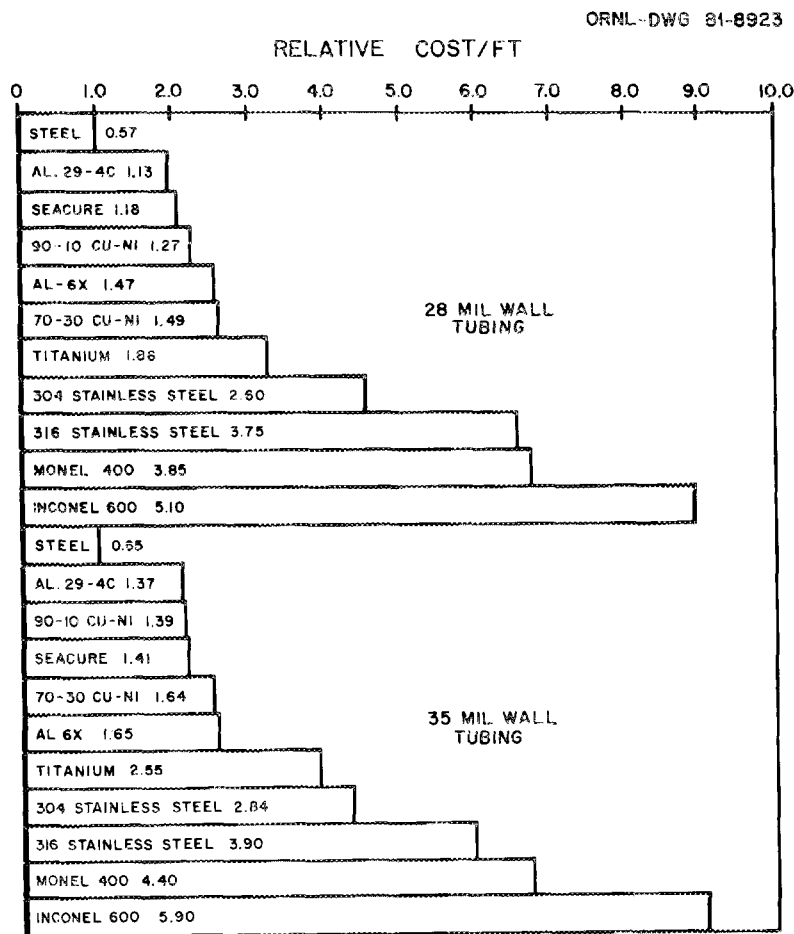


Fig. 29. Relative cost of saline resistant tube materials  
(March 15, 1981).

There remains development work to be done on the VFTCs. Plastic or rubber might be utilized for tube supports and baffles. Extrusion methods ought to be reinvestigated in an effort to reduce the cost of production of flutes. More expedient means of attaching tubes to the baffles need to be investigated.

Experimentally, we need to modify our test rig to extend the capabilities for testing tubes up to 9-m (30-ft) long to further investigate the effects of vertical tube lengths on condensing performance.

The effect of noncondensables on the overall heat transfer in condensers is not fully understood, and it is hoped that the test runs at the East Mesa test site on the ORNL condenser will shed some light on this dilemma. We intend to monitor the component gas concentrations, through the use of a gas chromatography, at six different elevations in the condenser via snorkel tubes that go to the center of the condenser to find exactly where the noncondensables accumulate and in what quality.

We will experimentally determine the effects of superheat coolant and vapor flow rates on the condensing pressure, which is a means of evaluating the condenser performance.

Resistance thermometers (RTDs) have been installed on the condenser to monitor the temperature rise in the coolant stream in conjunction with a orifice meter to accurately determine the total heat load on the condenser.

Recent test data from the Raft River geothermal test station on the 104-tube VFTC has been yielding overall heat transfer coefficient of about  $2270 \text{ W/m}^2\cdot\text{K}$  ( $400 \text{ Btu/h}\cdot\text{ft}^2\cdot{}^\circ\text{F}$ ) with the vapor containing 9K ( $25^\circ\text{F}$ ) more superheat than expected. We are trying to confirm whether increased superheat tends to reduce the efficiency of the condenser.

We would like to extend these experiments to cover condensing steam. This creates new problems such as corrosion, fatigue, and more vibration at higher velocities. Tube wall thickness might have to be increased with high pressure steams. New tube configurations may have to be developed for steam which has physical properties quite different from isobutane. There is some consolation in that much higher heat transfer coefficients can be obtained which should lead to more efficient condensers.



## 12. CONCLUSIONS AND RECOMMENDATIONS

We firmly believe that a VFTC having an overall heat transfer coefficient of greater than  $2840 \text{ w/m}^2 \cdot \text{K}$  ( $500 \text{ Btu/h} \cdot \text{ft}^2 \cdot {}^\circ\text{F}$ ) can be built for condensing isobutane. To accomplish this task, both inside and outside fouling would have to be cut to a minimum, the exchanger operated at the optimum heat flux, maximum tubeside velocity achieved, and probably most important, the isobutane kept free of oils and non condensables.

A recapitulation of the good points of the VFTC includes the fact that the tube count of a horizontal-smooth-tube unit can be reduced by a factor of at least five. An added advantage is that when the number of tubes are decreased, the shell diameter is also decreased, thus saving both shell and structural material.

VFTCs can be built by standard heat exchanger manufacturers if one is willing to accept responsibility for the heat transfer performance. The manufacturers will build the unit in conformance with TEMA standards and negotiate any necessary deviations.

The major task in this effort was the design and procurement of the fluted tubes. The cost of the fluting is a flat "per foot" cost. With inexpensive tube material, the fluting cost is, therefore, relatively high: about 75% of the total cost of the fluted tube; with expensive tube material, it can be relatively low: about 20% of the total cost.

The advantage of using vertical-fluted-tube exchangers is obtaining higher overall heat transfer coefficients and condensing more vapor per unit cost than either horizontal- or vertical-smooth-tube exchangers requiring the same total tube length. The disadvantages are higher tubing cost, cost of sealing the tubes to the baffles, and having to resort to multipassing the coolant to achieve the desired high coolant velocities. In spite of this, fluted tubes are attractive alternatives to smooth-tube-horizontal heat exchangers for low-temperature waste heat utilization. If some of these disadvantages could be overcome, it would make the fluted tube units even more attractive.

One means of accomplishing this objective is employing a bayonet design with the fluted tube as the sheath with a plastic tube as a

bayonet. Using this method, there would be less than a 0.05 K (0.1°F) temperature increase in the coolant in the plastic tube. This means that the bayonet condenser would be truly counter-current with the condensation split evenly between the tubes. Plastic baffles might be used that could be attached to the tubes by application of heat. To fabricate the bayonet, the fluted tube would have to be provided with a hollow spherical tip. These and other methods are under current investigation as are cost comparisons on various tubing materials suitable for use with geothermal brines and brackish water. As manufacturers become more familiar with fluted tubes and fluted tube exchangers, the fabrication costs will be reduced and we should see more of these units in industrial usage.

#### ACKNOWLEDGMENTS

This report was done in cooperation with the Energy Division through J. W. Michel as part of the Waste Heat Rejection Program sponsored by the U.S. Department of Energy, Division of Geothermal Energy, under Contract No. W-7405-end-26 with Union Carbide Corporation's Nuclear Division (UCC-ND).

I wish to acknowledge the help of several members of the UCC-ND staff who made contributions to this report as well as to the design and development of the East Mesa condenser:

Dr. K. H. Luk of the Systems Engineering Department performed the vibrational analysis and verified the arrangement of the baffles and tube supports.

W. D. Hoyle did the drafting work and contributed many original ideas to the conceptual design of the condenser. T. Whitus and D. J. Kincaid did the excellent graphics contained in the report.

J. W. Wells and W. P. Huxtable, although not assigned to the project, are thanked for their consultation on condensation theory and excellent references.

I also wish to express my appreciation to J. W. Michel of the Energy Division and the Project Manager, who orginally suggested the project, and to Drs. R. W. Murphy and M. Siman-Tov, who reviewed the report and offered technical consultation.



#### REFERENCES

1. K. J. Bell, Condensation, 8th International Heat Transfer Conference, Paris, France, August 1978, Vol. III, pp. 361-375.
2. Vehara Hervo, *Design of Condensers*, Thermal Pollution Administration (Netsu Kanri to Kogai), 28(9-12).
3. Jerry Taborek, *Heat Exchanger Design*, 6th International Heat Transfer Conference, Paris, France, August 1978, Vol. III, pp. 269-283.
4. Jerry Taborek, "Evolution of Heat Exchanger Design Techniques," *Heat Transfer Engineering*, 1(1): 15-29 (July-September 1979).
5. R. Gregorig, "Hautkondensation an feingewelten oberflachen bei Berksichtigung der Oberflachen spannungen," *Z. angew. Math. Phys.*, V, 36-49 (1954).
6. R. L. Webb, "A Generalized Procedure for the Design and Optimization of Gregoric Condensing Surfaces," *J. Heat Transfer*, 101, 335-339 (May 1979).
7. T. C. Carnavos, "Augmenting Heat Transfer in Desalination Equipment with Fluted Surfaces," Office of Saline Water Symposium on Enhanced Tubes for Distillation Plants, Washington, D.C. (March 1969).
8. L. G. Alexander and H. W. Hoffman, *Improved Heat Transfer Systems for Evaporators -- Performance Characteristics of Advanced Evaporator Tubes for Long Tube Vertical Evaporators*, ORNL/TM-2951 (January 1971).
9. D. G. Thomas, "Enhancement of Film Condensation Heat Transfer Rates on Vertical Tubes by Vertical Wires," *Am. Int. Chem. Eng. J.*, 14, 644 (1968).
10. D. G. Thomas, "Enhancement of Film Condensation Rate on Vertical Tubes by Longitudinal Fins," *Am. Int. Chem. Eng. J.*, 14(4): 644-649 (July 1968).

11. A. E. Bergles and M. K. Jensen, *Enhanced Single Phase Heat Transfer for Ocean Thermal Energy Conversion Systems*, ORNL/Sub-77/14216/1 (April 1977).
12. S. K. Combs, *An Experimental Study of Heat Transfer Enhancement for Ammonia Condensing on Vertical Fluted Tubes*, ORNL-5356 (January 1978).
13. S. K. Combs, *Experimental Data for Ammonia Condensation on Vertical and Inclined Tubes*, ORNL-5488 (January 1979).
14. C. B. Panchal and K. J. Bell, "Analysis of Nusselt-Type Condensation on a Vertical Fluted Surface," *Condensation Heat Transfer*, 18th National Heat Transfer Conference, San Diego, California, Aug. 6-8, 1979.
15. Y. Mori, K. Hijikata, S. Hirasawa, and W. Nakayamo, "Optimized Performance of Condensers with Outside Condensing Surface," *Condensation Heat Transfer*, 18th National Heat Transfer Conference, San Diego, California, Aug. 6-8, 1979.
16. C. F. Gottzmann, P. S. O'Neill, and P. E. Minton, "High Efficiency Heat Exchangers," *Chem. Eng. Prog.*, 69(7): 69-75 (July 1973).
17. R. M. Milton and C. F. Gottzmann, "High Efficiency Reboilers and Condensers," *Chem. Eng. Prog.*, 68(9): 56-61 (September 1972).
18. W. Wolf, "Heat Flux Tubing Conserves Energy," *Chem. Eng. Prog.*, 72(7) (July 1976).
19. S. K. Combs, G. S. Mailen, and R. W. Murphy, *Condensation of Refrigerants on Vertical Tubes*, ORNL/TM-5848 (August 1978).
20. J. W. Michel, "Enhancement on Vertical Fluted Surfaces," *Power Condenser Heat Transfer Technology*, P. J. Marto and R. H. Nunn, eds., Hemisphere Publishing Corporation, Washington, D.C., 1981.
21. R. W. Murphy, and N. Domingo, *Field Tests of 2-Tube and 40-Tube Condensers at the East Mesa Geothermal Test Site*, ORNL-5852.

22. N. A. Samurain and J. R. Shields, "Preliminary Design of Axial Flow Hydrocarbon Turbine," *Generator Set for Geothermal Applications*, EPRI ER 513 (May 1979).
23. K. E. Starlings, *Fluid Thermodynamic Properties for Light Hydrocarbon Systems*, Gulf Publishing Company, Houston, Texas, 1973.
24. D. H. Riemer, H. R. Jacobs, R. F. Boehm, and D. S. Cook, "A Computer Program for Determining the Thermodynamic Properties of Light Hydrocarbons," UTEC ME 76-211.
25. American Petroleum Institute, *Technical Data Book, Petroleum Refining*, 2d ed., 1970.
26. W. M. Rohsenow and J. P. Hartnett, *Handbook of Heat Transfer*, pp. 7-32, McGraw Hill, New York, 1973.
27. J. H. Perry, *Chemical Engineers Handbook*, 4th ed., pp. 10-14, McGraw Hill, New York.
28. David Butterworth and L. B. Cousins, "Use of Computer Programs in Heat Exchanger Design," *Chem. Eng. (N.Y.)*, 83(14): pp. 72-76 (July 5, 1976).
29. D. F. Othmer, Ph.D. Thesis, University of Michigan (1927), *Ind. Eng. Chem.* 21, 576 (1929).
30. F. C. Standiford, W. L. Badger Associates, Inc., Greenbank, Washington, "Effect of Noncondensibles on Condenser Design and Heat Transfer," *Chem. Eng. Prog.*, 75(7): 59 (July 1979).
31. A. P. Colburn and O. A. Houghton, "Design of Condensers for Mixtures of Vapors with Noncondensing Gases," *Ind. Eng. Chem.*, 26(11): 1170-82 (November 1934).
32. R. G. E. Franks, *Modeling and Simulation in Chemical Engineering*, Wiley-Interscience, New York, 1972.
33. J. Prausnitz, T. Anderson, E. Grens, C. Eckert, R. Hsieh, and J. O'Connell, *Computer Calculations for Multicomponent Vapor-Liquid and Liquid-Liquid Equilibria*, Prentice-Hall International Series in the Physical and Chemical Engineering Sciences, Prentice Hall, Inc., Englewood Cliffs, New Jersey, 1980.

34. N. Domingo, *Condensation of Refrigerant-11 on the Outside of Vertical Enhanced Tubes*, ORNL/TM-7797 (August 1981).
35. C. H. Gilmore, "No Fooling, No Fouling," *Chem. Eng. Prog.*, 61(7): 49-54 (July 1965).
36. *Standards of Tubular Exchanger Manufacturers Association*, 6th ed., New York, 1978.
37. D. Q. Kern, *Process Heat Transfer*, p. 845, McGraw Hill Book Company, New York, 1950.
38. C. J. Dobratz and C. F. Oldershaw, "Desuperheating Vapors in Condensers Unnecessary," *Chem. Eng. (N.Y.)*, 74, 146 (July 31, 1967).
39. S. W. Churchill, "Friction-factor Equation Spans all Fluid-Flow Regimes," *Chem. Eng. (N.Y.)*, 84(24), 91-92 (November 3, 1977).
40. D. Q. Kern, *Process Heat Transfer*, p. 273, McGraw-Hill Book Company, New York, 1950.
41. K. J. Bell, "Final Report of the Cooperative Research Program on Shell and Tube Heat Exchangers," Bulletin #5, University of Delaware, Newark, Delaware (June 1953).
42. J. W. Palen and Jerry Taborek, "Solution of Shell Side Flow Pressure Drop and Heat Transfer by Stream Analysis Method," *Chem. Eng. Prog. Symp. Ser.*, Heat Transfer -- Philadelphia 92(65): 53-63.
43. J. H. Perry, *Chemical Engineering Handbook*, 4th ed., pp. 5-30, Eq. (5-91), McGraw-Hill Book Company, New York.
44. D. A. Donahue Heat Transfer and Pressure Drop in Heat Exchangers, *Ind. Eng. Chem.*, 41: 2499 (1943).
45. D. F. Rudd and C. C. Watson, *Strategy of Process Engineering*, pp. 40-50, John Wiley & Sons, New York, 1968.
46. S. Timoshenko and D. H. Young, *Vibration Problems in Engineering*, p. 338, 3d ed., D. Van Nostrand Company, 1966.
47. K. H. Luk, ORNL Engineering Division, private communication, June 1979.

48. P. M. Morse, *Vibration and Sound*, 2d ed., McGraw-Hill, 1948.
49. J. F. Whitbeck, "Measurement and Control Techniques in Geothermal Power Plants," TREE-1312 (January 1979).
50. L. G. Lewis and N. F. Sather, *OTEC Performance Tests of the Carnegie-Mellon University Vertical Fluted Tube Condenser*, ANL/OTEC-PS-4 (May 1979).
51. James Lorentz, D. T. Yung, D. L. Hillis, and N. F. Sather, *OTEC Performance Tests of the Carnegie-Mellon University Vertical Fluted Tube Evaporator*, ANL/OTEC-PS-5 (July 1979).



## BIBLIOGRAPHY

- Adler, S. B., and Dominic F. Palazzo, "Sure You Are Using the Right 'K'?", *Chem. Eng. (NY)*, 66(13) 95-100 (1959).
- Afgan, N. H. and E. U. Schulünder, *Heat Exchangers: Design and Theory Sourcebook*, McGraw Hill, New York, 1974.
- Balekjian, G. and D. L. Katz, "Heat Transfer from Supertreated Vapors to a Horizontal Tube, *A.I.Ch.E. J.*, 4(1) 43-48, (March 1958).
- Beaty, K. O. and D. L. Katz, "Condensation of Vapors on Outside of Finned Tubes, *Chemical Engineering Progress*, Vol. 44, pp. 55 (1948).
- Bell, K. J., and M. H. Ghalay, "An Approximate Generalized Design Method for Multicomponent/Partial Condensers," *AIChE Heat Transfer Symposium Series No. 131* Vol. 69.
- A. E. Bergles, "Enhancement of Heat Transfer," 6th International Heat Transfer Conference Paris France, Volume III, pp. 89-108, August 1978.
- Cary, J. R., "Fast Convenient Approach to Sizing Heat Exchangers," *Chem. Eng. (NY)*, pp. 169-174, (May 18, 1959).
- Chen, N. H., "Tubeside Heat Transfer Coefficients for Streamline and Turbulent Flow," *Chem. Eng. (NY)*, pp. 114-126, (Jan. 12, 1959).
- \_\_\_\_\_, "Heat Transfer and Pressure Drop in Transverse Finned Shell-and-Tube Exchangers," *Chem. Eng. (NY)*, pp. 153-156, (Oct. 20, 1958).
- \_\_\_\_\_, "An Explicit Equation for Friction Factor in Pipe," *Ind. Eng. Chem. Fundam.*, 18(3) (1979).
- Cox, B. and P. A. Jallouk, *Experimental Determination of the Performance Characteristics of Eight Compact Heat Transfer Surfaces*, K-1832, Oak Ridge Gaseous Diffusion Plant (December 1972).
- Coury & Associates, Inc., *Heat Exchanger Design for Desalination Plant*, ORNL/TM-6734 (March 1979).

- Diehl, J. K. and C. H. Unruh, "Two Phase Pressure Drop for Horizontal Crossflow through Tube Banks," *Pet. Refiner*, 37(10) 124-120 (October 1958).
- D. M. Eissenberg et al, *Enhanced Tubes for Seawater Distillation Plants*, ORNL-TM-2611 (August 1969).
- Edwards, D. K., K. D. Gier, P. S. Ayyaswamy, and I. Cotton, "Evaporation and Condensation in Circumferential Grooves on Horizontal Tubes," ASME Publication, 73-HT-251 (1973).
- Ellis, P. F., II and M. F. Conover, *Materials Selection Guidelines for Geothermal Energy Utilization Systems*, DOE/RA/27026-1 (January 1981).
- Fanaritis, J. P. and J. W. Bevevino, "Designing Shell and Tube Heat Exchangers," *Chem. Eng. (NY)*, 62-71 (July 7, 1976).
- Foxhall, D. H. and P. T. Gilhert, "Selecting Tubes for CPI Heat Exchangers," *Chem. Eng. (NY)*, pp. 148-150, (April 12, 1976); II, pp. 101-104 (April 26, 1976); III, pp. 133-135 (May 10, 1976).
- Fujii, T. and H. Honda, "Laminar Filmwise Condensation on a Vertical Single Fluted Plate," *Proceedings of 6th International Heat Transfer Conference*, Vol. 2, pp. 419-424 (1978).
- Fujii, T. et al., "Heat Transfer and Flow Resistance in Condensation of Low Pressure Steam Flowing Through Tube Banks," *International Journal of Heat and Mass Transfer* Vol. 15 347-359, Pergamon Press, London, England.
- Gallant, R. W., "Sizing Pipe for Liquids and Vapors," *Chem. Eng. (NY)*, pp. 96-104, (Feb. 24, 1969).
- Ganapathy, V., "Quick Calculation for Exchanger Tubeshell Thickness," *Chem. Eng. (NY)*, p. 114, May 12, 1975.
- Gloyer, Walter, Thermal Design of Mixed Vapor Condensers, *Hydrocarbon Process.*, Part 1: pp. 103-107, (June 1970); Part 2: pp. 107-110 (July 1970).
- Green, M. A. and H. S. Pines, *Calculation of Geothermal Power Plant Cycles Using Program GEOTHM*, LBL-3238, (October 1975).

Gutteman, G., "Specify the Right Heat Exchanger," *Hydrocarbon Process.*, pp. 161-163, (April 1980).

Halford, J. A., ORICON: *A Fortran Code for the Calculation of A Steam Condenser of Circular Cross Section*, ORNL-TM-4248, (July 1973).

*Heat Exchange Institute Standards for Steam Surface Condensers*, Seventh Edition.

Heidemann, R. A., "Three-Phase Equilibria Using Equations of State," *AIChE J.* 20 (5) 847-855 (September 1974).

Hirasawa, S., K. Hijikata, Y. Mori, and W. Nakayama, "Effect of Surface Tension on Laminar Film Condensation along a Vertical Plate with a Small Leading Radius, *Proceedings of Sixth International Heat Transfer Conference*, Vol. 2, pp. 413-418 (1978).

\_\_\_\_\_, "Effect of Surface Tension on Laminar Film Condensation (Study of Condensate Film in a Small Groove)," *Transactions of JSME*, Vol. 44, pp. 2041-2048 (1978).

Holt, Co., Ben, *Geothermal Heat Exchanger Test at Heber, California*, EPRI ER-572 (August 1978).

Johnson, R. W., H. R. Jacobs, and R. F. Boehm, *Direct Contact Heat Transfer Between Two Immiscible Liquids in Laminar Flow Between Parallel Plates*, DCE/1549-1 (December 1975).

Kestin, Joseph, *Available Work in Geothermal Energy*, COO-4051-25, USDOE Geothermal Energy (July 1978).

\_\_\_\_\_, *Source Book on the Production of Electricity from Geothermal Energy*, DOE/RA/28320-2, U.S. Department of Energy (March 1980).

Khalifa, H. E. and Michaelides, *The Effect of Noncondensable Gases on the Performance of Geothermal Steam Power Systems*, COO-4051-36 (November 1978).

Krishna, Rajamani and C. B. Panchal, "Condensation of a Binary Vapor Mixture in the Presence of an Inert Gas," *Chemical Engineering Science* 12, 741-745, Pergamon Press, Great Britain, 1977.

- Krishna, R. et al., "An Ackerman-Colburn and Drew Type Analysis for Condensation of Multicomponent Mixtures," *Letters in Heat and Mass Transfer*, 3, 163-172 (1976).
- Kruger, Paul and Carel Otte, *Geothermal Energy Resources, Production, and Simulation*, Stanford University Press, Stanford, Calif., 1973.
- Lahaye, P. G., F. J. Neugebauer, R. K. Sahuja, A Generalized Prediction of Heat Transfer Surfaces, *J. Heat Transfer*, pp. 511-517 (November 1974).
- Leach, M. J., "An Approach to Multiphase Vapor-liquid Equilibria," *Chem. Eng. (NY)*, pp. 137-140, (May 23, 1977).
- Levi, J. E., "New Developments in Basics of Cooling Water Treatment," *Chem. Eng. (NY)*, pp. 88-92, (June 10, 1974).
- Lord, R. C., P. E. Minton, and R. P. Slusser, "Guide to Trouble Free Heat Exchangers," *Chem. Eng. (NY)*, pp. 153-160 (June 1, 1970).
- Matheson Company, *Matheson Gas Data Book*, Matheson Co. Inc., East Rutherford, N.J.
- Michel, J. W., and R. W. Murphy, "Enhanced Condensation Heat Transfer," *Heat Transfer - Orlando AIChE Symposium Series* pp. 183-191, (1980).
- Milora, S. L. and S. K. Combs, *Thermodynamic Representations of Ammonia and Isobutane*, ORNL/TM-5847 (May 1977).
- Milora, S. L. and J. W. Testor, *Geothermal Energy as A Source of Electric Power*, MIT Press, Cambridge, Mass., and London, England, 1976.
- Mothershed, C. T., *ORMEF: A FORTRAN Code for Computing Detail Multi-effect Multistage Flash Evaporation Desalination Plant Designs*, ORNL/TM-1560 (August 1966).
- MPR Associates, *Assessment of Condenser Leakage Problems*, EPRI-NP-1467 (August 1980).
- Mueler, Alfred C., "An Inquiry of Selected Topics on Heat Exchanger Design," Donald Q. Kern Award Lecture, 1975, Sixteenth National Heat Transfer Conference, St. Louis, Mo., (August 9, 1976).

- Nakayama, W., T. Daikoku, H. Kuwahara, and K. Kakizaki, "High-Flux Heat Transfer Surface 'THERMOEXCELL'," *Hitachi Review*, 24 (8), pp. 329-334 (1975).
- Neill, D. T., *Geothermal Shell and Tube Heat Exchanger Augmentation*, TREE-1023, (November 1976).
- Neitzel, J. W., *Cooling Methods Study for the Proposed Raft River Geothermal Power Plant*, ANCR-1203 (April 1975).
- Newson, I. H. and T. D. Hodgson, "The Development of Enhanced Heat Transfer Condenser Tubing," *Desalination*, Vol. 14, pp. 291, (1978).
- ORNL Engineering, *Design Guide for Heat Transfer Equipment in Water Cooled Nuclear Reactor Systems*, ORNL/TM-3573 (July 1975).
- Ramalho, R. S. and F. M. Tiller, "Improved Design Methods for Multipass Exchangers" *Chem. Eng. NY*, pp. 87-92, (March 29, 1965).
- Robertson, R. C., *Waste Heat Rejection from Geothermal Power Stations*, ORNL/TM-6533 (December 1978).
- Row, M. et al., "Heat Transfer and Air Blanketing in Steam Condensers," *I Mech E*, pp. 153-162 (1979).
- Schrodt, J. Thomas, "Simultaneous Heat and Mass Transfer from Multi-component Condensing Vapor-Gas Systems," *AICHE J.*, 19(4), pp. 753-759 (July 1973).
- Short, B. E., "Heat Transfer and Pressure Drop in Heat Exchanges," Engineering Research Series No. 37, Bureau of Engineering Research, University of Texas Publication No. 4324 (June 22, 1943).
- Spencer, R. A., Jr., "Predicting Heat-Exchanger Performance by Successive Summation," *Chem. Eng.*, pp. 121-124, (Dec. 4, 1978).
- Starczewski, J., "Short-Cut Method to Exchanger Tube Side Pressure Drop," *Hydrocarbon Proc.* pp. 121-124 (May 1971).
- Starling, K. E. and L. W. Fish, *HSGC, A Mixture Thermodynamic Computer Program*, ORO-4944-2 (December 1975).

Stephan, K., "Application of Multicomponent Thermodynamics to the Calculation of Thermal Separation Processes," *Cer. Chem. Eng.*, pp. 269-278 (1980).

Stern, Frederick and Votta Ferdinand, "Condensation from Superhead Gas-Vapor Mixtures," *AICHE J.* 14(6) (November 1968).

Taborek, J., "Evolution of Heat Exchanger Design," *Heat Transfer Engineering*, 1, 15-28 (July-Sept. 1979).

Tallackson, J. R., *CACHE-An Extended BASIC Program Which Computes the Performance of Shell and Tube Heat Exchangers*, ORNL/TM-4952 (March 1976).

Taneyama, T. and S. Simizu, "On the Transition of Dropwise-Film Condensation," *Proc. of 5th International Heat Transfer Conference*, Vol. 3, pp. 274 (1974).

Tleimat, B. W. et al., *Hydrocarbon Heat Transfer Coefficients Preliminary Isobutane Results*, LBL-8645 (February 1979).

Turner, S. E. and W. W. Madsen, *HEDCOR, A Heat Exchanger and Design Optimization Routine*, TREE-1112 (April 1977).

Uehara, H., K. Masutani, and M. Miyoshi, "Heat Transfer of Condensation on Vertical Fluted Tubes," pp. 146-160 in *Proceedings of the 5th Ocean Thermal Energy Conversion Conference*, Miami Beach, Fla., Feb. 20-22, 1978. DOE Report CONF-780236, Vol. 3, Sec 6.

Wahl, E. F. and F. B. Boucher, *Theory and Practice of Near Critical Pressure Direct Contact Heat Exchange*, SNA/1076-1 (October 1977).

Webb, R. L., and M. J. Scott, "A Parametric Analysis of the Performance of Internally Finned Tubes for Heat Exchanger Application," *Transactions of the ASME Journal of Heat Transfer*, 102, 38-42 (February 1980).

Wenzel, H. and W. Rupp, "Calculation of Phase Equilibria in Systems Containing Water and Supercritical Components," *Chemical Engineering Science*, 33, 683-687 (1978).

Williams, A. G., S. S. Nandapurkar, and F. A. Holland, "A Review of Methods for Enhancing Heat Transfer Rates in Surface Condensers, *The Chemical Engineer*, No. 233, pp. CE 367-373 (1968).

Wilson, J. L., "The Design of Condensers by Digital Computers," Paper presented at the Symposium on Design Decision and the Computer, Institution of Chemical Engineers, England (1972).

Yamamoto, Hiroshi and Toyoaki Ishibachi, "Calculation of Condensation Heat Transfer Coefficients of Fluted Tubes. The effects of gravitation and valley flow," *Heat Transfer - Jpn. Res.*, 7(3) 49-54 (Eng.) (1978).



Appendix A  
CONVERSIONS (METRIC/ENGLISH, ENGLISH/METRIC)

All quantities used in this report have been expressed in Scientific International (SI) units with the corresponding American Common Usage (ACU) units. Table A.1 gives the factors to convert from ACU units to the corresponding SI units. Table A.2 gives the factors to convert from SI units into the corresponding ACU units.

Table A.1. Factors to convert from American Common Usage (ACU) units into Scientific International (SI units)

To convert from	To	Multiply by
Btu/h	W	0.2929
Btu/h·ft <sup>2</sup>	W/m <sup>2</sup>	2.152
Btu/h·ft·°F	W/m·K	1.730
Btu/h·ft <sup>2</sup> ·°F	W/m <sup>2</sup> ·K	5.675
Btu/lb <sub>m</sub>	J/kg	2.324 × 10 <sup>3</sup>
Btu/lb <sub>m</sub> ·°F	J/kg·K	4.184 × 10 <sup>3</sup>
ft	m	0.3048
lb/h	kg/s	1.263 × 10 <sup>-4</sup>
ft <sup>2</sup>	m <sup>2</sup>	0.0929
ft/h <sup>2</sup>	m/s <sup>2</sup>	2.35 × 10 <sup>-8</sup>
fps	m/s	0.3048
gpm	m <sup>3</sup> /s	6.309 × 10 <sup>-5</sup>
in.	cm	2.54
lb/h	kg/s	1.263 × 10 <sup>4</sup>
lb <sub>f</sub> /ft	N/m	14.59
lb <sub>m</sub> /ft <sup>3</sup>	kg/m <sup>3</sup>	16.02
lb <sub>m</sub> /h·ft	Pa·s	4.134 × 10 <sup>-4</sup>
lb <sub>m</sub> /h·ft <sup>2</sup>	Pa·s/m	1.356 × 10 <sup>-3</sup>
psia	Pa	6.895 × 10 <sup>3</sup>
Δ(°F)	Δ(K) or (°C)	0.5556
Temperature conversion: T(K) = 5/9 [T(°F) - 32] + 273.15		

Table A.2. Factors to convert from Scientific International (SI) units into American Common Usage (ACU) units

To convert from	To	Multiply by
W	Btu/h	3.414
W/m <sup>2</sup>	Btu/h·ft <sup>2</sup>	0.3173
W/m·K	Btu/h·ft·°F	0.5780
W/m <sup>2</sup> ·K	Btu/h·ft <sup>2</sup> ·°F	0.1762
J/kg	Btu/lb <sub>m</sub>	4.303 × 10 <sup>-4</sup>
J/kg·K	Btu/lb <sub>m</sub> ·°F	2.390 × 10 <sup>-4</sup>
m	ft	3.281
cm	in.	0.3937
m <sup>2</sup>	ft <sup>2</sup>	10.764
m/s <sup>2</sup>	ft/h <sup>2</sup>	4.255 × 10 <sup>7</sup>
m/s	ft/s	3.281
m <sup>3</sup> /s	gpm	1.585 × 10 <sup>-4</sup>
N/m	lb <sub>f</sub> /ft	0.0685
kg/s	lb <sub>m</sub> /h	7.920 × 10 <sup>3</sup>
kg/m <sup>3</sup>	lb <sub>m</sub> /ft <sup>3</sup>	0.0624
Pa·s	lb <sub>m</sub> /h·ft	3.190 × 10 <sup>3</sup>
Pa·s/m	lb <sub>m</sub> /h·ft <sup>2</sup>	7.375 × 10 <sup>2</sup>
Pa	psia	1.450 × 10 <sup>-4</sup>
Δ(K) or Δ(°C)	ΔT(°F)	1.8
Temperature conversions: T(°F) = [1.8 T(°C)] + 32		

Appendix B  
PROPERTIES OF ISOBUTANE

Appendix B contains data on pertinent thermodynamic and physical properties of isobutane. Figure B.1 shows the latent heat of isobutane as a function of temperature at a pressure of 1 atm. Figure B.2 shows the vapor pressure of isobutane as a function of temperature. Figure B.3 shows the specific heat of isobutane gas at 1 atm as a function of temperature. Figure B.4 is a diagram showing the enthalpy of isobutane as a function of temperature and pressure. Figure B.5 shows the solubility of both propane and isobutane in water as functions of temperature. Figure B.6 shows the solubility of water in propane and isobutane as functions of temperature. These data have been abstracted from equations presented in Ref. 25.

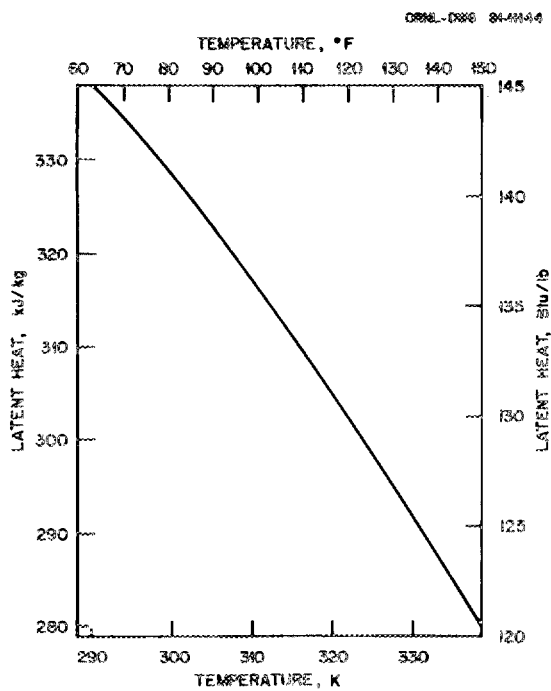


Fig. B.1. Latent heat of isobutane as a function of temperature at a pressure of 1 atm.

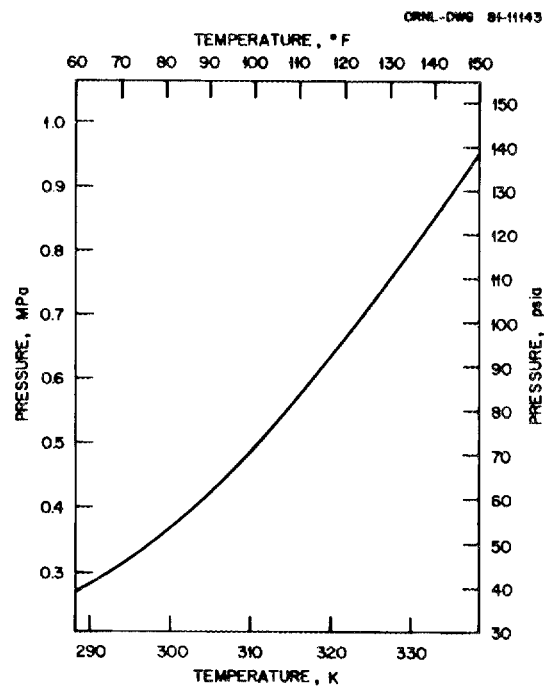


Fig. B.2. Vapor pressure of isobutane as a function of temperature.

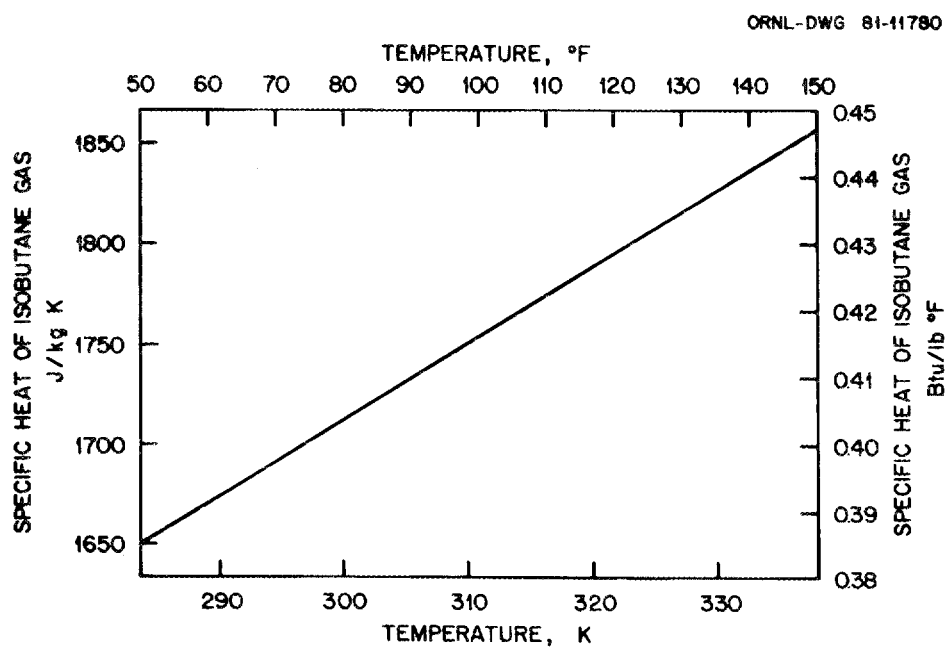


Fig. B.3. Specific heat of isobutane gas at 1 atm.

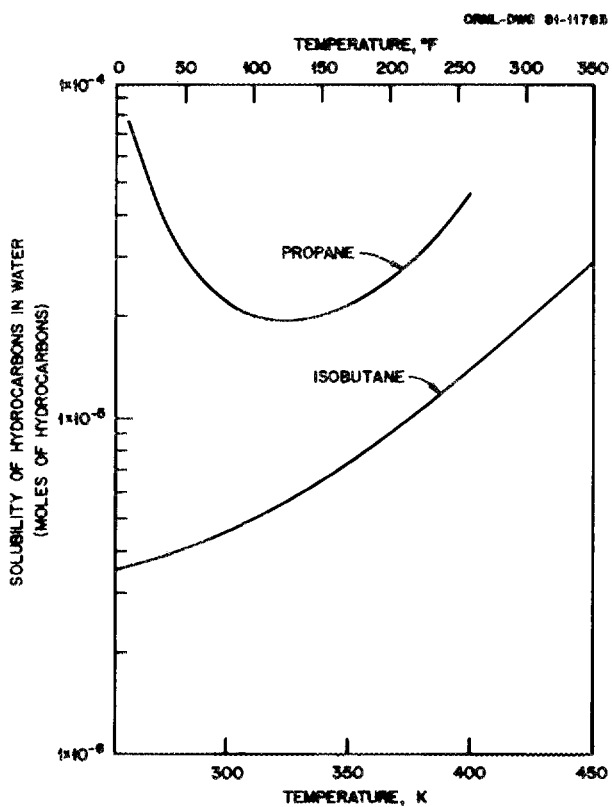


Fig. B.4. Enthalpy of isobutane as a function of temperature and pressure.

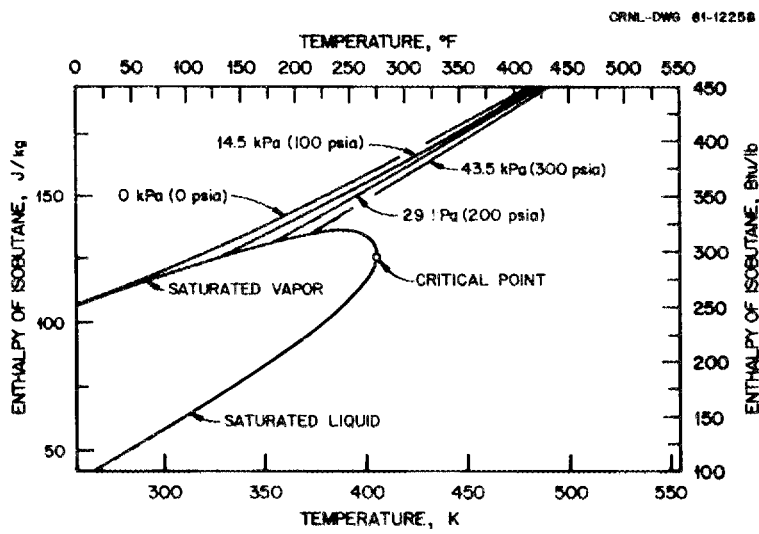


Fig. B.5. Solubility of propane and isobutane in water as functions of temperature.

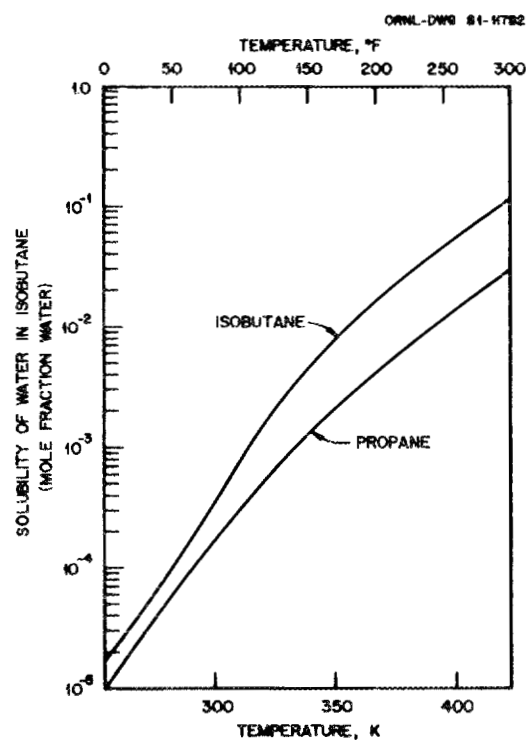


Fig. B.6. Solubility of water in propane and isobutane as functions of temperature.

Appendix C  
PROPERTIES OF WATER

Table C.1 shows the physical properties of water over the appropriate temperature range of the cooling water. The properties include the density, dynamic viscosity, thermal conductivity and Prandtl Number. The specific heat of water is assumed to be constant over the temperature range considered.

Table C.1. Properties of saturated water<sup>a</sup>

T		$\rho$		$\mu$		k		$N_{Pr}$
k	$^{\circ}F$	kg/m <sup>3</sup>	lb/ft <sup>3</sup>	Pas	lb/ft <sup>2</sup> ·h	W/m K	Btu/h·ft <sup>°</sup> F	
273	32	1000	62.42	0.00179	4.33	0.566	0.327	13.37
277	40	1000	62.42	0.00155	3.75	0.574	0.332	11.36
283	50	999	62.38	0.00130	3.17	0.585	0.338	9.41
289	60	999	62.34	0.00112	2.71	0.595	0.344	7.88
294	70	998	62.27	0.00098	2.37	0.604	0.349	6.78
300	80	996	62.17	0.00086	2.08	0.614	0.355	5.85
305	90	995	62.11	0.00076	1.85	0.623	0.360	5.13
311	100	993	61.99	0.00068	1.65	0.630	0.364	4.52
316	110	991	61.84	0.00062	1.49	0.637	0.368	4.04
322	120	989	61.73	0.00056	1.36	0.644	0.372	3.65
327	130	986	61.54	0.00051	1.24	0.649	0.375	3.30
333	140	983	61.39	0.00047	1.14	0.654	0.378	3.01
339	150	980	61.20	0.00043	1.04	0.659	0.381	2.72

<sup>a</sup>T = temperature,  $C_p$  = specific heat = 1.0 Btu/lb<sup>°</sup>F or cal/gm<sup>°</sup>K,  
 $\rho$  = density,  $\mu$  = dynamic viscosity, k = thermal conductivity, and  
 $N_{Pr}$  = Prandtl Number (dimensionless).



Appendix D  
SHELLSIDE PRESSURE DISTRIBUTION

Appendix D shows the pressure distribution in the East Mesa condenser. The vapor velocity, the amount of condensate obtained on each row, the total condensate obtained, and the incurred pressure drop are tabulated for each row of each shell pass. Tables D.1 through D.6 show the data for the first pass through the sixth pass and indicate the baffle spacing for each pass. The following is the same for all passes: baffles, 6; total tube length, 6, 6168 m (20,239 ft); temperature, 307.57 K (94.0°F); pressure, 493.68 kPa (71.60 psi); gas flow rate, 12.55 kg/s (99,400 lb/h); entrance loss to be added to total pressure drop, 715.22 Pa (0.1037 psi).

Table D.1. Pressure distribution through the first shell pass of the East Mesa condenser with a baffle spacing of 1.52 m (60 in.)

Row number	Number of tubes	Vapor velocity		Condensed/row		Total condensed		Pressure drop	
		(m/s)	(ft/s)	(liters/s)	(gal/min)	(liters/s)	(gal/min)	kPa	psi
1	30	3.269	10.73	0.188	2.973	0.188	2.97	0.020	0.003
2	31	3.142	10.31	0.194	3.072	0.381	6.05	0.039	0.006
3	32	3.021	9.91	0.200	3.171	0.581	9.22	0.056	0.008
4	34	2.823	9.26	0.213	3.369	0.794	12.59	0.071	0.010
5	35	2.719	8.92	0.219	3.468	1.013	16.05	0.085	0.012
6	36	2.620	8.60	0.225	3.568	1.238	19.62	0.099	0.014
7	37	2.526	8.29	0.231	3.667	1.469	23.29	0.111	0.016
8	38	2.435	7.99	0.238	3.766	1.707	27.05	0.123	0.018
9	40	2.291	7.52	0.250	3.964	1.957	31.02	0.134	0.019
10	40	2.265	7.43	0.250	3.964	2.207	34.98	0.144	0.021
11	40	2.239	7.35	0.250	3.964	2.457	38.95	0.154	0.022
12	41	2.160	7.09	0.256	4.063	2.713	43.01	0.164	0.024
13	41	2.134	7.00	0.256	4.063	2.970	47.07	0.173	0.025
14	41	2.108	6.92	0.256	4.063	3.226	51.13	0.182	0.026
15	41	2.082	6.83	0.256	4.063	3.482	55.20	0.191	0.028
16	41	2.056	6.74	0.256	4.063	3.739	59.26	0.199	0.029
17	41	2.030	6.66	0.256	4.063	3.995	63.32	0.208	0.030
18	41	2.004	6.57	0.256	4.063	4.251	67.39	0.216	0.031
19	41	1.978	6.49	0.256	4.063	4.508	71.45	0.224	0.033
20	41	1.952	6.40	0.256	4.063	4.764	75.51	0.232	0.034
21	40	1.973	6.47	0.250	3.964	5.014	79.48	0.240	0.035
22	40	1.947	6.39	0.250	3.964	5.264	83.44	0.248	0.036
23	40	1.921	6.30	0.250	3.964	5.514	87.40	0.256	0.037
24	38	1.993	6.54	0.238	3.766	5.752	91.17	0.264	0.038
25	37	2.019	6.62	0.231	3.667	5.983	94.84	0.272	0.039
26	37	1.993	6.54	0.231	3.667	6.215	98.50	0.280	0.041
27	36	2.020	6.63	0.225	3.568	6.440	102.07	0.289	0.042
28	34	2.109	6.92	0.213	3.369	6.652	105.44	0.298	0.043
29	34	2.083	6.83	0.213	3.369	6.865	108.81	0.307	0.044
30	33	2.118	6.95	0.206	3.270	7.071	112.08	0.316	0.046
31	31	2.224	7.30	0.194	3.072	7.265	115.15	0.326	0.047
32	30	2.269	7.45	0.188	2.973	7.453	118.13	0.336	0.049

Table D.2. Pressure distribution through the second shell pass of the East Mesa condenser with a baffle spacing of 1.11 m (44 in.)

Row number	Number of tubes	Vapor velocity		Condensed/row		Total condensed		Pressure drop	
		(m/s)	(ft/s)	(liters/s)	(gal/min)	(liters/s)	(gal/min)	kPa	psi
1	30	3.064	10.05	0.138	2.180	7.590	120.31	1.231	0.179
2	31	2.943	9.66	0.142	2.253	7.732	122.56	1.248	0.181
3	32	2.828	9.28	0.147	2.326	7.879	124.88	1.263	0.183
4	34	2.642	8.67	0.156	2.471	8.035	127.35	1.277	0.185
5	35	2.543	8.34	0.160	2.544	8.195	129.90	1.289	0.187
6	36	2.448	8.03	0.165	2.616	8.360	132.51	1.301	0.189
7	37	2.358	7.74	0.170	2.689	8.530	135.20	1.312	0.190
8	38	2.272	7.45	0.174	2.762	8.704	137.96	1.323	0.192
9	40	2.136	7.01	0.183	2.907	8.888	140.87	1.332	0.193
10	40	2.110	6.92	0.183	2.907	9.071	143.78	1.341	0.194
11	40	2.084	6.84	0.183	2.907	9.254	146.69	1.350	0.196
12	41	2.009	6.59	0.188	2.980	9.442	149.67	1.358	0.197
13	41	1.982	6.50	0.188	2.980	9.630	152.64	1.366	0.198
14	41	1.956	6.42	0.188	2.980	9.818	155.62	1.374	0.199
15	41	1.930	6.33	0.188	2.980	10.006	158.60	1.382	0.200
16	41	1.904	6.25	0.188	2.980	10.194	161.58	1.390	0.202
17	41	1.878	6.16	0.188	2.980	10.382	164.56	1.397	0.203
18	41	1.852	6.08	0.188	2.980	10.570	167.54	1.404	0.204
19	41	1.826	5.99	0.188	2.980	10.758	170.52	1.411	0.205
20	41	1.800	5.91	0.188	2.980	10.946	173.50	1.418	0.206
21	40	1.818	5.96	0.183	2.907	11.130	176.41	1.425	0.207
22	40	1.792	5.88	0.183	2.907	11.313	179.32	1.432	0.208
23	40	1.766	5.79	0.183	2.907	11.496	182.22	1.438	0.209
24	38	1.830	6.00	0.174	2.762	11.671	184.98	1.445	0.210
25	37	1.851	6.07	0.170	2.689	11.840	187.67	1.452	0.211
26	37	1.825	5.99	0.170	2.689	12.010	190.36	1.459	0.212
27	36	1.848	6.06	0.165	2.616	12.175	192.98	1.467	0.213
28	34	1.927	6.32	0.156	2.471	12.331	195.45	1.474	0.214
29	34	1.902	6.24	0.156	2.471	12.487	197.92	1.482	0.215
30	33	1.931	6.34	0.151	2.398	12.638	200.32	1.490	0.216
31	31	2.025	6.64	0.142	2.253	12.780	202.57	1.498	0.217
32	30	2.064	6.77	0.138	2.180	12.918	204.75	1.507	0.219

Table D.3. Pressure distribution through the third shell pass of the East Mesa condenser with a baffle spacing of 0.86 m (34 in.)

Row number	Number of tubes	Vapor velocity		Condensed/row		Total condensed		Pressure drop	
		(m/s)	(ft/s)	(liters/s)	(gal/min)	(liters/s)	(gal/min)	kPa	psi
1	30	2.722	8.93	0.103	1.635	12.021	206.39	2.398	0.348
2	31	2.612	8.57	0.107	1.690	13.127	208.08	2.412	0.350
3	32	2.507	8.23	0.110	1.744	13.238	209.82	2.424	0.352
4	34	2.339	7.67	0.117	1.853	13.354	211.67	2.435	0.353
5	35	2.248	7.38	0.120	1.908	13.475	213.58	2.445	0.355
6	36	2.162	7.09	0.124	1.962	13.599	215.54	2.454	0.356
7	37	2.079	6.82	0.127	2.017	13.726	217.56	2.463	0.357
8	38	2.000	6.56	0.131	2.071	13.856	219.63	2.472	0.358
9	40	1.877	6.16	0.138	2.180	13.994	221.81	2.479	0.360
10	40	1.851	6.07	0.138	2.180	14.132	223.99	2.486	0.361
11	40	1.825	5.99	0.138	2.180	14.269	226.17	2.493	0.362
12	41	1.756	5.76	0.141	2.235	14.410	228.41	2.500	0.363
13	41	1.730	5.68	0.141	2.235	14.551	230.64	2.506	0.363
14	41	1.704	5.59	0.141	2.235	14.692	232.87	2.512	0.364
15	41	1.678	5.51	0.141	2.235	14.833	235.11	2.518	0.365
16	41	1.652	5.42	0.141	2.235	14.974	237.34	2.524	0.366
17	41	1.626	5.33	0.141	2.235	15.115	239.58	2.530	0.367
18	41	1.600	5.25	0.141	2.235	15.256	241.81	2.535	0.368
19	41	1.574	5.16	0.141	2.235	15.397	244.05	2.541	0.368
20	41	1.548	5.08	0.141	2.235	15.538	246.28	2.546	0.369
21	40	1.559	5.12	0.138	2.180	15.676	248.46	2.551	0.370
22	40	1.533	5.03	0.138	2.180	15.813	250.64	2.556	0.371
23	40	1.507	4.94	0.138	2.180	15.951	252.82	2.561	0.371
24	38	1.558	5.11	0.131	2.071	16.081	254.89	2.566	0.372
25	37	1.573	5.16	0.127	2.017	16.209	256.91	2.572	0.373
26	37	1.547	5.07	0.127	2.017	16.336	258.93	2.577	0.374
27	36	1.562	5.12	0.124	1.962	16.460	260.89	2.582	0.375
28	34	1.625	5.33	0.117	1.853	16.576	262.74	2.588	0.375
29	34	1.599	5.25	0.117	1.853	16.693	264.60	2.593	0.376
30	33	1.619	5.31	0.113	1.799	16.807	266.39	2.599	0.377
31	31	1.694	5.56	0.107	1.690	16.913	268.08	2.605	0.378
32	30	1.722	5.65	0.103	1.635	17.017	269.72	2.612	0.379

Table D.4. Pressure distribution through the fourth shell pass of the East Mesa condenser with a baffle spacing of 0.61 m (24 in.)

Row number	Number of tubes	Vapor velocity		Condensed/row		Total condensed		Pressure drop	
		(m/s)	(ft/s)	(liters/s)	(gal/min)	(liters/s)	(gal/min)	kPa	psi
1	30	2.338	7.67	0.075	1.189	17.092	270.91	3.500	0.508
2	31	2.239	7.35	0.078	1.229	17.169	272.14	3.510	0.509
3	32	2.146	7.04	0.080	1.268	17.249	273.41	3.519	0.510
4	34	1.998	6.56	0.085	1.348	17.334	274.75	3.527	0.512
5	35	1.917	6.29	0.088	1.387	17.422	276.14	3.535	0.513
6	36	1.840	6.04	0.090	1.427	17.512	277.57	3.542	0.514
7	37	1.766	5.79	0.093	1.467	17.604	279.03	3.549	0.515
8	38	1.695	5.56	0.095	1.506	17.699	280.54	3.555	0.516
9	40	1.587	5.21	0.100	1.586	17.799	282.13	3.560	0.516
10	40	1.561	5.12	0.100	1.586	17.899	283.71	3.565	0.517
11	40	1.535	5.03	0.100	1.586	17.999	285.30	3.571	0.518
12	41	1.472	4.83	0.103	1.625	18.102	286.92	3.575	0.519
13	41	1.446	4.74	0.103	1.625	18.205	288.55	3.580	0.519
14	41	1.420	4.66	0.103	1.625	18.307	290.17	3.584	0.520
15	41	1.394	4.57	0.103	1.625	18.410	291.80	3.589	0.520
16	41	1.368	4.49	0.103	1.625	18.512	293.42	3.593	0.521
17	41	1.342	4.40	0.103	1.625	18.615	295.05	3.597	0.522
18	41	1.316	4.32	0.103	1.625	18.717	296.67	3.601	0.522
19	41	1.290	4.23	0.103	1.625	18.820	298.30	3.604	0.523
20	41	1.264	4.15	0.103	1.625	18.922	299.92	3.608	0.523
21	40	1.268	4.16	0.100	1.586	19.022	301.51	3.612	0.524
22	40	1.242	4.08	0.100	1.586	19.122	302.10	3.615	0.524
23	40	1.216	3.99	0.100	1.586	19.222	304.68	3.619	0.525
24	38	1.252	4.11	0.095	1.506	19.317	306.19	3.622	0.525
25	37	1.259	4.13	0.093	1.467	19.410	307.65	3.626	0.526
26	37	1.233	4.04	0.093	1.467	19.502	309.12	3.629	0.526
27	36	1.240	4.07	0.090	1.427	19.592	310.55	3.633	0.527
28	34	1.284	4.21	0.085	1.348	19.678	311.90	3.636	0.527
29	34	1.258	4.13	0.085	1.348	19.763	313.24	3.640	0.528
30	33	1.269	4.16	0.083	1.308	19.845	314.55	3.644	0.528
31	31	1.321	4.34	0.078	1.229	19.923	315.78	3.648	0.529
32	30	1.338	4.39	0.075	1.189	19.998	316.97	3.652	0.530

Table D.5. Pressure distribution through the fifth shell pass of the East Mesa condenser with a baffle spacing of 0.46 m (18 in.)

Row number	Number of tubes	Vapor velocity		Condensed/row		Total condensed		Pressure drop	
		(m/s)	(ft/s)	(liters/s)	(gal/min)	(liters/s)	(gal/min)	kPa	psi
1	30	1.754	5.75	0.056	0.892	20.054	317.86	4.535	0.658
2	31	1.673	5.49	0.058	0.922	20.112	318.78	4.541	0.659
3	32	1.597	5.24	0.060	0.951	20.172	319.73	4.547	0.659
4	34	1.481	4.86	0.064	1.011	20.236	320.75	4.551	0.660
5	35	1.414	4.64	0.066	1.041	20.301	321.79	4.556	0.661
6	36	1.350	4.43	0.068	1.070	20.369	322.86	4.560	0.661
7	37	1.289	4.23	0.069	1.100	20.438	323.96	4.564	0.662
8	38	1.230	4.04	0.071	1.130	20.510	325.09	4.567	0.662
9	40	1.145	3.76	0.075	1.189	20.585	326.28	4.570	0.663
10	40	1.119	3.76	0.075	1.189	20.660	327.46	4.573	0.663
11	40	1.093	3.59	0.075	1.189	20.735	328.65	4.576	0.664
12	41	1.041	3.42	0.077	1.219	20.812	329.87	4.578	0.664
13	41	1.015	3.33	0.077	1.219	20.889	331.09	4.581	0.664
14	41	0.989	3.25	0.077	1.219	20.965	332.31	4.583	0.665
15	41	0.963	3.16	0.077	1.219	21.042	333.53	4.585	0.665
16	41	0.937	3.07	0.077	1.219	21.119	334.75	4.588	0.665
17	41	0.911	2.99	0.077	1.219	21.196	335.97	4.590	0.666
18	41	0.885	2.90	0.077	1.219	21.273	337.19	4.591	0.666
19	41	0.859	2.82	0.077	1.219	21.350	338.40	4.593	0.666
20	41	0.833	2.73	0.077	1.219	21.427	339.62	4.595	0.666
21	40	0.827	2.71	0.075	1.189	21.502	340.81	4.597	0.667
22	40	0.801	2.63	0.075	1.189	21.577	342.00	4.598	0.667
23	40	0.775	2.54	0.075	1.189	21.652	343.19	4.600	0.667
24	38	0.788	2.58	0.071	1.130	21.723	344.32	4.601	0.667
25	37	0.782	2.57	0.069	1.100	21.793	345.42	4.603	0.668
26	37	0.756	2.48	0.069	1.100	21.862	346.52	4.604	0.668
27	36	0.750	2.46	0.068	1.070	21.930	347.59	4.606	0.668
28	34	0.767	2.52	0.064	1.011	21.993	348.60	4.607	0.668
29	34	0.741	2.43	0.064	1.011	22.057	349.61	4.608	0.668
30	33	0.736	2.42	0.062	0.981	22.119	350.59	4.610	0.669
31	31	0.756	2.48	0.058	0.922	22.117	351.52	4.611	0.669
32	30	0.754	2.47	0.056	0.892	22.233	352.41	4.613	0.669

Table D.6. Pressure distribution through the sixth shell pass of the East Mesa condenser with a baffle spacing of 0.33 m (13 in.)

Row number	Number of tubes	Vapor velocity		Condensed/row		Total condensed		Pressure drop	
		(m/s)	(ft/s)	(liters/s)	(gal/min)	(liters/s)	(gal/min)	kPa	psi
1	30	1.013	3.32	0.041	0.644	22.274	353.05	5.492	0.797
2	31	0.956	3.14	0.042	0.666	22.316	353.72	5.494	0.797
3	32	0.901	2.96	0.043	0.687	22.359	354.40	5.496	0.797
4	34	0.825	2.71	0.046	0.730	22.405	355.13	5.498	0.797
5	35	0.776	2.55	0.047	0.751	22.453	355.89	5.500	0.798
6	36	0.730	2.39	0.049	0.773	22.502	356.66	5.501	0.798
7	37	0.685	2.25	0.050	0.794	22.552	357.45	5.502	0.798
8	38	0.642	2.10	0.051	0.816	22.603	358.27	5.503	0.798
9	40	0.585	1.92	0.054	0.859	22.657	359.13	5.504	0.798
10	40	0.559	1.83	0.054	0.859	22.712	359.99	5.505	0.798
11	40	0.533	1.75	0.054	0.859	22.766	360.85	5.506	0.799
12	41	0.494	1.62	0.056	0.880	22.821	361.73	5.506	0.799
13	41	0.468	1.54	0.056	0.880	22.877	362.61	5.507	0.799
14	41	0.442	1.45	0.056	0.880	22.932	363.49	5.508	0.799
15	41	0.416	1.37	0.056	0.880	22.988	364.37	5.508	0.799
16	41	0.390	1.28	0.056	0.880	23.043	365.25	5.508	0.799
17	41	0.364	1.20	0.056	0.880	23.099	366.13	5.509	0.799
18	41	0.338	1.11	0.056	0.880	23.155	367.01	5.509	0.799
19	41	0.312	1.02	0.056	0.880	23.210	367.89	5.509	0.799
20	41	0.286	0.94	0.056	0.880	23.266	368.77	5.510	0.799
21	41	0.267	0.88	0.054	0.859	23.320	369.63	5.510	0.799
22	40	0.241	0.79	0.054	0.859	23.374	370.49	5.510	0.799
23	40	0.215	0.70	0.054	0.859	23.428	371.35	5.510	0.799
24	38	0.199	0.65	0.051	0.816	23.480	372.16	5.510	0.799
25	37	0.178	0.58	0.050	0.794	23.530	372.96	5.511	0.799
26	37	0.152	0.50	0.050	0.794	23.580	373.75	5.511	0.799
27	36	0.130	0.43	0.049	0.773	23.629	374.52	5.511	0.799
28	34	0.111	0.36	0.046	0.730	23.675	375.25	5.511	0.799
29	34	0.085	0.28	0.046	0.730	23.721	375.98	5.511	0.799
30	33	0.061	0.20	0.045	0.709	23.765	376.69	5.511	0.799
31	31	0.038	0.12	0.042	0.666	23.807	377.36	5.511	0.799
32	30	0.013	0.04	0.041	0.644	23.848	378.00	5.511	0.799



INTERNAL DISTRIBUTION

- |                                |  |
|--------------------------------|--|
| 1. H. G. Arnold                | 39-58. G. H. Llewellyn                 |
| 2. J. P. Belk                  | 59. R. H. Lyon (Consultant)            |
| 3. H. P. Blanco                | 60. K. H. Luk                          |
| 4. D. D. Cannon                | 61. R. E. MacPherson                   |
| 5. R. S. Carlsmith             | 62. H. A. McClain                      |
| 6. F. C. Chin                  | 63. V. C. Mei                          |
| 7. J. H. Clinton               | 64-73. J. W. Michel                    |
| 8. S. K. Combs                 | 74. S. L. Milora                       |
| 9. K. D. Cook                  | 75. L. I. Moss                         |
| 10. L. M. Cuddy                | 76. R. W. Murphy                       |
| 11. R. C. Devault              | 77. B. Neimann                         |
| 12. N. Domingo                 | 78. G. K. Oppegard                     |
| 13. D. M. Eissenberg           | 79. J. A. Parsons                      |
| 14. J. F. Fourman              | 80. F. S. Patton                       |
| 15. W. Fulkerson               | 81. F. J. Peretz                       |
| 16. W. R. Gambill              | 82. T. W. Pickel                       |
| 17. R. W. Glass                | 83. A. W. Reed                         |
| 18. R. E. Goodson (Consultant) | 84. W. R. Reed                         |
| 19. G. Grossman                | 85. R. C. Robertson                    |
| 20. G. R. Hadder               | 86. M. W. Rosenthal                    |
| 21. C. V. Hardin               | 87. T. H. Row                          |
| 22. V. O. Haynes               | 88. J. A. Seneker                      |
| 23. J. L. Heck                 | 89-93. M. Siman-Tov                    |
| 24. M. V. Helfrich             | 94. C. B. Smith                        |
| 25. L. C. Hensley              | 95. D. G. Thomas                       |
| 26. R. F. Hibbs                | 96. D. B. Trauger                      |
| 27. H. W. Hoffman              | 97. H. E. Trammell                     |
| 28. R. M. Holmes               | 98. E. A. Vinyard                      |
| 29. L. N. Howell               | 99. G. C. Wei                          |
| 30. W. D. Hoyle                | 100. J. T. Weir                        |
| 31. W. P. Huxtable             | 101. J. W. Wells                       |
| 32. L. Jung                    | 102. T. Whitus                         |
| 33. R. A. Just                 | 103. L. V. Wilson                      |
| 34. A. A. Khan                 | 104. ORNL Patent Office                |
| 35. D. J. Kincaid              | 105-107. Central Research Library      |
| 36. E. H. Krieg                | 108. Document Reference Section        |
| 37. T. R. LaPorte (Consultant) | 109-110. Laboratory Records Department |
| 38. B. Lieberman               | 111. Laboratory Records (RC)           |

## EXTERNAL DISTRIBUTION

112. A. A. Adduci, DOE, San Francisco Operations Office, 133 Broadway, Oakland, CA 94612
113. J. H. Anderson, Sea Solar Power, Inc., 2422 South Queen Street, York, PA, 17403
114. W. Aung, Division of Engineering, National Science Foundation, Washington, DC 20550
115. K. J. Bell, School of Chemical Engineering, Oklahoma State University, Stillwater, OK 74074
116. A. E. Bergles, Department of Mechanical Engineering, Iowa State University, Ames, IA 50010
117. C. H. Bloomster, Battelle-Pacific Northwest Laboratory, Richland, WA 99352
118. G. E. Brandvold, Sandia Laboratories, P. O. Box 5800, Albuquerque, NM 87115
119. E. S. Burcher, Division of Ocean Energy Technology, DOE, Forrestal Building, 1000 Independence Avenue SW, Washington, DC 20585
120. T. Carnavos, Noranda Metal Industries, Prospect Drive, Newton, CT 06470
121. N. R. Clevinger, Wolverine Division, 2100 Market St. SE, P. B. Box 2202, Decatur, AL 35601
122. R. L. Coit, Electric Power Research Institute, P. O. Box 10412, Palo Alto, CA 94303
123. N. M. F. Conover, Radian Corporation, P. O. Box 9948, Austin, TX 78766
124. R. B. Coryell, Geothermal Program, National Science Foundation, Washington, DC 20550
125. R. H. Dart, Idaho National Engineering Laboratory, Idaho Falls, ID 83415
126. O. J. Demuth, Idaho National Engineering Laboratory, Idaho Falls, ID 83415
127. R. L. Fulton, Lawrence Berkeley Laboratory, University of California, Berkeley, CA 94720
128. C. G. Gottsman, Union Carbide, Linde Division, P. O. Box 44, Tonawanda, NY 14150
129. T. C. Hinrichs, Magma Power Company, 5143 Sunset Blvd., Los Angeles, CA 92112
130. B. Hwang, Mail Code 2722, David Taylor Naval Ship R&D Center, Annapolis, MD 21402
131. I. J. Ingvarsson, Aerojet Nuclear Company, 550 Second Street, Idaho Falls, ID 83401
132. B. A. Johnson, Battelle-Pacific Northwest Laboratory, P. O. Box 999, Richland, WA 99352
133. E. G. Keshock, Aerospace and Mechanical Engineering Department, University of Tennessee, Knoxville, TN 37916
134. J. Kestin, Division of Engineering, Brown University, Box D, Providence, RI 02912
135. G. A. Kolstad, Office of Energy Research, DOE, Washington, DC 20545

136. R. Kornbau, David Taylor Naval Ship Research and Development Center, Annapolis, MD 21402
137. J. T. Kuwada, Rogers Engineering Company, Inc., 111 Pine Street, Sixth Floor, San Francisco, CA 94111
138. A. D. K. Laird, Mechanical Engineering Department, University of California, Lawrence Berkeley Laboratory, Berkeley, CA 94720
139. R. J. LaSala, Geothermal and Hydro Power Division, Department of Energy, 1000 Independence Avenue SW, Washington, DC 20585
140. A. Lavi, Department of Chemical Engineering, Carnegie-Mellon University, Schenley Park, Pittsburgh, PA 15213
141. G. W. Leonard, ATDD (P&E) HPDD, Department of the Navy, China Lake, CA 93555
142. R. Letan, Ben-Gurion University of the Negev, Department of Mechanical Engineering, P. O. Box 653, Beer Sheva, Israel
143. A. Lundberg, L-505, University of California, Lawrence Livermore Laboratory, P. O. Box 808, Livermore, CA 94550
144. W. W. Madsen, Idaho National Engineering Laboratory, Idaho Falls, ID 83415
145. P. H. McCabe, Route 1, Bedo, ID 83323
146. C. McFarland, Solar Research and Technology, Department of Energy, 1000 Independence Avenue SW, Washington, DC 20585
147. G. Mines, Idaho National Engineering Laboratory, Idaho Falls, ID 83415
148. P. E. Minton, Union Carbide, P. O. Box 8361, Bldg. 2000, S. Charleston, W. VA 25303
149. K. Mirk, Lawrence Berkeley Laboratory, University of California, Berkeley, CA 94720
150. W. C. Moore, York Division, Borg Warner Corporation, York, PA 17403
151. D. T. Neil, Idaho National Engineering Laboratory, Idaho Falls, ID 83415
152. K. Nichols, Barber-Nichols Engineering, 6325 West 55th Avenue, Arvada, CO 80002
153. F. Notaro, Union Carbide, Linde Division, P. O. Box 44, Tonawanda, NY 14150
154. J. Nugent, Geothermal Energy, San Diego Gas and Electric Company, P. O. Box 1831, San Diego, CA 92112
155. R. H. Nunn, Naval Postgraduate School, Monterey, CA 93940
156. R. Olander, Barber-Nichols Engineering, 6325 West 55th Avenue, Arvada, CO 80002
157. P. O. O'Neil, Union Carbide, Linde Division, P. O. Box 44, Tonawanda, NY 14150
158. W. L. Owens, Lockheed Missiles and Space Company, Inc., P. O. Box 504, Sunnyvale, CA 95088
159. R. W. Perkins, Spiral Tubing Corporation, 533 John Downey Drive, New Britain, CT 06051
160. J. J. Perona, Chemical and Metallurgical Engineering Department, University of Tennessee, Knoxville, TN 37916
161. G. Phillips, Barber-Nichols Engineering, 6325 West 55th Avenue, Arvada, CO 80002
162. W. L. Pope, Lawrence Berkeley Laboratory, University of California, Berkeley, CA 94720

163. T. Rabas, Steam-Turbine Generator Technical Operations Division, Westinghouse Electric Corporation, Lester Branch, P. O. Box 9175 N2, Philadelphia, PA 19113
164. K. F. Read, 448 Ferry Point Road, Annapolis, MD 21403
165. W. Rohsenow, Mechanical Engineering Department, Massachusetts Institute of Technology, 77 Massachusetts Avenue, Cambridge, MA 02139
166. R. R. Rothfus, Chemical Engineering Department, Carnegie-Mellon University, Schenley Park, Pittsburgh, PA 15213
167. J. D. Ryan, Technology Consumer Products Branch, DOE, Forestal Building, MS 6H-068, Washington, DC 20585
168. L. L. Simpson, Union Carbide, P. O. Box 8361, Bldg. 2000, S. Charleston, W. VA 25303
169. R. C. Somes, Westec Services, Inc., P. O. Box 791, Holtville, CA 92250
170. K. E. Starlings, School of Chemical Engineering and Materials Science, University of Oklahoma, 202 West Boyd, Norman, OK 53201
171. D. F. Sucui, Idaho National Engineering Laboratory, Idaho Falls, ID 83415
172. G. Schwartz, Union Carbide, P. O. Box 8361, Bldg. 2000, S. Charleston, W. VA 25303
173. J. W. Tester, Los Alamos Scientific Laboratory, P. O. Box 1663, Los Alamos, NM 87544
174. S. E. Turner, Idaho National Engineering Laboratory, Idaho Falls, ID 83415
175. W. H. Thielbahr, DOE, Idaho Operations Office, 550 Second Street, Idaho Falls, ID 83401
176. R. Webb, Department of Mechanical Engineering, Pennsylvania State University, 208 Mechanical Engineering Building, University Park, PA 16802
177. D. K. Werner, Barber-Nichols Engineering, 6325 West 55th Avenue, Arvada, CO 80002
178. J. F. Whitbeck, Idaho National Engineering Laboratory, Idaho Falls, ID 83415
179. G. Wildsmith, Research and Development, Yorkshire Imperial Metals, Ltd., P. O. Box 166, Leeds LS1 1 RD, England
180. W. Urbanek, DSS Engineers, Inc., 1850 NW 69th Avenue, Fort Lauderdale, FL 33313
181. J. S. Yampolsky, General Electric Company, P. O. Box 81608, San Diego, CA 92138
182. Office of Assistant Manager for Energy Research and Development, Department of Energy, ORO, Oak Ridge, TN 37830
- 183-612. Given distribution as shown in DOE/TIC-4500 under category UCC-66d (GE-Utilization Technology)